Nuclear Science

OECD

Physics of Plutonium Recycling

Volume VI: Multiple Plutonium Recycling in Advanced PWRs

NUCLEAR • ENERGY • AGENCY

Nuclear Science

Physics of Plutonium Recycling

Volume VI

Multiple Pu Recycling in Advanced PWRs

NUCLEAR ENERGY AGENCY
ORGANISATION FOR ECONOMIC CO-OPERATION AND DEVELOPMENT

ORGANISATION FOR ECONOMIC CO-OPERATION AND DEVELOPMENT

Pursuant to Article 1 of the Convention signed in Paris on 14th December 1960, and which came into force on 30th September 1961, the Organisation for Economic Co-operation and Development (OECD) shall promote policies designed:

- to achieve the highest sustainable economic growth and employment and a rising standard of living in Member countries, while maintaining financial stability, and thus to contribute to the development of the world economy;
- to contribute to sound economic expansion in Member as well as non-member countries in the process of economic development; and
- to contribute to the expansion of world trade on a multilateral, non-discriminatory basis in accordance with international obligations.

The original Member countries of the OECD are Austria, Belgium, Canada, Denmark, France, Germany, Greece, Iceland, Ireland, Italy, Luxembourg, the Netherlands, Norway, Portugal, Spain, Sweden, Switzerland, Turkey, the United Kingdom and the United States. The following countries became Members subsequently through accession at the dates indicated hereafter: Japan (28th April 1964), Finland (28th January 1969), Australia (7th June 1971), New Zealand (29th May 1973), Mexico (18th May 1994), the Czech Republic (21st December 1995), Hungary (7th May 1996), Poland (22nd November 1996), Korea (12th December 1996) and the Slovak Republic (14 December 2000). The Commission of the European Communities takes part in the work of the OECD (Article 13 of the OECD Convention).

NUCLEAR ENERGY AGENCY

The OECD Nuclear Energy Agency (NEA) was established on 1st February 1958 under the name of the OEEC European Nuclear Energy Agency. It received its present designation on 20th April 1972, when Japan became its first non-European full Member. NEA membership today consists of 28 OECD Member countries: Australia, Austria, Belgium, Canada, Czech Republic, Denmark, Finland, France, Germany, Greece, Hungary, Iceland, Ireland, Italy, Japan, Luxembourg, Mexico, the Netherlands, Norway, Portugal, Republic of Korea, Slovak Republic, Spain, Sweden, Switzerland, Turkey, the United Kingdom and the United States. The Commission of the European Communities also takes part in the work of the Agency.

The mission of the NEA is:

- to assist its Member countries in maintaining and further developing, through international co-operation, the scientific, technological and legal bases required for a safe, environmentally friendly and economical use of nuclear energy for peaceful purposes, as well as
- to provide authoritative assessments and to forge common understandings on key issues, as input to government decisions on nuclear energy policy and to broader OECD policy analyses in areas such as energy and sustainable development.

Specific areas of competence of the NEA include safety and regulation of nuclear activities, radioactive waste management, radiological protection, nuclear science, economic and technical analyses of the nuclear fuel cycle, nuclear law and liability, and public information. The NEA Data Bank provides nuclear data and computer program services for participating countries.

In these and related tasks, the NEA works in close collaboration with the International Atomic Energy Agency in Vienna, with which it has a Co-operation Agreement, as well as with other international organisations in the nuclear field.

FOREWORD

The OECD/NEA Working Party on the Physics of Plutonium Fuels and Innovative Fuel Cycles (WPPR) was established in 1993 and reports to the OECD/NEA Nuclear Science Committee. Its main activity has been to analyse physics code benchmarks for problems related to the physics of plutonium fuels. Past volumes of published work have examined the physics of plutonium-fuelled pressurised water reactors (PWRs), as well as the physics of metal- and oxide-fuelled fast reactors.

Some of the questions that the Working Group has attempted to address in the present and previous volumes include:

- What is the effect on the physics of the degradation in plutonium fissile quality that occurs with increasing burn-up and age of spent fuel?
- What is the impact on the physics of multiple recycling of plutonium if MOX assemblies are themselves reprocessed? What are the limitations associated with multiple recycling? Is there a point beyond which multiple recycling becomes no longer practicable in the present generation of PWRs?
- Are the present nuclear data libraries and neutronics codes capable of predicting the physics performance of MOX made from plutonium derived from high burn-up and/or multiple-recycling scenarios?
- Is thermal MOX recycling ultimately compatible with a fast-reactor fuel cycle? Can fast reactors be used in a flexible manner to address whatever requirements there might be to consume plutonium from a thermal MOX programme? Can plutonium-burning fast reactors be changed to plutonium breeding to maintain self-sufficiency in the longer term?
- How do the nuclear codes compare with real data from experiments?

The “Physics of Plutonium Recycling” series currently comprises the following titles:

- Volume I: Issues and Perspectives (OECD/NEA, 1995);
- Volume II: Plutonium Recycling in Pressurised Water Reactors (OECD/NEA, 1995);
- Volume III: Void Reactivity Effect in Pressurised Water Reactors (OECD/NEA, 1995);
- Volume IV: Fast Plutonium Burner Reactors: Beginning of Life (OECD/NEA, 1995);
- Volume V: Plutonium Recycling in Fast Reactors (OECD/NEA, 1996);
- Volume VI: Multiple Plutonium Recycling in Advanced PWRs (OECD/NEA, 2002).

Volumes VII and VIII, in preparation, will be devoted to a theoretical benchmark of a boiling water reactor (BWR) assembly containing mixed-oxide fuel rods, and to plutonium fuel in high-temperature reactors.

While all of the earlier work consisted of theoretical benchmarks comparing different nuclear codes and nuclear data libraries, comparisons against experimental measurements were made possible by SCK-CEN using data from the VENUS-2 reactor. The VENUS-2 data concerned an experimental mock-up of a PWR core containing UO_2 and mixed-oxide (MOX) assemblies. The results of this benchmark were published in *Benchmark on the VENUS-2 MOX Core Measurements* (OECD/NEA, 2000). The benchmark was carried out under the joint auspices of the WPPR and the Task Force on Reactor-based Plutonium Disposition (TFRPD). Another benchmark was undertaken for three critical core configurations of the KRITZ reactor: two with UO_2 fuel and one with MOX fuel. Measurements were performed for room temperature as well as elevated temperatures (~245°C). The results are due to be published soon.

TABLE OF CONTENTS

CONTRIBUTORS

CHAIR	*K. Hesketh*	BNFL	UK
SECRETARY	*E. Sartori*	OECD/NEA	
PRINICPAL AUTHORS	*M. Delpech*	CEA	France
	K. Hesketh	BNFL	UK
	D. Lutz	IKE	Germany
	E. Sartori	OECD/NEA	
PROBLEM SPECIFICATION	*M. Delpech*	CEA	France
SPECIAL CONTRIBUTION	*G. Schlosser*	Siemens/KWU	Germany
DATA COMPILATION AND ANALYSIS	*M. Delpech*	CEA	France
	I. Champtiaux	CEA	France
	M. Goutefarde	CEA	France
	M. Juanola	CEA	France
SPECIAL STUDY (CHAPTER 6)	*S. Cathalau*	CEA	France
	D. Lutz	IKE	Germany
	W. Bernnat	IKE	Germany
	M. Mattes	IKE	Germany
	T.T.J. M. Peeters	ECN	The Netherlands
	Y. Peneliau	CEA	France
	A. Puill	CEA	France
	H. Takano	JAERI	Japan
EDITOR	*K. Hesketh*	BNFL	UK
TEXT PROCESSING AND LAYOUT	*A. McWhorter*	OECD/NEA	
	H. Déry	OECD/NEA	

BENCHMARK PARTICIPANTS

Name	*Establishment*	*Country*
MALDAGUE, Thierry	Belgonucléaire	Belgium
HOEJERUP C. Frank	Risø	Denmark
BARBRAULT Patrick	EDF-Clamart	France
VERGNES Jean	EDF-Clamart	
DELPECH Marc	CEA-Cadarache	
COSTE Mireille	CEA-Saclay	
LEE Yi-Kang	CEA-Saclay	
PENELIAU Yannick	CEA- Saclay	
PUILL André	CEA- Saclay	
ROHART Michelle	CEA- Saclay	
TSILANIZARA Aimé	CEA- Saclay	
POINOT-SALANON Christine	FRAMATOME	
HESSE Ulrich	GRS	Germany
MOSER Eberhard	GRS	
LEHMANN Sven	U-Braunschweig	
BERNNAT Wolfgang	U-Stuttgart-IKE	
LUTZ Dietrich	U- Stuttgart -IKE	
MATTES Margerete	U- Stuttgart -IKE	
SCHWEIZER M.	U- Stuttgart -IKE	
KANEKO K.	ITIRO	Japan
AKIE Hiroshi	JAERI	
TAKANO Hideki	JAERI	
MISAWA Tsuyoshi	U-Nagoya	
TAKEDA Toshikazu	U-Osaka	
YAMAMOTO Toshihisa	U-Osaka	
FUJIWARA Daisuke	U-Tohoku	
IWASAKI Tomohiko	U-Tohoku	
KIM Young-Jin	KAERI	Republic of Korea
KLOOSTERMAN Jan Leen	Petten	The Netherlands
TSIBOULIA Anatoli	IPPE-Obninsk	Russian Federation
PARATTE Jean-Marie	PSI	Switzerland
CROSSLEY Steve	BNFL	United Kingdom
HESKETH Kevin	BNFL	
BLOMQUIST Roger N.	ANL	USA
GRIMM Karl	ANL	
HILL Robert N.	ANL	

EXECUTIVE SUMMARY

The recycling of plutonium in LWRs has for quite some time been seen as an important interim step prior to the large scale introduction of fast reactors; several countries have, in fact, been using MOX fuel in PWRs on a commercial scale for many years. Now that fast reactors are no longer expected to be introduced for some time, the need to manage existing plutonium stocks puts even more emphasis on LWR MOX. Even though there is sufficient experience of MOX in PWRs to be assured of satisfactory performance under existing conditions, the situation is not static and it is very important to address future requirements.

There are two main trends which need to be accounted for. First, discharge burn-ups are still increasing steadily. Second, the fissile quality of the plutonium is generally becoming poorer. The decline in fissile quality is partly a consequence of the higher burn-ups, but another major consideration is the effect of recycling MOX fuel itself. Multiple recycle scenarios cause a significant decline in fissile quality in each recycle generation. One consequence is that the initial plutonium content of MOX fuel is considerably increased in each recycle generation and this poses a considerable challenge to current nuclear design codes and the associated nuclear data libraries.

The OECD Working Group on the Physics of Plutonium Recycling (WPPR) has considered the issue of multiple recycle of MOX in PWRs in Volumes I and II of its report published in 1995. The main effort was directed towards an international benchmark exercise in which participants were invited to submit solutions to a fully defined problem representative of a multiple recycle scenario in a PWR. Such benchmark exercises are a valuable first step towards understanding the problems to be overcome before a future scenario can be realised in practice. They cannot, of course, identify the correct answer; this must wait until there is experimental or operational experience to learn from. However they can highlight the areas in which current calculational methods and nuclear data start to breakdown and thereby provide a rational basis for directing the research effort.

The earlier benchmark work identified major discrepancies between the various nuclear design codes and nuclear data libraries, specifically differences of up to 4%Δk in reactivities. A portion of the range of discrepancy was explained because some of the codes did not apply self-shielding to the resonance treatment of the higher plutonium isotopes; with the large concentration of ^{242}Pu specified in the benchmark, self-shielding in this nuclide was very important. Nevertheless the remaining discrepancy was considered sufficiently large that further work would clearly be necessary before the multiple recycle scenario envisaged in the specification could be implemented.

A shortcoming of the initial benchmark was that the cases considered only included one corresponding to today's situation (with plutonium of good isotopic quality), to one which might arise after many generations of MOX recycle (with extremely poor isotopic quality). Analysis of the intermediate steps was missing, and therefore there was no possibility of determining precisely where the nuclear codes and data libraries would start to lose their applicability. Accordingly, CEA suggested a benchmark in which five consecutive generations of multiple recycle in a PWR would be followed. In the specification of the benchmark, attempts were made to make it as realistic a

scenario as possible, taking account of such details as the length of time between recycle generations (accounting for the time delays in pond storage, MOX fabrication, etc.) and the dilution effect when MOX and UO_2 assemblies are co-reprocessed.

As in the previous benchmark exercise, the benchmark was restricted to the level of the lattice codes. This is the logical first step because it does not make sense to progress to the three-dimensional whole core codes until the underlying nuclear data and lattice code calculations show adequate agreement. Two cases were considered, one for a standard 17×17 PWR lattice such as used in many of today's PWRs (designated the STD PWR) and one for a lattice with an increased moderator/fuel ratio (3.5:1 compared with 2:1 for the STD PWR). The latter case, designated the HM PWR (for highly moderated), was intended to cover a proposed PWR design dedicated for use with MOX only. In such a PWR it would be possible to optimise the lattice to give increased moderation, thereby improving the efficiency with which the plutonium can be used.

Parameters examined in the benchmark exercise included end-of-cycle reactivity, which determines cycle length, the variation of reactivity with burn-up, reactivity coefficients, microscopic cross-sections, isotopic evolution and isotopic toxicity evolution with time. The detailed comparison of the results is very extensive and is not given in full in this report. The following are the broad conclusions and observations that have emerged:

Since the earlier benchmarks, considerable progress has been made in nuclear data libraries and methods. The discrepancies between the different data libraries and lattice methods, when applied to multiple recycle scenarios in PWR, are now generally within reasonable bounds. The observed spread of results is now consistent with the uncertainties in the underlying nuclear data and will require further experimental validation prior to practical implementation of multiple recycle. Multiple recycle scenarios therefore appear to be practicable and feasible in conventional PWRs, at least in the near term. Questions arising from a possible positive void coefficient would almost certainly preclude recycle beyond the second generation and even possibly even in the second generation in this particular scenario.

In the longer term, the HM PWR concept shows some merit. However, the principal advantage, that of needing a lower initial plutonium content with the same dilution ratio, is largely eroded in later recycle generations; in spite of the much improved moderation, the HM PWR degrades the plutonium isotopic quality more rapidly than the STD PWR, to a large extent negating the benefit of the softer spectrum. The HM PWR case also seems to pose more difficulties for present nuclear data libraries and codes, as evidenced by the larger number of discrepant results seen in the HM PWR benchmark. Therefore, even the HM PWR is of questionable practicability with respect to the later recycle generations.

In view of these considerations, at its last meeting the WPPR agreed that there is no compelling reason to continue further benchmark studies at the level of the lattice codes. Suggestions for future work include examining existing experimental configurations where the specifications are freely available, and also the re-examination of the problem at the level of whole-core calculations, in order to be able to understand more clearly how the lattice codes results relate to whole-core reactivity coefficients and other important parameters for the design and safety analyses. With such studies it is hoped to be able to make a definitive judgement as to where the limits of multiple recycle in PWRs are.

Chapter 1

INTRODUCTION

Background

The recycling of plutonium as PuO_2/UO_2 mixed oxide (MOX) fuel is already established in pressurised water reactors (PWR) in several countries on a commercial scale. The discharge burn-up of MOX fuel, and indeed its overall performance, is essentially the same as that of UO_2 fuel. Thus the MOX fuel currently being irradiated in PWRs is typically intended to be discharged at burn-ups of 40 to 45 MWd/t. The initial plutonium content needed to achieve such burn-ups varies depending on the precise source of the plutonium, but is typically in the range 7 to 8 w/o total plutonium, expressed as an average over the whole assembly. The experience of MOX utilisation in PWRs has been positive and there are no outstanding operational or safety issues to be resolved. However the situation is not static, and such issues will have to be addressed in the near future as the background conditions change.

The fundamental changes are that discharge burn-ups are continuing to trend upwards, while there will also arise a need to recycle the plutonium from discharged MOX assemblies. Both these changes will manifest themselves as a decrease in isotopic quality of the plutonium that is available for recycle. For thermal reactors the even isotopes of plutonium (238, 240 and 242) do not contribute significantly to fissions. The ratio ($^{239}Pu + {}^{241}Pu$)/(total plutonium) is thus denoted the fissile fraction of the plutonium and is a measure of plutonium quality for thermal reactor MOX. The problem is that plutonium quality decreases as the discharge burn up increases and decreases yet further following recycle of the plutonium recovered from MOX. Combined with the self-evident need to increase plutonium content to reach higher burn-ups, it will be necessary to significantly increase the total plutonium content of the MOX fuel.

Compared with conventional UO_2 fuel, MOX fuel is already significantly different from a neutronic point of view, there being a much smaller thermal flux for a given rating. This is due to the combined effects of the higher fission and absorption cross-sections of ^{239}Pu and ^{241}Pu compared with ^{235}U, exacerbated by the significant absorption of the ^{240}Pu and the ^{242}Pu. The difference in spectrum affects the core performance because the control, reactivity coefficient and transient behaviours are all altered. Increasing the total plutonium content beyond present levels exaggerates all these effects further. Ultimately, the deterioration in parameters such as control rod reactivity worth, boron reactivity worth and moderator void and temperature coefficients may become a barrier to further utilisation of MOX in PWRs, at least in conventional lattices. The question is, therefore, at what precise point will such considerations present a barrier. Also, it is important to ask whether present nuclear data libraries and nuclear codes agree as to where this point occurs.

It was against this background that the OECD/NEA Working Group on the Physics of Plutonium Recycle (WPPR) initiated an earlier benchmark studies for PWR MOX. This was reported in 1995 (refer to Vol. I and Vol. III). The benchmarks in question considered first a PWR MOX infinite lattice

cell and a multi-assembly arrangement designed to test the nuclear data libraries and lattice codes and to test core-wide calculational methods respectively.

The infinite lattice benchmark considered the identical geometrical arrangement of the lattice both a good and a poor isotopic quality for the plutonium as part of the specification. The good quality case was considered in order to provide a reference point for comparison, by showing how well the various solutions were in agreement for a situation that was prototypic of the present generation MOX. The poor isotopic quality case was intended to be an extreme test of the nuclear data and codes. While the various solutions were in reasonable (but not perfect agreement) for the former case, they were very discrepant in the case of the latter. Predictions of k-infinity versus burn-up were different by more than 4% Δ-k. This was a very serious discrepancy, and called into doubt the ability of the nuclear data libraries and codes to model the future situation. An explanation for some of the discrepancy, due to some of the codes ignoring resonance self-shielding in ^{242}Pu, was noted. Nevertheless, the remaining discrepancies were considered unacceptable for design and licensing applications.

The multi-assembly Benchmark was intended to explore the void reactivity coefficient, to see whether the various codes were in agreement as to the point where it becomes positive. The void coefficient is very important for safety and should be negative, or at least non-positive to ensure negative feedback. The void coefficient tends to become less negative the higher the total plutonium content and in the conventional PWR lattice changes sign from negative to positive at a total plutonium concentration of between 10 and 12 w/o. The benchmark comparisons showed reasonably satisfactory level of agreement between the various solutions submitted.

The present benchmark was intended to complement the earlier two as explained in the next section.

Current objectives

Multiple recycle scenarios presently form a very important topic for MOX recycle in LWRs. With the prospects for large scale deployment of fast reactors having receded in recent years, MOX is becoming more significant as a means of utilising plutonium stocks that were originally intended to start fast reactor cycles. The existence of surplus ex-weapons plutonium and establishing a means for its consumption or disposal has, at the same time, added further urgency and importance. The question of how many times plutonium recovered from MOX assemblies can be re-used in PWRs is important strategically and logistically. Strategically, it is important because it affects the energy potential that is available from plutonium. Logistically it determines whether there will be a need to store or dispose of MOX assemblies and/or plutonium and some future point if indefinite recycle does not prove practical.

Each recycle generation involves irradiation of MOX fuel (lasting typically 4-5 years), followed by pond cooling (typically 5 years), followed by reprocessing and re-fabrication as MOX (taking a further 2 years). Thus each generation of multiple recycle will last at least 11 years. Multiple recycle scenarios therefore extend over very long periods measured in decades. It is clear that over such extended timescales there will be ample opportunity for major changes in world energy requirements and strategies. It may well be the case that the scenario considered here is overtaken by events well before even the first or second generations of recycle are completed. Nevertheless, it is important to analyse such scenarios, just to be sure that they are practical technically, strategically, logistically and to establish their impact on environmental and safety considerations.

The present benchmark is for a standard lattice PWR and a highly moderated PWR operating with a moderately high burn-up fuel cycle (51 MWd/t discharge burn-up), which is expected to be representative of PWR operation in the next decade. The specification calls for the reprocessing of MOX fuel along with a certain fraction of UO_2 assemblies, as will be required in the current generation of reprocessing plants for technical reasons. The emphasis was on specifying a benchmark problem that was as realistic as possible, but keeping within the bounds of what is known from current technology and not relying on extrapolation to an uncertain future. This latter constraint may mean that the benchmark may turn out to have been pessimistic by not accounting for technological developments, but this is unavoidable. A fuller description of the benchmark is provided in Chapter 2, while Appendix A gives the complete specification as issued to the individual contributors.

The primary objectives of the benchmark were:

- to compare reactivities, reactivity coefficients and isotopic evolution calculations obtained with different lattice codes and their associated nuclear data libraries;

- to determine at what point, if any, the calculations diverge to such an extent that the physics predictions must be considered unreliable;

- to determine at what point, if any, further generations of recycle are excluded on technical grounds such as unacceptable reactivity coefficient characteristics;

- to evaluate the environmental impact of multiple recycle.

The rationale behind including a highly moderated PWR lattice is that theoretically, such a lattice may show technical advantages in multiple recycle scenarios. The idea would be to dedicate a small number of new PWRs to MOX usage only. With no need to accommodate UO_2 fuel, the reactor designer could then choose to optimise the moderator/fuel volume ratio for plutonium. It turns out that the optimum occurs at moderator/fuel volume ratio of about 3.5, compared with 2.0 for uranium fuel in a standard lattice. This could be achieved by preserving the fuel rod design and dimensions and simply increasing the rod to rod pitch. The reactor core would be marginally bigger in its radial dimensions, but otherwise the reactor design and the associated equipment would be much as for a conventional PWR.

The present benchmark was naturally specified for PWRs, as all commercial experience of MOX usage has so far been obtained in them. However, the lessons learned are expected to be broadly applicable to BWRs as well, although the details will inevitably be different.

Important physics issues

The key physics issues that this collaboration was intended to address are those of:

- The variation of k-infinity with burn-up for the MOX infinite lattice calculations with burn-up during each recycle generation. It is important for nuclear designers to be able to predict the k-infinity behaviour with a good degree of confidence if cycle lengths predictions are to be accurate enough for a utility's requirements.

- The behaviour of reactivity coefficients with recycle generation. Reactivity coefficients such as boron, fuel temperature (Doppler), moderator temperature and moderator void are key parameters that will largely determine the practicability of multiple recycle. Determining

precisely at what point any of these coefficients would become unacceptable is outside the scope of this study, as it necessarily requires a core-wide spatial analysis. Nevertheless, establishing the underlying trends with the number of recycle generations is a valuable first step.

- The calculation of the isotopic evolution in each recycle generation. Particularly in respect to plutonium, the burn-up calculations will determine the dependence of initial plutonium content with recycle generation. In turn, the initial plutonium content has major impacts for fuel fabrication, reprocessing, fuel thermo-mechanical and physics behaviour.

- The comparison of the highly moderated MOX lattice with a standard MOX lattice. To test, in particular, whether such lattices would be advantageous in a multiple recycle scenario.

Outline of this volume

Chapter 2 provides a summary description of the present benchmark. Chapter 3 lists the participants in the benchmark and describes the lattice codes and nuclear data libraries. Chapter 4 presents a summary of the principal results of the benchmark. Full details of the results are too voluminous for inclusion in this report, but are available on request from the OECD/NEA on computer disks. Chapter 5 discusses the results of the benchmarks and their significance to the practical situation. Chapter 6 describes a supplementary benchmark carried out in parallel to the main benchmark that offers further insights to the problem. Finally, Chapter 7 presents the conclusions and recommendations.

Chapter 2

BENCHMARK SPECIFICATION

Pin cell geometry

This chapter provides an outline description of the benchmark and comments on it. The full specification, as given to participants beforehand, is reproduced here in Appendix A. The purpose was to test the various nuclear data libraries and lattice codes in the simplest possible geometry of an infinite lattice cell or pin cell. Two pin cells were examined, as illustrated in Figure 2.1:

Figure 2.1. Schematic of standard (STD) lattice and highly moderated (HM) lattice pin cells

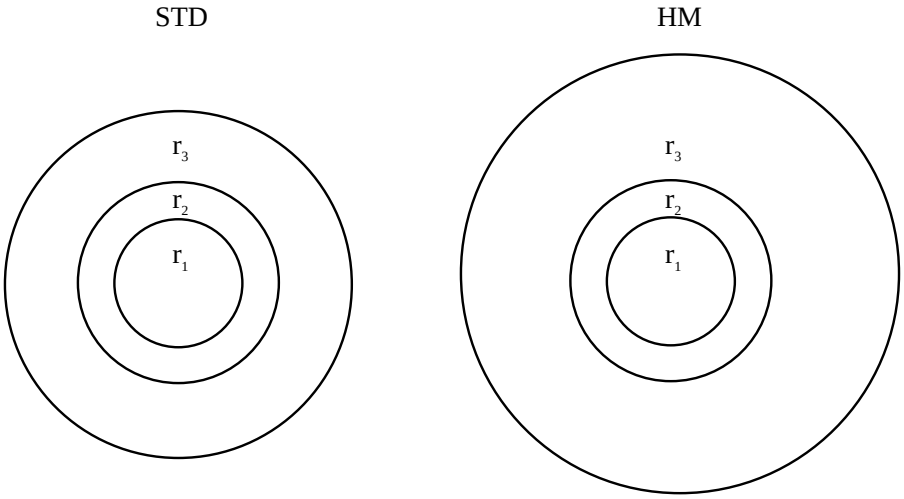

r_1: MOX fuel, 0.4127 cm
r_2: Zirconium clad, 0.4744 cm
r_3: Water + 500 ppm dissolved boron, 0.7521 cm STD, 0.9062 cm HM

The first was intended to be representative of a modern PWR assembly design and is designated the STD pincell in this report. Specifically, it represents a 17×17 MOX assembly design with 25 guide and instrument tubes and 264 fuel rods, illustrated schematically in Figure 2.2. Table 2.1 lists details of the main geometrical data for the assembly, which is modelled on the design in use in EdF's three and four loop plants. The outer diameter of the moderator region of the pincell was specified so that the overall moderator/fuel ratio (at approximately 2:1) matches that of the full assembly, including the guide and instrument thimbles and outside water gaps. Complications such as the absorption effect of grids, guide thimble tubes burnable poisons, etc. were avoided by ignoring them in the pincell specification. Their neglect does not affect the benchmark's aims, and so is not considered important.

Figure 2.2. Schematic of multiple recycle logistics

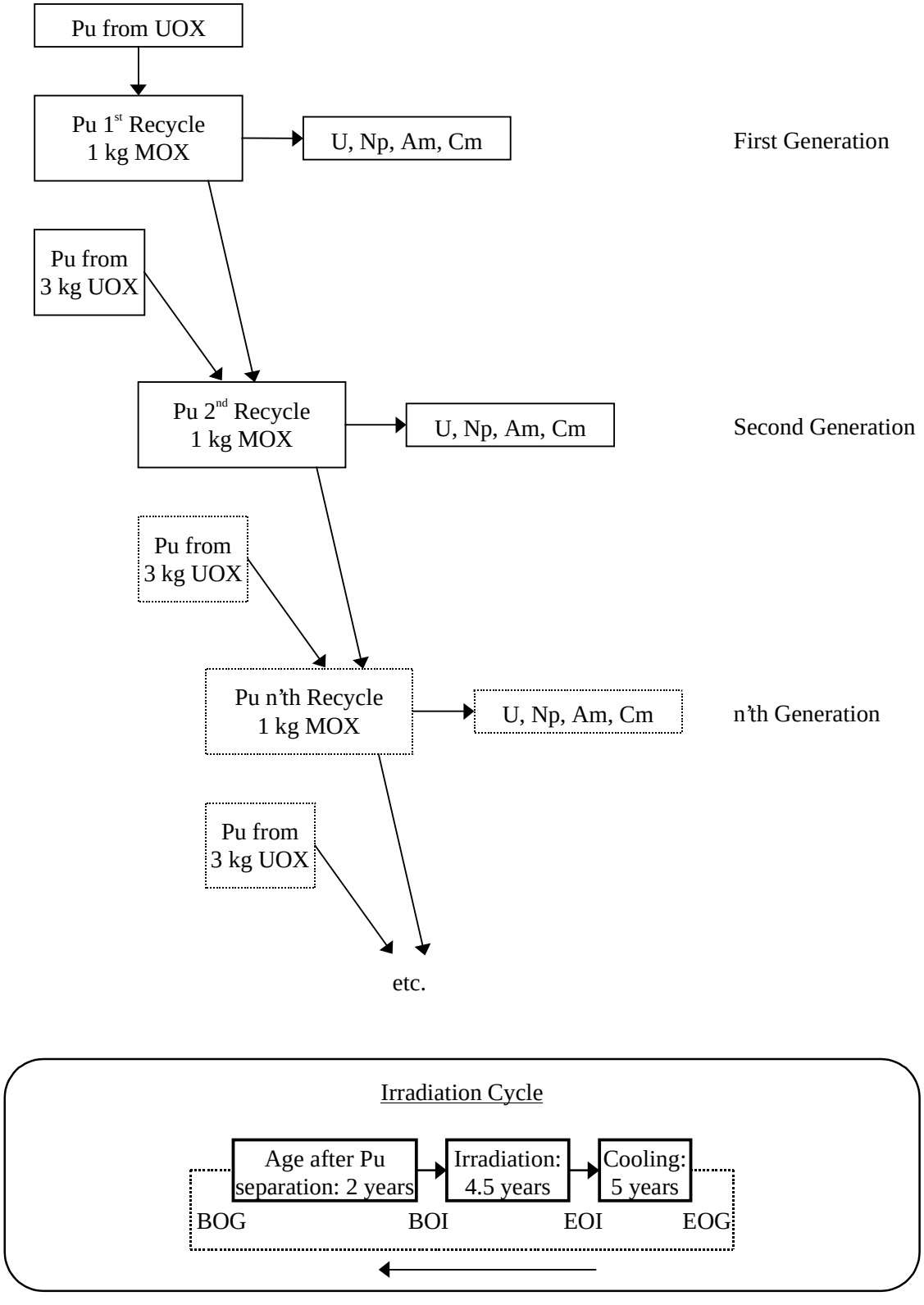

The second pincell was intended to represent a proposed assembly design for a highly moderated MOX fuelled PWR, with the designation HM pincell. This design has been proposed for a small family of future PWRs that would be wholly fuelled with MOX. In the conventional lattice assembly, the moderator/fuel ratio is too low to be optimal for plutonium fuel; a higher value of around 3.5:1 has been shown to be better suited for plutonium, as it is nearer the optimum for reactivity. In theory, a MOX fuelled reactor with a moderator/fuel ratio of 3.5 would need a lower plutonium concentration and would have better reactivity control and shutdown characteristics. The exclusive use of MOX assemblies would eliminate the boundary effects between UO_2 and MOX assemblies that necessitates multiple plutonium enrichments in a conventional MOX assembly.

The highly moderated design is most easily implemented by simply increasing the pin to pin pitch while retaining the pin design unmodified. This implies that the radial dimension of the core needs to be increased and with it the diameter of the pressure vessel. Other than this relatively minor change, the remainder of the plant would be based on existing, well proven components. Table 2.1 identifies where the HM assembly differs geometrically from the STD assembly.

Table 2.1. Main geometrical parameters of standard (STD) and highly moderated (HM) assemblies

	STD Pincell	HM Pincell
Lattice	17×17-25*	17×17-25*
Fuel pellet radius (cm)	0.4127	0.4127
Clad outer radius (cm)	0.4744	0.4744
Clad thickness (cm)	0.0617	0.0617
Pin to pin pitch (cm)		
Outer radius of equivalent pin-cell (cm)	0.7521	0.9062
Moderator/fuel ratio	2.0	3.5

* Guide thimbles (see Appendix A)

Material compositions

Table 2.2 summarises the material composition data which are common to the two pincells. For the three main components of fuel pellet, clad and moderator the following observations apply.

Pellet

The fuel pellet consists of UO_2/PuO_2 mixed oxide at a density of 10.02 g/cm^3. This corresponds to a nominal density of 95% of the theoretical density of 10.96 g/cm^3, with allowance for the loss of volume due to end-dimples and pellet chamfers. The fuel temperature, used to specify the Doppler broadening parameters, is representative of nominal full power operation.

Clad

For the purposes of the benchmark, the clad is assumed to be composed of natural zirconium. In reality, of course, Zircaloy is used, but the neglect of the minor alloying elements has no implications for the benchmarks. The temperature is again representative of full power operation.

Table 2.2. Material compositions common to STD and HM pincells

	STD & HM Pincells
MOX Fuel Pellet	
Density (g/cm^3)	10.02
Temperature (K)	900
Uranium carrier enrichment (w/o)	0.25
Clad	
Material	Zirconium
Density (g/cm^3)	6.55
Temperature (K)	600
Zr number density (b cm)	4.3248E-2
Moderator	
Material	H_2O + dissolved boron
Density (g/cm^3)	0.71395
Temperature (K)	573.16
Dissolved boron concentration (ppm)	500
H_2O Number density (barn cm)	2.386013E-2
B-10 Number density (barn cm)	3.92943E-6
B-11 Number density (barn cm)	1.59162E-5
	1 barn cm = 1E-24 cm^2

Moderator

The moderator is light water at a density of 0.71395 g/cm^3, representative of the average density in nominal full power operation. At the nominal working pressure of 155.5 Bars, this density corresponds with a moderator temperature of 306°C (579.16 K). However, the specification sets the temperature at precisely 300°C (573.16 K) so that MCNP data libraries can be used by participants wishing to contribute a Monte Carlo solution, this being one of the standard temperature tabulations. The difference in temperature has a small effect on the neutron spectrum that is of no significance for the benchmarks. The specification calls for the pincell depletions to be carried out with 500 ppm dissolved boron. This is roughly the lifetime average value in a modern PWR. It is important to carry out the depletion in this manner in order to correctly capture the average spectral history effect. However, certain calculations called for the boron to be set to zero, as discussed in the following section.

Fuel depletion

The fuel depletion specifications are the same for each generation of recycle. The underlying assumption is that the fuel management remains the same throughout all five generations of recycle considered. Of course, it is unlikely to be the case in practice, but it is necessary in order to define a manageable problem.

The fuel management is a three batch 18-month fuel cycle, with a discharge burn-up of 51 MWd/kg. Thus at each refuelling outage, the 1/3 of the fuel assemblies resident longest in the core

are discharged and replaced with fresh fuel. Such a fuel management scheme is a little outside present experience with both UO_2 and MOX, but is certainly realistic for a few years hence.

Table 2.3 summarises the fuel depletion parameters. The rating is at nominal full power for the reactor. The depletion to 51 MWd/kg, at constant 500 ppm boron, is followed by five years' pond cooling before reprocessing and recycle back into the next generation after a further two years. The pond cooling and recycle delays are important because of the decay of ^{241}Pu to ^{241}Am, and the consequent impact on the physics. The effect of refuelling shutdowns are neglected. Since each refuelling cycle lasts for 18 months, the complete fuel depletion lasts for 4.5 years and therefore the complete cycle from fresh fuel of one generation to fresh fuel of the next generation occupies 11.5 years.

Table 2.3. Fuel depletion parameters

	STD Pincell	HM Pincell
Ageing after fabrication and before irradiation (years)	2	2
Linear rating during irradiation (W/cm)	178	280
Mass rating (W/g of heavy metal)	37.7	59.3
Constant concentration of dissolved boron in moderator (ppm)	500	500
Cooling time after irradiation before reprocessing (years)	5	5

The linear and mass ratings for the STD pincell are the nominal full power values for the current 17×17 fuel assembly. Those for the HM pincell are a factor 1.57 higher than for the STD pincell. The design intent for the HM PWR would be to maintain the enthalpy rise in the moderator roughly in line with that of the STD PWR, otherwise the thermal hydraulic conditions of the primary system would be affected and thermal efficiency reduced. The enthalpy rise depends on the energy deposited by the fuel rods and the coolant flow rate. Optimisation between the coolant flow speed and the fuel linear heating allows to reach a moderation ratio of 4 in standard PWR (EPR) with a 19×19 lattice.

Multiple recycle logistics

This is the essence of these benchmarks and requires careful explanation. The benchmark calls for the plutonium to be followed through five recycle generations, as illustrated in Figure 2.2. Each recycle generation consists of a two-year ageing period from recovery of the plutonium from reprocessing to loading of MOX fuel in reactor. There then follows the irradiation of the fuel, which lasts 4.5 years and the subsequent five-year pond cooling period. The bottom part of Figure 2.2 is a schematic showing the three phases. The points denoted BOG, BOI, EOI and EOG stand for Beginning of Generation, Beginning of Irradiation, End of Irradiation and End of Generation.

The first generation simply involves taking the plutonium obtained from reprocessing a number of UOX assemblies and recycling it as MOX. The UOX assemblies, assumed to be discharged at 51 MWd/kg, contain 12.4 kg/tU total plutonium at discharge (where it is understood that the mass of uranium refers to the initial value). With the isotopic composition of this plutonium, the initial plutonium content of the first generation MOX needed to attain the 51 MWd/kg fuel cycle was determined by CEA to be 10.15 w/o or 101.5 kg/t HM). This value was taken to be the specification

for the first generation MOX assembly, with all participants expected to use the same value. The reasoning here was that since there was no expectation of major discrepancies in the first generation (which is already proven in commercial reactors), it would be better to specify the starting point in order to be able to have a reference point for comparison in the later generations.

In the second, third, fourth and fifth generations, the plutonium from the MOX assemblies was assumed to be recovered by co-reprocessing with conventional UOX assemblies in a ratio of 3 UOX: 1 MOX. There are two main reasons why this is appropriate:

1. It is not envisaged that reprocessing plants specifically dedicated to MOX will be built, so that the MOX assemblies would necessarily have to be reprocessed in plants primarily intended for reprocessing UOX. This being the case, there are technical reasons why it would not be practicable to recycle MOX assemblies on their own, or why it would be uneconomic to do so. These have to do with factors such as heat generation in the reprocessing liquors (which is higher in MOX) and activity level from minor actinides (also higher). Therefore, the only practical scenario is where UOX and MOX assemblies are reprocessed together, with a 3:1 ratio advised as being a technically sound value.

2. For the STD pincell at least, it is not intended to irradiate MOX assemblies alone in the core; there will also be UOX assemblies. Therefore a utility's spent fuel arisings will consists of a mix of the two types and it would make sense to reprocess them together. For the HM pincell, although the HM core will only consist of MOX assemblies, it is envisaged that the utility operating the HM PWR would have other conventional PWRs running on UOX only, or on UOX and mixed UOX/MOX. Indeed, this is practically a **requirement**, since otherwise the utility would have no source of plutonium to fuel its HM PWRs. Therefore, the utility's spent fuel arisings would still consist of a mix of UOX and MOX and co-reprocessing is the only sensible scenario.

Therefore in the second generation MOX and all later generations, the plutonium from each MOX assembly derives from a number of MOX assemblies and **three** times that number of UOX assemblies. Before discussing how many MOX and UOX assemblies are needed in the (n-1)'th generation to fuel the MOX in the n'th generation, two important points should be made:

1. The plutonium isotopic quality degrades during each MOX irradiation, as the non-fissile even isotopes accumulate. Therefore the role of the UOX assemblies can be seen as providing a measure of dilution of the plutonium, thereby helping to improve the isotopic quality.

2. The MOX assemblies contain at discharge upwards of 80 kg/t HM of plutonium, compared with just 12.4 kg/tU for the UOX assemblies. Therefore in terms of plutonium (rather than assembly masses or volumes), the dilution factor is much smaller than 3:1 and this means that the degradation of plutonium isotopic quality proceeds quickly in spite of the dilution.

The mass logistics from the (n-1)'th to the n'th generation depends on:

1. The initial plutonium content needed in the n'th generation MOX to provide the required 51 MWd/kg lifetime with the isotopic composition of the (n-1)'th generation plutonium.

2. The plutonium mass at discharge of the (n-1)'th generation MOX.

Suppose that the initial plutonium concentration of the n'th generation MOX is required to be p_i^n kg/t HM (how this is determined is explained in the following section). Suppose also that the

plutonium concentration at discharge of the (n-1)'th generation MOX is $p_d^{(n-1)}$ kg/t HM. Then assuming that the UOX plutonium content remains at 12.4 kg/tU, for each tonne of MOX discharged in the (n-1)'th generation there will be available ($p_d^{n-1} + 3 \times 12.4$) kg of plutonium. To fabricate one tonne of n'th generation MOX therefore requires $p_i^n / (p_d^{n-1} + 3 \times 12.4)$ tonnes of (n-1)'th generation MOX. In practice, this ratio is always greater than one, so that the number of tonnes of MOX in the n'th generation is less than that in the (n-1)'th. This is a result of the fact that $p_i^n > p_i^{n-1}$ always applies, because of the isotopic degradation. Also, $p_i^n > p_d^n$, because PWR MOX assemblies are incapable of breeding plutonium and the plutonium content at discharge must always be less than that loaded. These inequalities are such that in practice, the infusion of the 3×12.4 kg from the UOX assemblies is insufficient to keep the MOX mass from decreasing in each generation.

End of cycle reactivity

The concept of equivalent end of cycle reactivity is used to determine the initial plutonium content of a MOX assembly. A utility would usually wish a MOX assembly to substitute directly for a UOX assembly. Although there are occasionally exceptions, this normally means that the MOX assembly will contribute the same reactivity as a UOX assembly, when **averaged over its lifetime** in the core. MOX and UOX assemblies, having different reactivity characteristics (specifically, very different gradients of k-infinity with burn-up), cannot be matched for reactivity at more than one time in life. Equivalence in terms of end of cycle reactivity defines what time this should be:

Consider the three batch 18 month fuel cycle used in this benchmark. In the equilibrium fuel cycle, there will be 1/3-core of assemblies having been irradiated for one cycle, 1/3-core of two cycle assemblies and 1/3-core three cycle assemblies. Making the gross simplifications that the reactivity versus burn-up is linear and that the burn-up accumulated in each cycle is the same, the reactivity/burn-up relations of a UOX and a MOX assembly are as illustrated in Figure 2.3. Thus the first cycle regions will have accumulated a burn-up of 17 MWd/kg at the end of the cycle, the second cycle regions will be at 34 MWd/kg and the third cycle fuel at 51 MWd/kg.

The reactor will need to be refuelled when the average k-infinity of the three regions (i.e. the average of points A, B and C for the UOX assembly and a, b and c for the MOX assembly) is just sufficient to cover neutron leakage from the core. In a modern PWR, the leakage amounts to approximately 3.7 %Δk, so this implies the end of cycle occurring when the average k-infinity for the points (A, B, C) or (a,b,c) is 1.037.

Figure 2.3 has been contrived so that Points B and b are precisely at 1.037. In this case, the UOX and MOX assemblies would contribute equally to the core's lifetime reactivity and there would be no loss or gain in equilibrium cycle length if a MOX assembly was substituted for a UOX assembly. Although Figure 2.3 is idealised, it captures the concept perfectly. Note that the reactivity of the fuel at zero burn-up does not figure in the calculation, so that the effect of burnable poisons does not affect the lifetime reactivity provided the poison material is substantially used up by Point A or a.

For the present benchmark, the initial plutonium content needed at the start of each MOX generation was defined by requiring k-infinity to be 1.037 at 34 MWd/kg exposure, corresponding to Point b in Figure 2.3. Since the end of the cycle is defined as the point at which the dissolved boron concentration reduces to near zero, it is clear that k-infinity at Point b should be calculated with zero

Figure 2.3. Schematic of reactivity vs. burn-up for UOX and MOX

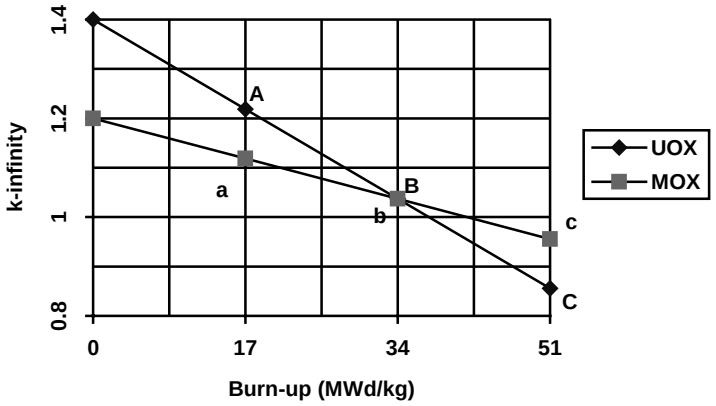

boron. However, it would be incorrect to assume zero boron applies throughout the depletion, since this would introduce a significant error from the incorrect spectral history this implies. A more realistic spectral history can be obtained with the lifetime average boron concentration in the depletion calculations and in this case a nominal value of 500 ppm was applied. The need to calculate Point b at zero ppm still applies, however, and this implies a branch calculation to zero ppm at 34 MWd/kg.

Thus lifetime reactivity equivalence amounts in this case to adjusting the initial plutonium content so that k-infinity for the MOX assembly, at zero ppm, 34 MWd/kg is precisely 1.037.

Plutonium isotopics and concentrations

The benchmark specification called for each participant to start off the first MOX generation with a given total plutonium content (10.15 w/o) and isotopic composition of the plutonium, as shown in Table 2.1. These data were calculated by CEA using the APOLLO code. As first formulated, each participant was then to deplete the MOX assembly to 51 MWd/kg, age for seven years and then recycle the as-calculated plutonium isotopics as detailed in the section entitled *Multiple recycle logistics*. However, it was felt that this might complicate comparisons between different solutions if carried out in isolation, since there is scope for both the reactivity determination and the plutonium isotopic calculation to deviate. Accordingly, it was agreed early on that the multiple recycle strategy would be carried out in two separate stages In the first stage, the isotopic number densities are imposed and in the second they are individually calculated by participants.

- ***Stage I***
  In Stage I the APOLLO code was used as a reference for all other participants, in that the plutonium concentrations and plutonium isotopics calculated by APOLLO were to be treated as given and used as inputs at the start of all five generations of MOX. Table 2.4 lists all the given data. APOLLO was chosen as the reference only because the APOLLO calculations were available prior to other submissions and does not necessarily imply that it is any better than any other code. Indeed, for the purposes of this benchmark, any of the solutions submitted would have served. Carrying out this intermediate step provides a reference point for comparing the reactivity calculations without the complications of having different plutonium contents at the start of each irradiation.

Table 2.4. Initial plutonium (total) contents and plutonium isotopics as calculated with APOLLO

STD PWR

Generation	1	2	3	4	5
Total Pu content (w/o)	10.15	13.625	15.981	17.779	19.228
^{238}Pu (%)	4.0000	4.8260	5.2880	5.5389	5.6633
^{239}Pu (%)	50.4000	42.6180	39.1890	37.1235	35.6755
^{240}Pu (%)	23.0000	26.9270	28.2750	28.9289	29.2940
^{241}Pu(%)	13.5000	13.4140	12.8570	12.3085	11.8480
^{242}Pu (%)	9.1000	12.2150	14.3910	16.1003	17.5181
^{235}U (%)	0.2500	0.2500	0.2500	0.2500	0.2500
^{238}U (%)	99.7500	99.7500	99.7500	99.7500	99.7500

HM PWR

Generation	1	2	3	4	5
Total Pu content (w/o)	6.703	9.636	12.107	14.374	16.583
^{238}Pu (%)	4.0000	4.6484	4.9674	5.1382	5.2151
^{239}Pu (%)	50.4000	36.9325	31.5575	28.5209	26.4344
^{240}Pu (%)	23.0000	29.0647	29.6867	29.3443	28.7947
^{241}Pu (%)	13.5000	13.0907	12.7012	12.1591	11.6091
^{242}Pu (%)	9.1000	16.2637	21.0871	24.8376	27.9467
^{235}U (%)	0.2500	0.2500	0.2500	0.2500	0.2500
^{238}U (%)	99.7500	99.7500	99.7500	99.7500	99.7500

- ***Stage II***
  Stage II called for each participant to submit a set of solutions in which both the initial plutonium content and the plutonium isotopic vector was calculated by each participant independently. In this case, differences in calculating the end of cycle reactivity and the evolution of plutonium isotopics would have the opportunity to accumulate between each generation, providing a test of the relative performances of the complete code systems.

The Stage I Benchmark called for the participants to report:

1. k-infinity versus burn-up at 500 ppm boron, for each of the five MOX generations.

2. k-infinity at 34 MWd/kg, zero boron, for the five generations.

3. Number densities of specified uranium, plutonium, minor actinides and selected fission products at the BOG, BOI, EOI and EOG conditions previously discussed in the section *Multiple recycle logistics*.

4. Net changes in the masses of uranium, plutonium, minor actinides and selected fission products at BOG, BOI, EOI and EOG, in kg/tHM. Also isotopic compositions of same in per cent.

5. Microscopic cross-sections of uranium, plutonium, and minor actinides at 0, 8.5, 17, 25.5, 34, 42.5 and 51 MWd/kg during the irradiation of each generation.

6. Selected macroscopic cross-section at 0 and 51 MWd/kg burn-up (BOI and EOI).

7. Fission energy release for the fissioning nuclides.

8. Delayed neutron fraction (β-eff) data at 51 MWd/kg (EOI).

9. Reactivity balance with constant 500 ppm dissolved boron, being the reactivity difference between the 0.5 and 51 MWd/kg irradiation steps [k(0.5)-k(51)]/50.5, in units of 10^{-5}.

These data were requested largely in order to assist with identifying the reasons for any discrepancies that might have arisen between different participants. In Phase II, the participants were asked to report all of the above and the following additional results:

10. The mass of fuel at BOG, BOI, EOI, and EOG.

11. The isotopic composition of the fuel at BOG, BOI, EOI and EOG.

12. The global activity of the fuel at BOG and EOG for decay timescales from five years to one million years.

13. Radiotoxicities at BOG and EOG for decay timescales between five years and one million years using given half-lives and radiotoxity factors.

These additional data in Stage II largely relate to the question of the long term activity and radiotoxicity, of interest in order to see whether there is significant divergence in predictions of the environmental implications.

Reactivity coefficients

In addition to the calculations just described, the benchmark specification called for reactivity coefficients to be calculated in each generation at irradiations of 0.5, 17, 34 and 51 MWd/kg. Being able to calculate reactivity coefficients with confidence is essential if multiple recycle is to be realised. It is likely that if any limitation to multiple recycle are identified, it will be the reactivity coefficients which will be the determining factors.

The reactivity coefficients examined were the following:

1. Boron efficiency, calculated by perturbing the dissolved boron concentration from 500 to 600 ppm and reporting the boron reactivity coefficient [1/k(500)-1/k(600)]/100, in units of 10^{-5}/ppm. The boron coefficient is important for reactivity balance during normal operation and for emergency shutdown in a PWR.

2. Moderator temperature coefficient calculated by perturbing the moderator temperature and densities between hot and cold states, accordance with the given steam tables (cold state 569.16 K, water density 2.456146E-2 molecules/barn cm, hot state 589.16 K, water density 2.307541E-2 molecules/barn cm). The moderator temperature coefficient is defined as [1/k(cold)-1/k(hot)]/20, in units of 10^{-5}/K.

3. Fuel temperature coefficient calculated by perturbing fuel temperature between 890 and 910 K. The definition of fuel temperature coefficient is [1/k(cold)-1/k(hot)]/20, in units of 10^{-5}/K .

4. Global void effect calculated by changing the moderator density from 100% to 1% of nominal density and defined as [1/k(unvoided)-1/k(voided]/100, in units of 10^{-5}, with given values of moderator density in the unvoided and voided conditions. The calculation is carried out both with a no leakage spectrum and with a critical leakage spectrum in which the buckling parameter has been adjusted to ensure k-eff = 1.

Chapter 3

PARTICIPANTS AND METHODS

Twenty solutions from 10 countries were sent for the benchmark. The main characteristics of method and data used are described in the following table:

		Code	Flux calculation	Self-shielding	Library	HN chain FP chain
1.*	ANL	WIMS-D4M	Monte Carlo		ENDF/B.V, 32 gr. (0-10 MeV)	$^{233}U \rightarrow ^{241}Am$
2.*		CASMO 3		σ_{equi} from 4 eV to 9 kev	ENDF/B.IV, 23 gr. (0-10 MeV)	$^{234}U \rightarrow ^{244}Cm$
3.	Belgonucléaire	WIMS 6	Pij		JEF 2, 172 gr. (0-20 MeV)	
4.	BNFL	WIMS	Pij	sub-group applied to ^{235}U, ^{238}U, ^{239}P and ^{240}P	JEF 2 (0-20 MeV)	$^{233}U \rightarrow ^{245}Cm$
5.	CEA	APOLLO 2	Pij	σ_{equi} + sub-group for E > 0.1 eV	JEF 2, 172 gr. (0-20 MeV)	$^{234}U \rightarrow ^{247}Cm$
6.	ECN	Code system: OCTOPUS	Transport P_3S_g and Monte Carlo	Bondarenko: unresolved region + Nordheim: resolved energy region	JEF 2	Pseudo F.P. for flux ORIGEN-S updated library for depletion
7.	EDF	APOLLO 1	Pij	σ_{equi} for E > 2.6 eV	JEF 1 (0-10 MeV) + ENDF/B.IV, 99 gr.	$^{234}U \rightarrow ^{245}Cm$ 89 F.P.
8.	GRS	Code system: OREST-96			ENDF/B.V	
9.**	IFRR	SPEKTRA			JEF 2	
10.	IKE	RESMOD, RSYST 3, ORIGEN-2	Pij	Self and mutual shielding, 13000 gr. from 3 eV to 1 keV	JEF 2	$^{234}U \rightarrow ^{245}Cm$ 41 HN, 222 F.P.
11.**	IPPE	WIMS (ABBN)			POND-2, 66 gr.	
12.	JAERI	SRAC-95	Pij	Self and mutual shielding below 1 keV	JENDL 3.2	$^{230}Th \rightarrow ^{246}Cm$ 65 F.P.
13.	KAERI	HELIOS	Pij	Subgroups applied to 31 isotopes	ENDF/B.VI, 89 gr.	$^{230}Th \rightarrow ^{246}Cm$ 114 F.P.
14.*		CASMO 3	Pij	σ_{equi} from 4 eV to 9 keV	ENDF/B.VI, 70 gr.	$^{234}U \rightarrow ^{244}Cm$
15.	NAGOYA Univ.	SRAC	Pij	Self and mutual shielding below 130 eV	JENDL 3.1, 107 gr.	$^{233}U \rightarrow ^{245}Cm$ 65 F.P.
16.	PSI	BOXER	Pij	8000 points for 1.3 eV to 907 eV equi, th; for E > 907 eV	JEF 1, 70 gr.	$^{230}Th \rightarrow ^{248}Cm$ 55 F.P., 2 P.F.P
17.	OSAKA Univ.	RESPLA/CP	Pij	Self and mutual shielding below 130 eV	JENDL 3.1	$^{233}U \rightarrow ^{245}Cm$ 65 F.P.
18.		RESPLA/DC				
19.	TOHOKU Univ.	SRAC, ORIGEN 2	Pij	Self and mutural shielding below 1 keV	JENDL 3.2	ORIGEN-2
20.*	RISØ	CCMO-U			ENDF/B.VI, 76 gr.	

* Withdrawn ** Incomplete

Not all participants strictly complied with the benchmark specifications. The two stages of this benchmark imply a large effort, thus, some participants only presented solutions for Stage I. Nevertheless, the majority provided solutions for both stages. Solutions 1, 2, 14 and 20 were withdrawn because the methods used were not considered appropriate for this study.

A large number of solutions is based on flux calculations using the collision probability method, connected to an evolution module or code including more or less isotopes (heavy nuclides and fission products). These codes or systems provide a means of calculating reactivity evolution during depletion.

The main differences stem from the different data and methods used, particularly:

- the data libraries: JENDL, ENDF, JEF;
- the depletion chains: heavy nuclides and fission products;
- the self-shielding methods:
  - equivalent method;
  - sub-group method;
  - ultra-fine group method;
  - Monte Carlo;
- the fission yield and the energy per fission or per reaction.

Based on experience gained from the previous Phase I benchmark, the options used are relatively homogenous:

- the resonance self-shielding is applied to the main plutonium isotopes;
- the chains range from at least ^{234}U to ^{244}Cm.

This shows that there is a common understanding of the physics of plutonium in PWRs and thermal spectrum.

Most of the schemes are similar to those described in Volume II of the *Physics of Plutonium Recycling* series, entitled *Plutonium Recycling in Pressurised Water Reactors*.

Chapter 4

PRESENTATION OF RESULTS

Introduction

This chapter presents a summary of the principal results of the benchmark exercises. This is necessarily incomplete due to the enormous volume of data involved. For the sake of clarity, the Stage I and Stage II exercises are presented in turn and separate discussion provided for each. For Stage I, the results are compared with the APOLLO 2 results regarded as a reference. As discussed earlier, this is purely for convenience and does not imply any special status for APOLLO 2 and serves to highlight the relative spread of results. The Stage II exercise is considered the more fundamental, as the solutions represent what each individual contributor would predict for the evolution of the multi-recycle scenario.

The results presented for Stage I mainly comprise microscopic cross-sections and reactivity balance. Since the initial isotopic content is prescribed at the start of each recycle generation, the reactivity differences can be assumed to be primarily due to:

- data differences (in the nuclear data libraries);
- flux calculations (spectrum);
- self-shielding effects affecting the calculation of resonance absorptions;

Thus, the analysis of the results for Stage I is mainly concentrated on the spreads in microscopic cross-sections and reactivities. For the reactivities, three parameters are linked:

- the initial reactivity value;
- the reactivity balance under irradiation, meaning the change in reactivity with burn-up;
- the end of cycle reactivity value, as defined in Chapter 2.

To analyse all the amount of results, we divide the problem into two distinct parts:

- *Initial reactivity values ⇔ Microscopic cross-sections value*, keeping in mind that ^{239}Pu is the main contributor for fission (75%) and for capture (50%) in the neutronic balance. JAERI performed a comparison on ^{239}Pu source, JEF2, JENDL3 or ENDF/B.VI which shows the impact of data file evaluation and data treatments.
- *Reactivity balance under irradiation ⇔ Microscopic cross-sections value and fission rate*.

The reactivity adjustment value is a combination of the two effects, initial reactivity level and reactivity balance under irradiation.

The analysis of Stage II is mainly focused on the major physical parameters for plutonium recycling in the multiple recycle scenario such as initial plutonium content, reactivity coefficient values and minor actinide production.

Some helpful reference points are given by a Monte Carlo calculation using TRIPOLI 4 and JEF2 (CEA) for initial reactivity values and some reactivity values obtained for the reactivity coefficients conditions.

Standard PWR – Stage I Benchmark

This section presents the results of the benchmark for the standard (STD) PWR, with a moderation ratio of 2 (Vm/Vf) or 4.26 ($n_H/n_{H.N.}$), where n_H is the number density of hydrogen and $n_{H.N.}$ that of the heavy nuclides, with the initial fuel composition at the start of each recycle generation prescribed.

Microscopic cross-sections spreads: ^{238}U, ^{239}Pu, ^{240}Pu, ^{241}Pu, ^{242}Pu

The comparison of microscopic fission and capture cross-sections is shown in Figures 4.1 to 4.7 for all the plutonium isotopes, up to ^{242}Pu. ^{242}Pu becomes increasingly important in the later recycle generations as its concentration increases. The comparison is shown for only the first recycle generation; subsequent recycle generations shows qualitatively similar results.

The spread of values on the microscopic fission cross-sections is about ±2% for ^{239}Pu and -5% to +4% for ^{241}Pu.

The spreads are about ±2% for the microscopic capture cross-section of the main isotopes: ^{239}Pu and ^{238}U. For the latter, the trends with irradiation are rather different, one group which shows a decreasing cross-section trend with burn-up and second one (EDF, ECN, JAERI, PSI, TOHOKU, OSAKA) which has an increasing cross-section tendency with burn-up compared with the CEA.

For higher isotopes, the spreads are larger:

- from -0% to +6% for ^{240}Pu;
- from -4% to +4% for ^{241}Pu;
- from -6% to +2% for ^{242}Pu.

Figure 4.1. STD PWR – Stage I – First recycle:
^{239}Pu fission cross-section – Comparison with CEA values

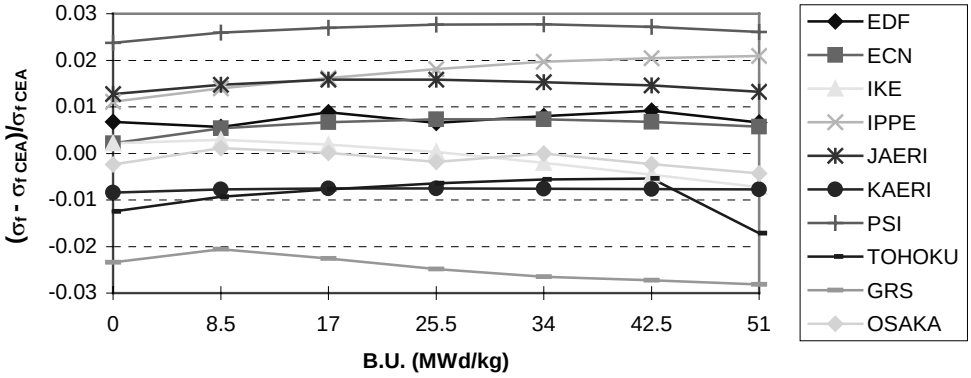

CEA values							
B.U (MWd/kg)	0	8.5	17	25.5	34	42.5	51
σ_f ^{239}Pu (barn)	21.85	22.08	22.90	23.84	24.90	26.06	27.32

Figure 4.2. STD PWR – Stage I – First recycle:
^{241}Pu fission cross-section – Comparison with CEA values

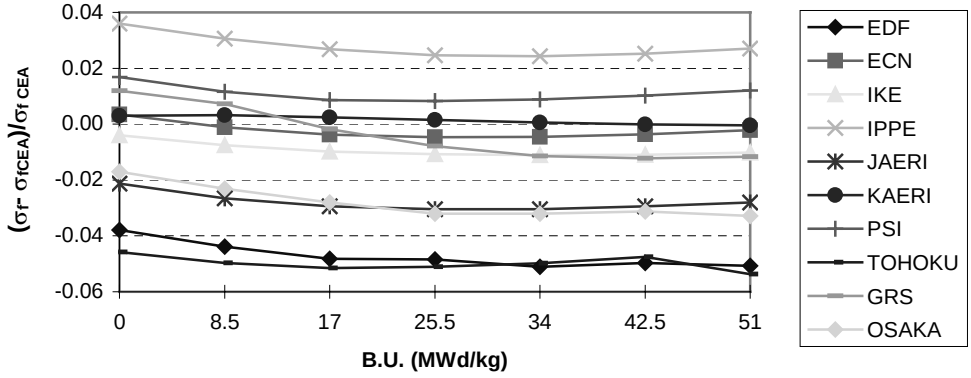

CEA values							
B.U (MWd/kg)	0	8.5	17	25.5	34	42.5	51
σ_f ^{241}Pu (barn)	28.89	28.97	29.73	30.58	31.51	32.52	33.60

Figure 4.3. STD PWR – Stage I – First recycle:
^{238}U capture cross-section – Comparison with CEA values

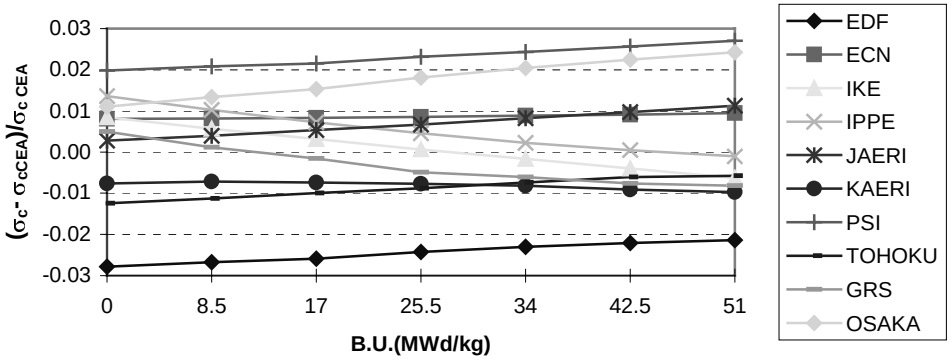

CEA values							
B.U MWd/kg	0	8.5	17	25.5	34	42.5	51
σ_c ^{238}U (barn)	0.82	0.82	0.82	0.83	0.83	0.83	0.83

Figure 4.4. STD PWR – Stage I – First recycle:
^{239}Pu capture cross-section – Comparison with CEA values

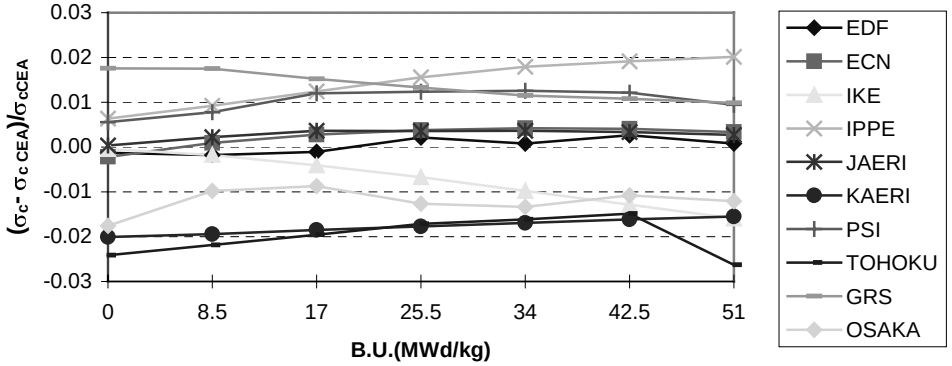

CEA values							
B.U (MWd/kg)	0	8.5	17	25.5	34	42.5	51
σ_c ^{239}Pu (barn)	12.22	12.42	12.91	13.47	14.09	14.76	15.49

Figure 4.5. STD PWR – Stage I – First recycle:
^{240}Pu capture cross-section – Comparison with CEA values

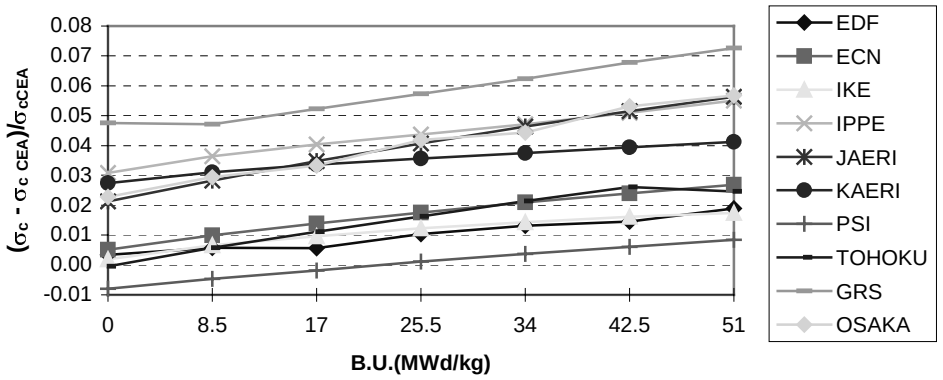

CEA values							
B.U MWd/kg	0	8.5	17	25.5	34	42.5	51
σ_c ^{240}Pu (barn)	25.81	25.35	25.26	25.34	25.57	25.92	26.40

Figure 4.6. STD PWR – Stage I – First recycle:
^{241}Pu capture cross-section – Comparison with CEA values

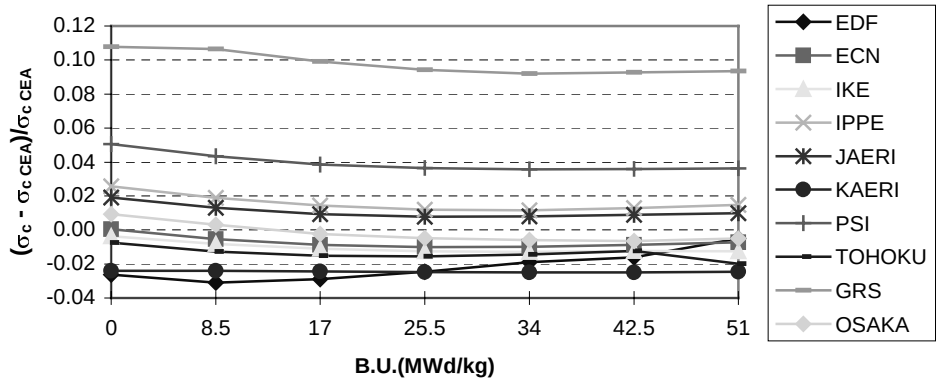

CEA values							
B.U (MWd/kg)	0	8.5	17	25.5	34	42.5	51
σ_c ^{241}Pu (barn)	9.03	9.09	9.37	9.68	10.01	10.37	10.75

Figure 4.7. STD PWR – Stage I – First recycle:
^{242}Pu capture cross-section – Comparison with CEA values

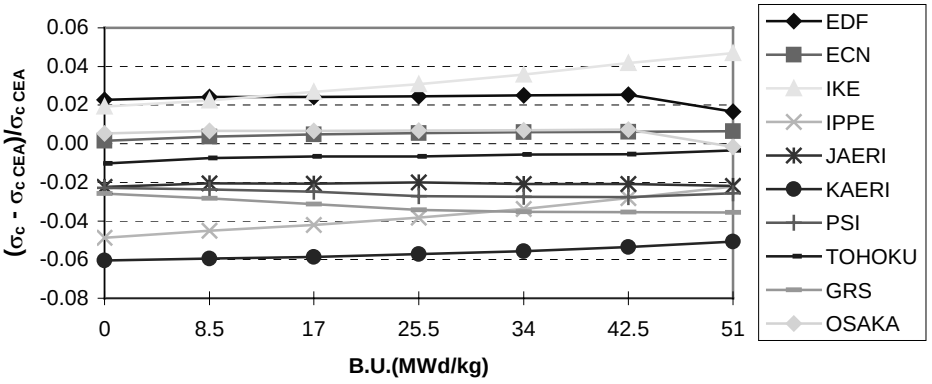

CEA values							
B.U MWd/kg	0	8.5	17	25.5	34	42.5	51
σ_c ^{242}Pu (barn)	11.54	11.42	11.33	11.22	11.12	11.02	10.92

On the microscopic (n,2n) cross-sections

Figures 4.8 and 4.9 show the microscopic (n,2n) cross-sections for ^{238}U and ^{244}Cm. The order of magnitude of the cross-sections for this reaction type in the neutronic balance is small, but it is of interest to show these two for illustration. The differences are large, even between for data based on the same evaluated data file and are largely due to the nuclear data, but there are also contributions from the different treatments of this reaction in each code, at high energy.

Figure 4.8. STD PWR – Stage I – Recycle:
^{238}U (n,2n) cross-section – Comparison with CEA values

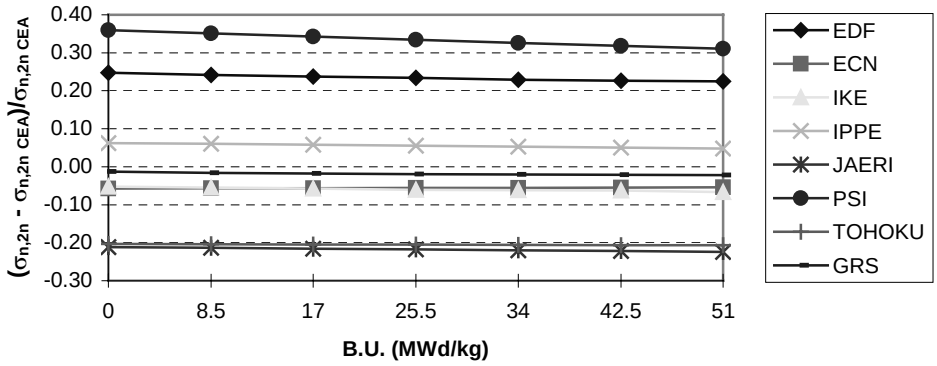

CEA values							
B.U (MWd/kg)	0	8.5	17	25.5	34	42.5	51
$\sigma_{n,2n}$ ^{238}U (barn)	5.72E-03	5.74E-03	5.75E-03	5.76E-03	5.77E-03	5.77E-03	5.78E-03

Figure 4.9. STD PWR – Stage I – First recycle:
^{244}Cm (n,2n) cross-section – Comparison with CEA values

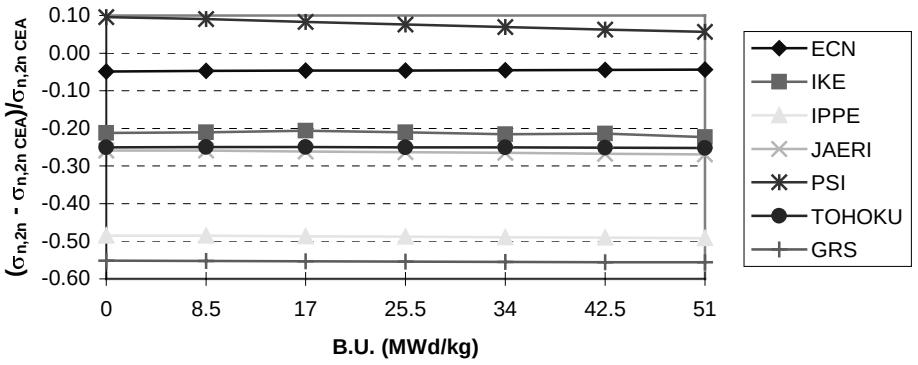

CEA values							
B.U (MWd/kg)	0	8.5	17	25.5	34	42.5	51
$\sigma_{n,2n}$ ^{244}Cm (barn)	2.19E-03	2.19E-03	2.20E-03	2.20E-03	2.20E-03	2.20E-03	2.21E-03

On the ν *values*

The differences are small for this parameter (the mean number of neutrons per fission). Figure 4.10 shows the comparison of ν values for the main contributing isotope, ^{239}Pu:

Figure 4.10. STD PWR – Stage I – First recycle:
^{239}Pu ν values

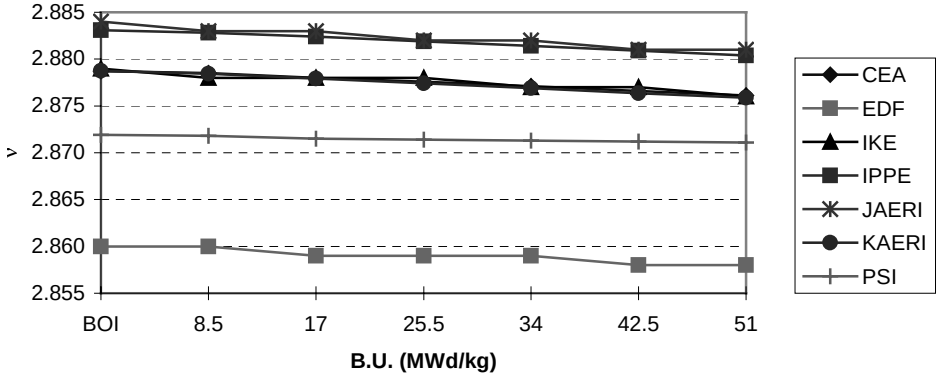

On the fission capture ratio cross-sections

Apart from the GRS values, all of the participants show positive differences between 0 to 2% (Figure 4.11). This implies that the main isotope for the reactivity balance is more fissile and therefore the reactivity value must be larger than CEA for the majority of participants.

For ^{241}Pu, the differences are larger in a range of +2% to -4%.

Figure 4.11. STD PWR – Stage I – First recycle:
^{239}Pu ratio fission/capture – Comparison with CEA values

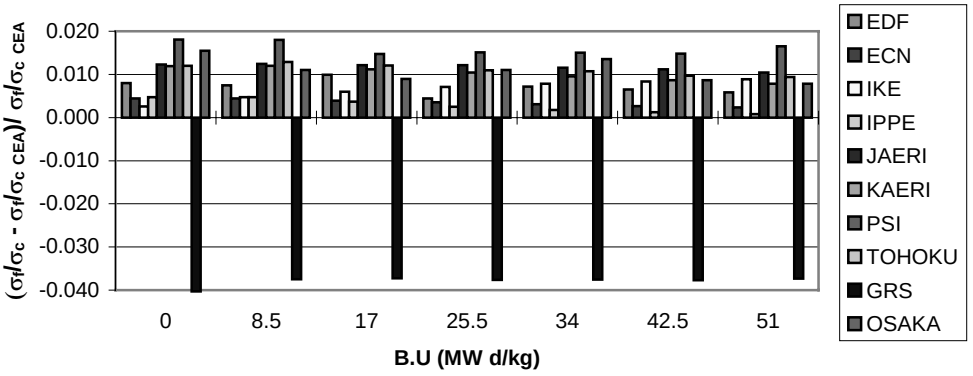

CEA values							
B.U (MWd/kg)	0	8.5	17	25.5	34	42.5	51
σ_f/σ_c ^{239}Pu	1.789	1.777	1.773	1.770	1.767	1.766	1.764

Microscopic differences as per evaluated data file

When the microscopic cross-sections are grouped together by nuclear data library, as in Figures 4.12 and 4.13, more consistent results are observed, as would be expected. The comparison is again with the CEA results, based on JEF:

Figure 4.12. STD PWR – Stage I – First recycle:
^{239}Pu ratio fission/capture – Comparison with CEA values – JENDL library

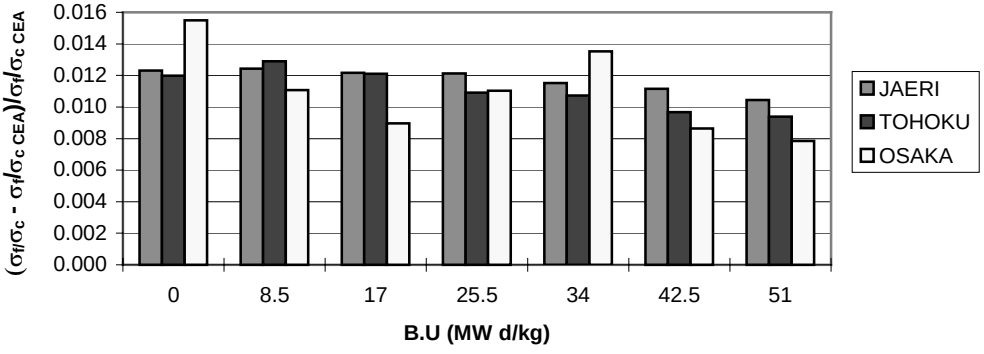

Figure 4.13. STD PWR – Stage I – First recycle:
^{239}Pu ratio fission/capture – Comparison with CEA values – JEF library

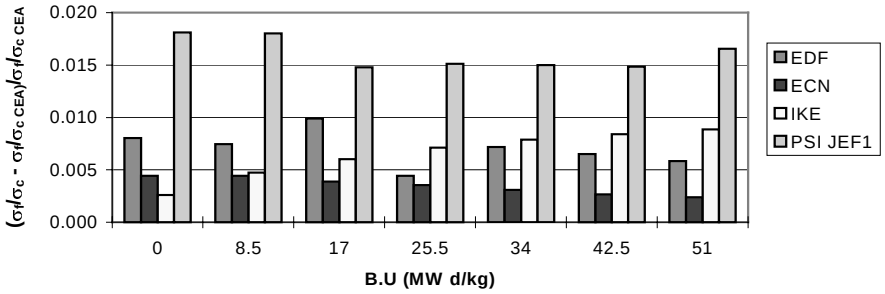

Spread in reactivities

For reactivity and the other major nuclear design parameters, representative results are presented. Although in some cases the results are presented for all five recycle generations, in most cases only the first and fifth generations are shown where there is no exceptional behaviour in the intermediate ones. Thus Figures 4.14 and 4.15 show the comparisons of reactivities versus cell irradiation for the first and fifth recycle generations, compared with CEA values as a reference:

Figure 4.14. STD PWR – Stage I – First recycle:
Reactivity swing – Comparison with CEA values

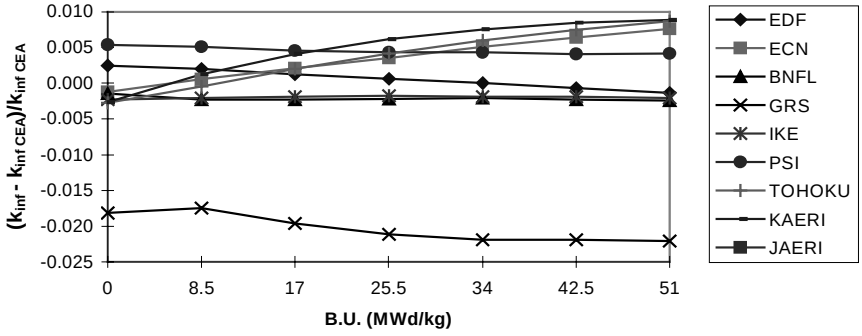

Figure 4.15. STD PWR – Stage I – Fifth recycle:
Reactivity swing – Comparison with CEA values

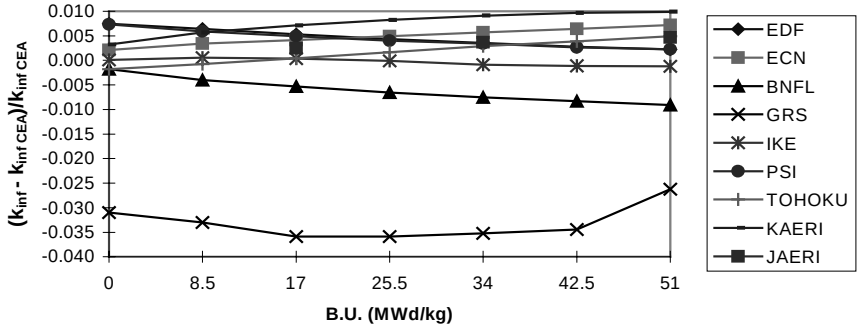

Disregarding the anomalous GRS results, two distinct trends are seen in respect of the reactivity variation with cell irradiation:

1. one in which reactivity decreases less rapidly with burn-up than CEA (KAERI, TOHOKU, ECN);

2. one for which reactivity decreases as per the CEA case.

The figure for the first recycle generation above is the reference case for setting the end-of-cycle reactivity for which we observe two groups of solutions:

1. BNFL, CEA, EDF, IKE, IPPE (smaller than 1.04);

2. ECN, JAERI, OSAKA, PSI, TOHOKU (larger than 1.04).

The differences observed do not increase during later recycle generations; all the results fall within a range of 1% in reactivity. This is small compared with the reduction in reactivity with irradiation, which is about 20% in the first recycle generation and 13% for the fifth generation.

Reactivity balance under irradiation

The value of the reactivity balance, being the change in reactivity with burn-up, is about 0.4% per MWd/kg for the first recycle generation and 0.25% per MWd/kg for the fifth generation as shown in Figure 4.16:

Figure 4.16. STD PWR – Stage I:
Reactivity balance – Comparison with CEA values

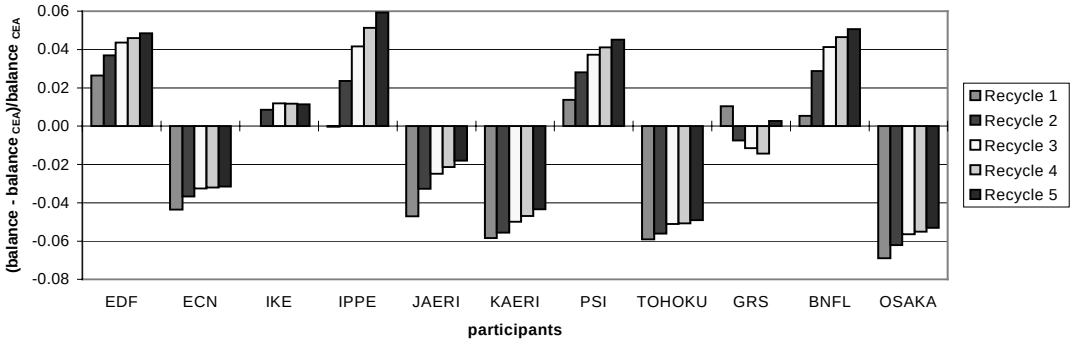

CEA values					
	Recycle 1	Recycle 2	Recycle 3	Recycle 4	Recycle 5
Reactivity balance	363	306	284	272	264

The reactivity balance under irradiation is linked to the fission rate, the cross-section data and the isotopic evolution chain. For most of the participants, the trend compared with CEA is for the reactivity balance to increase with increasing recycle generation, so that those cases starting out more positive than CEA initially become more positive still, while those starting out more negative than CEA become less negative.

Figure 4.17 shows the spread in the reactivity adjustment values, these being the end-of-cycle k-infinities calculated by each participant with the given initial plutonium isotopics and concentrations. Again, the CEA values are regarded as the reference. If there was complete agreement, all participants would return the value 1.037. Table 4.1 lists the k-infinities by participant and recycle generation.

Disregarding the anomalous GRS results, the largest change between first and fifth recycle generation is about 0.55% (BNFL). The spread between participants increases with recycle generation from 0.9% in reactivity up to 1.4% at the fifth recycle. Table 4.2 lists the minimum and maximum values of end-of-cycle k-infinity and the largest differences obtained.

Figure 4.17. STD PWR – Stage I:
Reactivity value adjustment – Comparison with CEA values

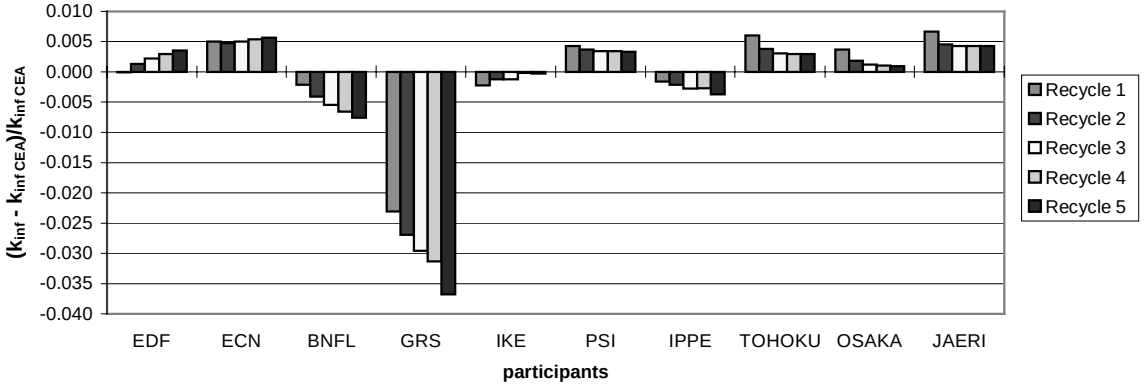

Table 4.1. End-of-cycle k-infinities by participant and recycle generation

	Recycle 1	Recycle 2	Recycle 3	Recycle 4	Recycle 5
CEA	1.03726	1.03726	1.03727	1.03723	1.03728
EDF	1.03720	1.03856	1.03955	1.04031	1.04089
ECN	1.04247	1.04219	1.04247	1.04279	1.04310
BNFL	1.03509	1.03303	1.03162	1.03045	1.02945
GRS	1.01338	1.00934	1.00666	1.00480	0.99919
IKE	1.03500	1.03600	1.03600	1.03700	1.03700
PSI	1.04169	1.04106	1.04086	1.04076	1.04073
IPPE	1.03566	1.03506	1.03435	1.03443	1.03348
TOHOKU	1.04354	1.04124	1.04045	1.04033	1.04031
OSAKA	1.04112	1.03922	1.03856	1.03832	1.03821
JAERI	1.04417	1.04199	1.04168	1.04163	1.04168

Table 4.2. End-of-cycle k-infinities – Extreme values

	Recycle 1	Recycle 2	Recycle 3	Recycle 4	Recycle 5
Min.	1.035	1.033028	1.031616	1.030452	1.02945
Max.	1.044166	1.04219	1.04247	1.04279	1.0431
Largest difference	0.009166	0.009162	0.010854	0.012338	0.01365

Spread in fission rates

Figure 4.18 shows the spread in fission rates calculated by the various participants.

Figure 4.18. STD PWR – Stage I – Fission rate differences (in %)

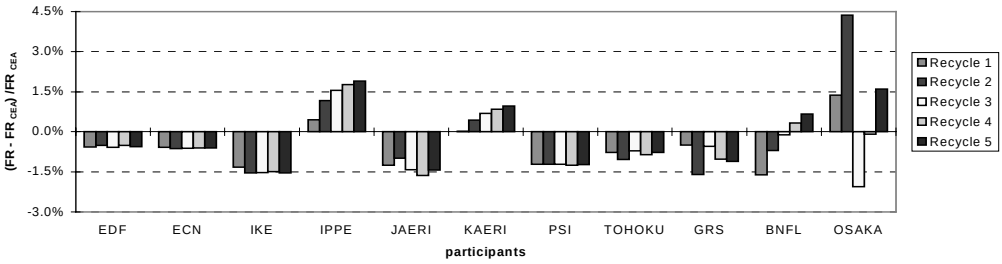

CEA values					
	Recycle 1	Recycle 2	Recycle 3	Recycle 4	Recycle 5
Fission rate (fraction)	0.05215	0.05215	0.05215	0.05217	0.05218

The differences are almost constant for the majority of the participants and fall within a range of 1.5% (EDF, ECN, IKE, PSI), although three participants show an increasing trend with recycle generation. 1% in fission ratio is equivalent to 0.5 MWd/kg, and thus, to 0.2% in reactivity for the first recycle generation and 0.15% for the fifth recycle generation. These differences are therefore insufficient to explain the discrepancies seen in the reactivity balance.

Spread in reaction rates

From the relatively small number of participants who provided reaction rates for comparison, the spread of results (illustrated in Figure 4.19 for the first recycle generation) is quite small and it is difficult to spot any underlying trends. Both absorption and production terms increase from the first recycle generation through to the fifth generation, due to the increasing plutonium content.

These results give us the order of magnitude between the different reactions in the different materials at the end of the life of the fuel (51 MWd/kgHM) for cycles one and five. The values are in a similar range.

Figure 4.19. STD PWR – Stage I – Reaction rates

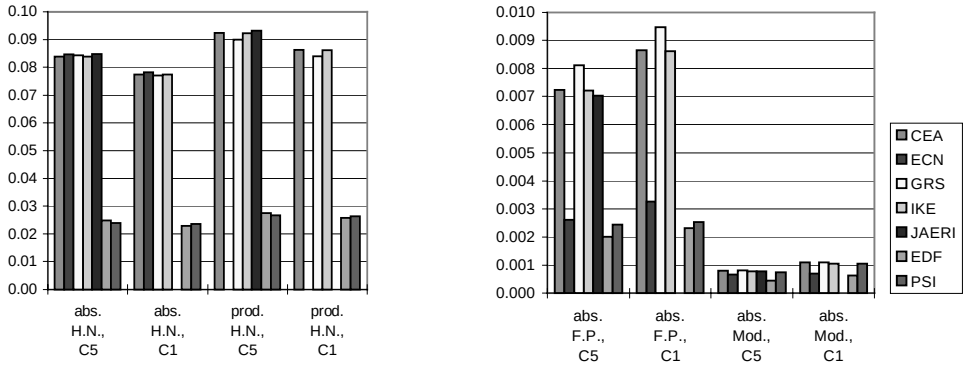

* *Production = ν fission*

Reactivity coefficients

The boron, moderator temperature and fuel temperature coefficients are important feedback parameters which normally have negative values. For convenience, the absolute values of these coefficients are plotted in this section. All three coefficients are actually negative.

The boron reactivity coefficients calculated by the various participants are generally in very good agreement, and show very similar trends as a function of cell burn-up. They are illustrated below in Figures 4.20 and 4.21 for the first and fifth recycle generation cases, plotted versus cell irradiation. Given that in Stage I the initial compositions are given, the 0.5 MWd/kg burn-up steps should be virtually identical in each case, as the reactivity and spectral effects of boron are well defined. Yet the JAERI and GRS solutions stand out as having a lower absolute value, particularly in the fifth recycle generation, implying differences arising from the solution method.

Figure 4.20. STD PWR – Stage I – First recycle: Boron efficiency

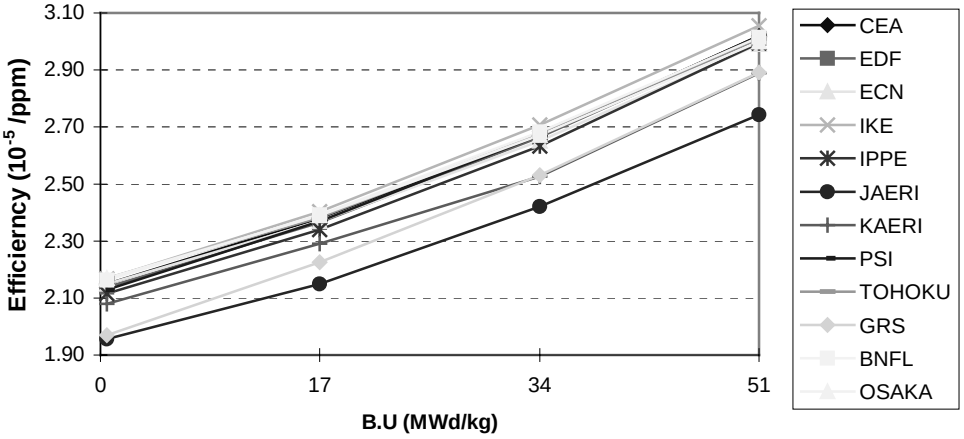

Figure 4.21. STD PWR – Stage I – Fifth recycle: Boron efficiency

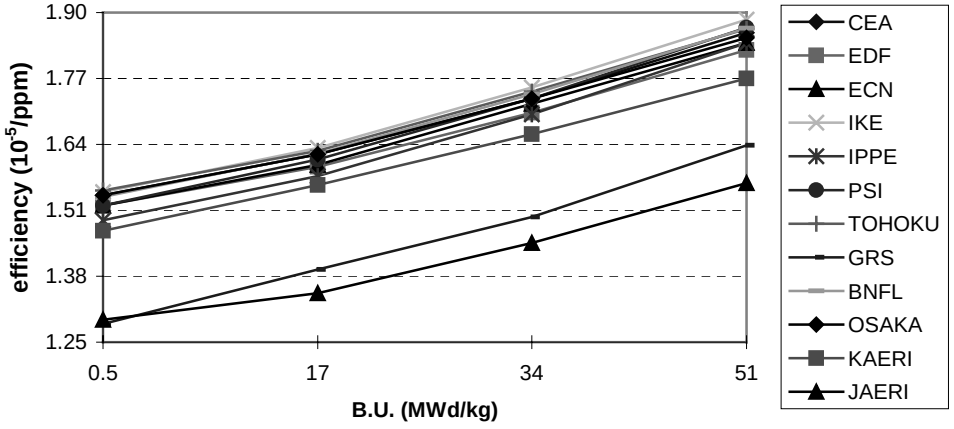

For the majority of participants, the boron coefficients are close for the beginning-of-irradiation step (0 MWd/kg). For the end-of-irradiation step (51 MWd/kg), the differences are about 0.2×10^{-5}/ppm of soluble boron. This implies a difference of 0.4% in reactivity effect for 2 000 ppm of soluble boron. This is an acceptable variation arising from a combination of depletion calculation, flux calculation and nuclear data.

It is notable that there is a large decrease in the magnitude of the boron efficiency between the first and fifth recycle generations, due to the rapid increase in plutonium content and the consequent effect of hardening of the neutron spectrum.

Figures 4.22 and 4.23 show the moderator temperature coefficients for the first and fifth recycle generations as a function of cell irradiation:

Figure 4.22. STD PWR – Stage I – First recycle: Moderator temperature coefficient

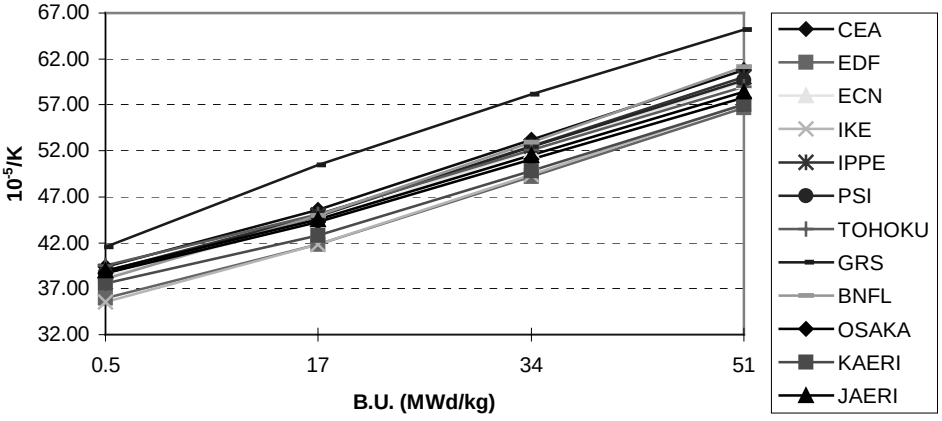

Figure 4.23. STD PWR – Stage I – Fifth recycle: Moderator temperature coefficient

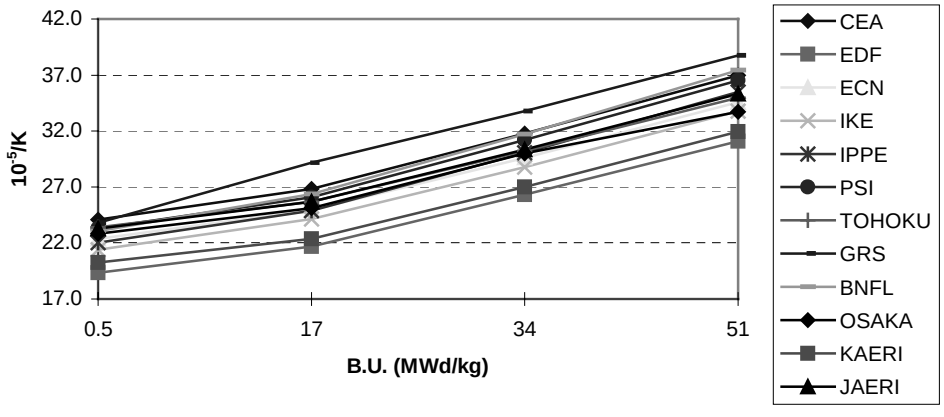

The moderator temperature coefficient values are spread very closely and the general trends are very similar for all participants. The absolute value decreases between the first and the fifth recycle generation, meaning that the moderator temperature coefficient becomes less negative, mainly due to the positive density effect with the increasing plutonium content.

Figures 4.24 and 4.25 show the fuel temperature (Doppler) coefficient as a function of cell irradiation and participant for the first and fifth recycle generations:

Figure 4.24. STD PWR – Stage I – First recycle:
Fuel temperature coefficient

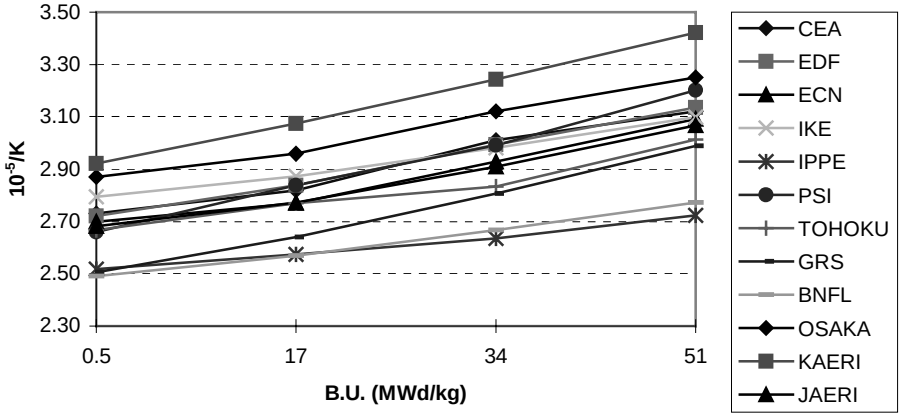

Figure 4.25. STD PWR – Stage I – Fifth recycle:
Fuel temperature coefficient

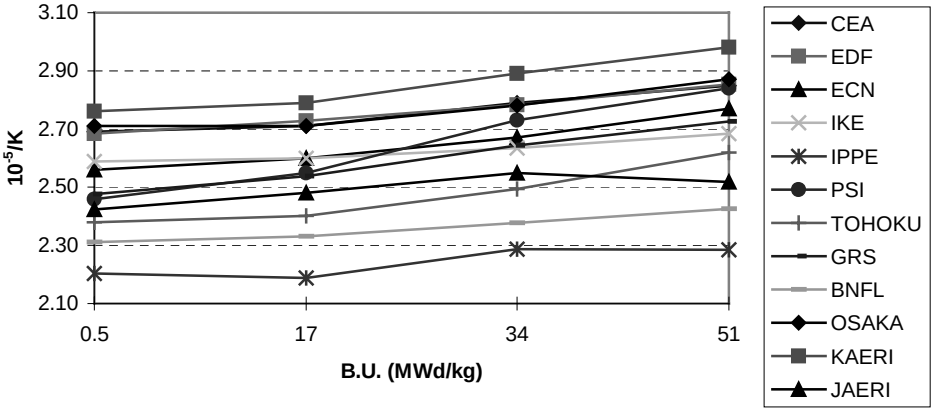

The fuel temperature coefficient values show a larger spread than either the boron coefficient or the moderator coefficient. The underlying trends with cell burn-up are not consistent and the discrepancies tend to increase in the later recycle generations. Isotopic degradation of the plutonium is probably at least partially responsible for these differences. The methods used to treat the temperature dependence of the plutonium resonances are different between the various participants and this may be a contributing factor. Overall it is clear the fuel temperature coefficient is not satisfactory and should be improved. More detailed investigation is required.

Figures 4.26 and 4.27 show the global void effect as a function of cell irradiation. This is the reactivity change caused by completely replacing the moderator by a low density void. A negative value is desirable, as it indicates negative feedback will apply in the event of accidental steam voiding in the core.

Figure 4.26. STD PWR – Stage I – Recycle:
Global void effect with no leakage

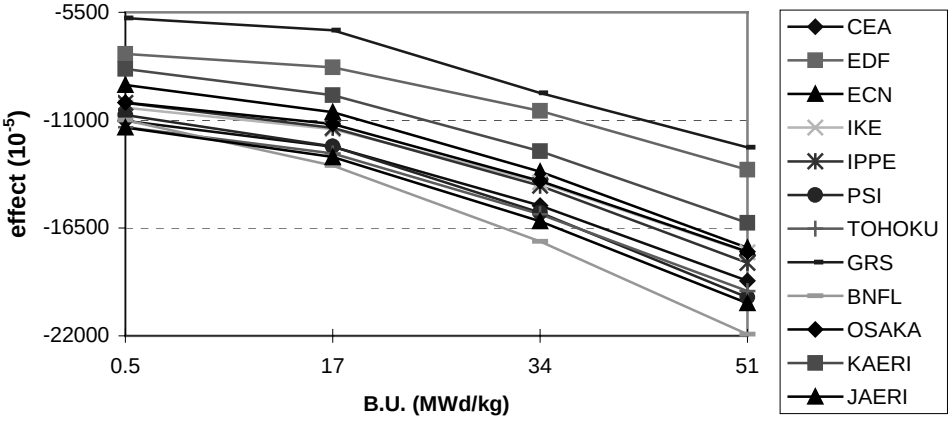

Figure 4.27. STD PWR – Stage I – Fifth recycle:
Global void effect with no leakage

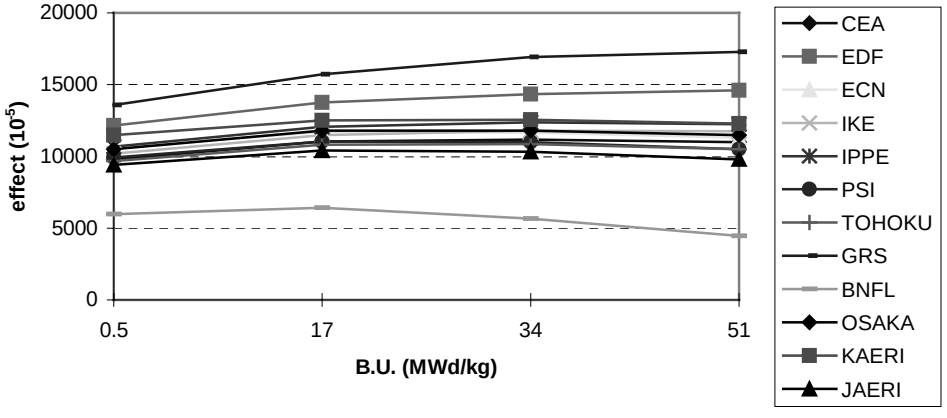

The various participants agree on the magnitude of the void reactivity effect to within a range of 10% in reactivity. The trend with irradiation is similar for all participants, with similar behaviour in all recycle generations.

β_{eff} *values*

Figure 4.28 shows a comparison of the delayed neutron fraction β_{eff}, measured in 10^{-5} reactivity (pcm). This an important indicator of the transient response of the core. Generally, it should be large in magnitude to slow down the onset of prompt criticality in the event of a reactivity insertion fault.

Figure 4.28. STD PWR – Stage I:
β_{eff} value at end of irradiation

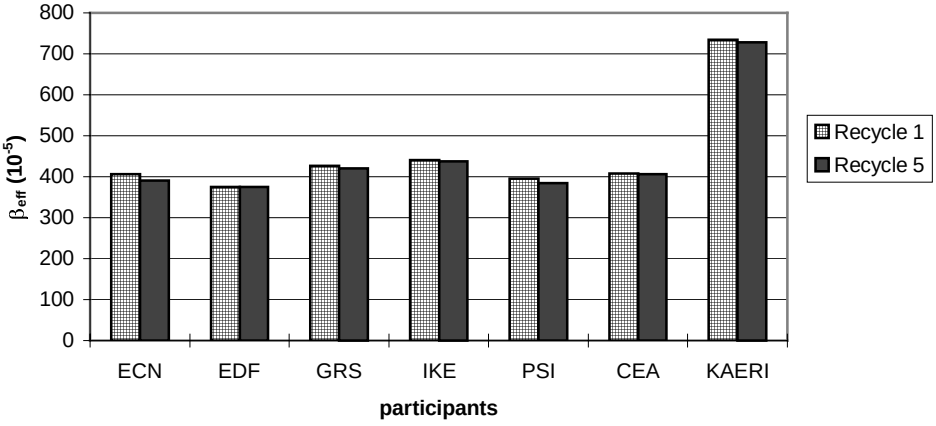

There is a large spread in delayed neutron fractions (β_{eff}), which must arise from underlying discrepancies in the nuclear data.

Standard PWR – Stage II Benchmark

In the Stage II Benchmark, each participant was asked to calculate its own plutonium isotopic assay at the start of irradiation and to fix the total plutonium content in accordance with the method specified in Chapter 2. IPPE and PSI did not keep exactly the agreed specification for the dilution between the plutonium from MOX and UO_2. Their results are not comparable to the others and where appropriate, they are not shown.

Initial plutonium content

Figure 4.29 shows a comparison of the initial plutonium content by recycle generation and participant, with CEA as the reference.

The spread of values increases in later recycle generations, up to a maximum of approximately 1 w/o in the absolute plutonium content. This represents, for a standard PWR of 1 300 MWe, around 1 metric tonne for the plutonium inventory of the whole core.

End-of-cycle reactivity value

Figure 4.30 shows the end-of-cycle k-infinity calculated by each participant in the first recycle generation. The first generation values are subsequently used as targets to be attained in the subsequent recycle generations by adjusting the initial plutonium content. As previously seen in Stage I, the results divide into two populations, one giving a smaller k-infinity than 1.04 and one larger than 1.04. Overall the calculations are fairly consistent, apart from GRS as a clear outlier.

Figure 4.29. STD PWR – Stage II:
Pu content at BOC – Comparison with CEA values

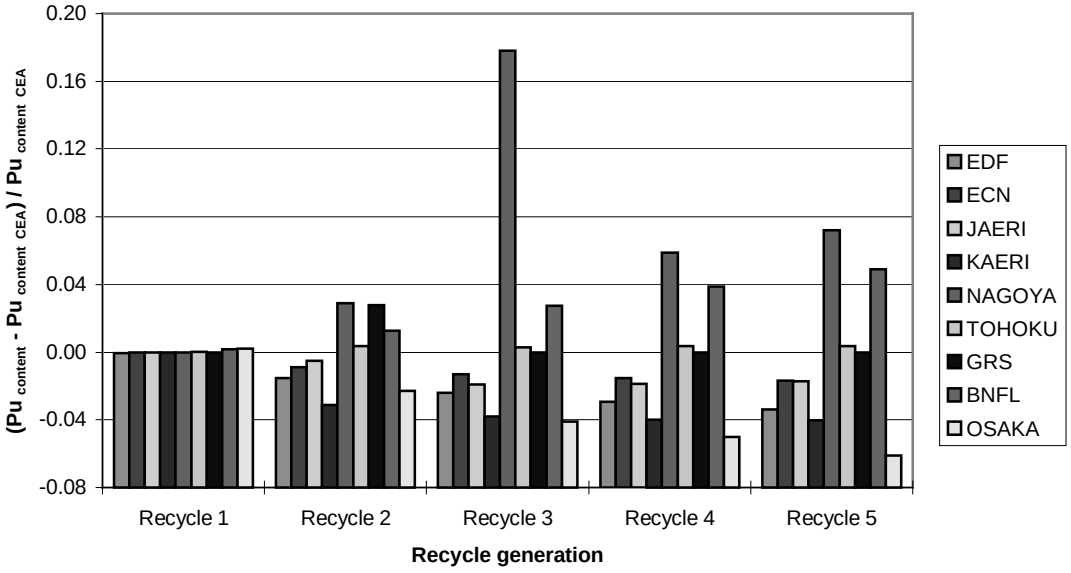

CEA values					
	Recycle 1	Recycle 2	Recycle 3	Recycle 4	Recycle 5
Pu content	10.09%	13.53%	15.87%	17.66%	19.10%

Figure 4.30. STD PWR – Stage II – First recycle: End-of-cycle-reactivity

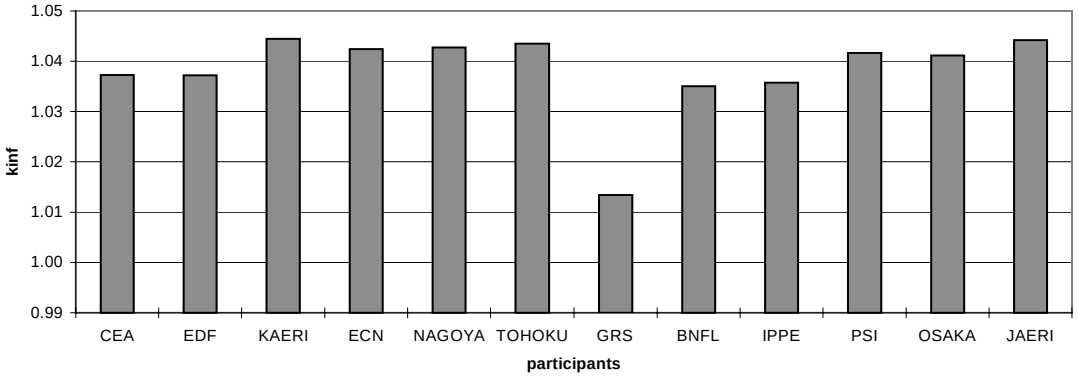

Reactivity parameters values

Figures 4.31 and 4.32 show the boron reactivity coefficients in the first and fifth recycle generations respectively, as a function of cell irradiation:

Figure 4.31. STD PWR – Stage II – First recycle: Boron efficiency

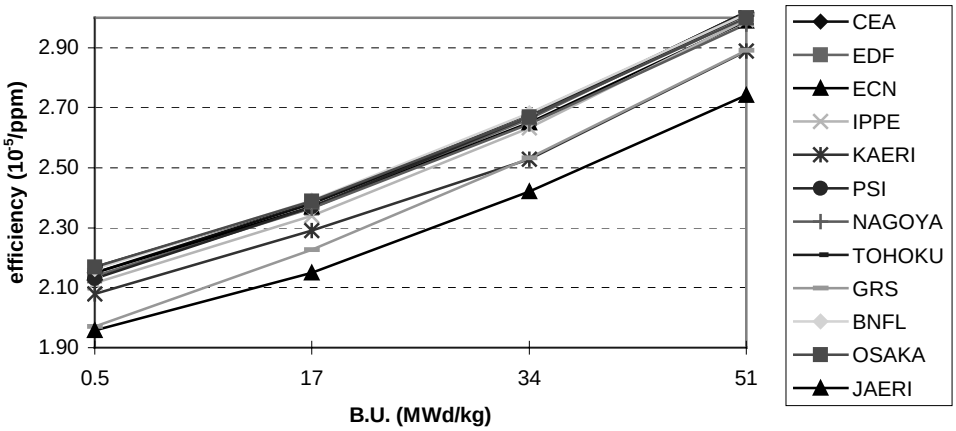

Figure 4.32. STD PWR – Stage II – Fifth recycle: Boron efficiency

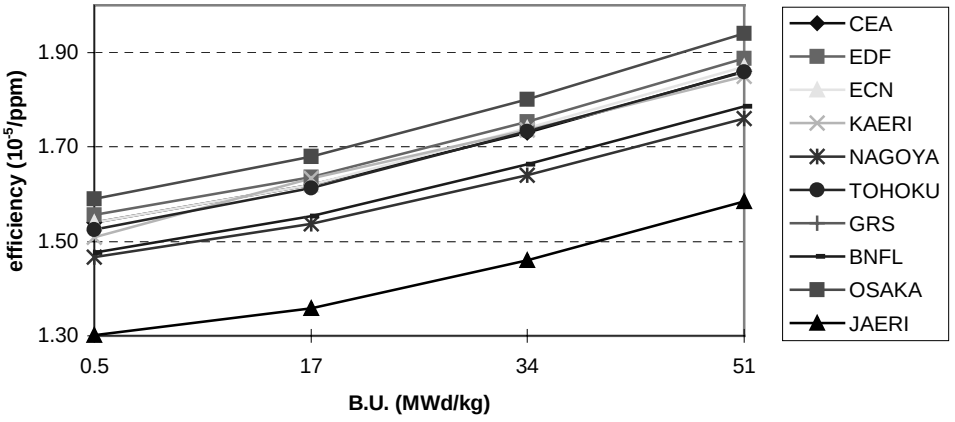

As in the Stage I Benchmark, the boron coefficients are generally in good agreement and show similar trends with cell irradiation. The absolute magnitude of the boron coefficients is very small in all recycle generations (*cf.* typical figure for UO_2: -8 pcm/ppm, 1 pcm = 10^{-5}). This will make satisfactory control and operation of the core more difficult to achieve, particularly in the later recycle generations.

Figures 4.33 and 4.34 show the moderator temperature coefficient for recycle generations one and five respectively.

Figure 4.33. STD PWR – Stage II – First recycle: Moderator temperature coefficient

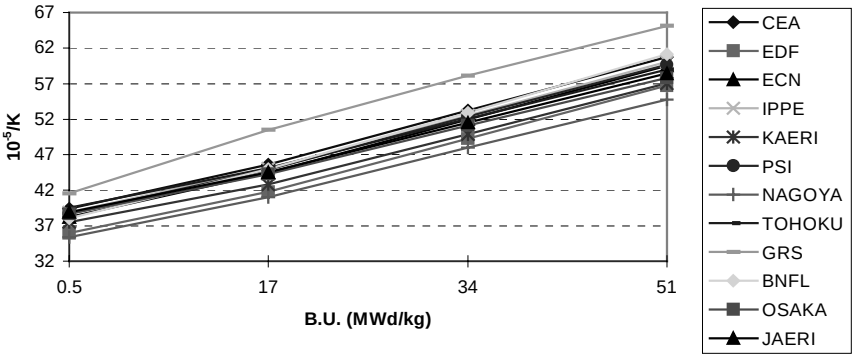

Figure 4.34. STD PWR – Stage II – Fifth recycle: Moderator temperature coefficient

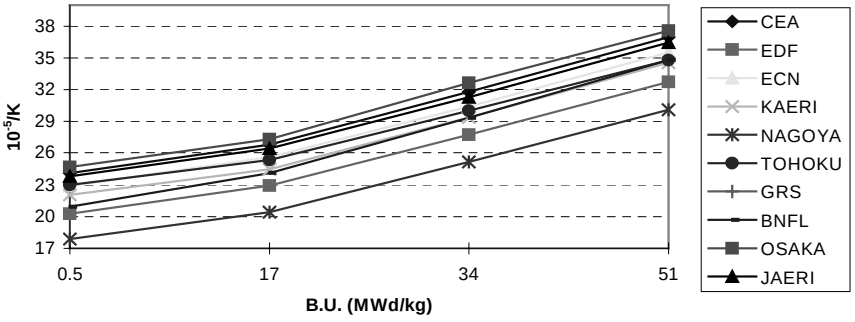

The trends are similar to those seen in the Stage I Benchmark. During later recycle generations, the absolute value moderator temperature coefficient becomes larger, as does the spread between the participants.

Figures 4.35 and 4.36 show the fuel temperature coefficients for the first and fifth recycle generations.

Figure 4.35. STD PWR – Stage II – First recycle: Fuel temperature coefficient

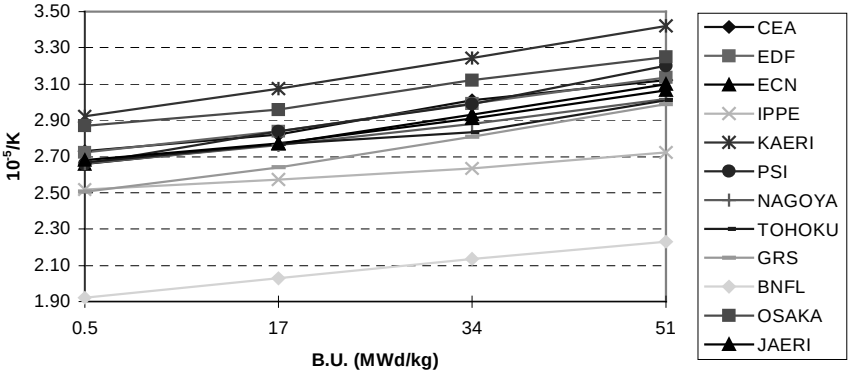

Figure 4.36. STD PWR – Stage II – Fifth recycle: Fuel temperature coefficient

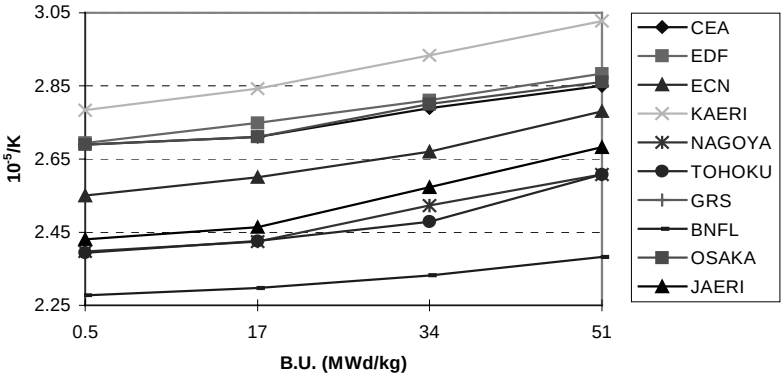

Compared with the Stage I Benchmark, similar trends are obtained, but with the spread of results increased, due to the larger initial differences combined with the plutonium content, which is also different for each participant. The BNFL results are discrepant, probably due to an inconsistent definition of the fuel temperature coefficient.

Figures 4.37 and 4.38 show the global void effect. This parameter is negative in the first recycle generation, but becomes more positive in later recycle generations such that all participants show positive values for the fifth recycle generation.

Figure 4.37. STD PWR – Stage II – First recycle: Global void effect with no leakage

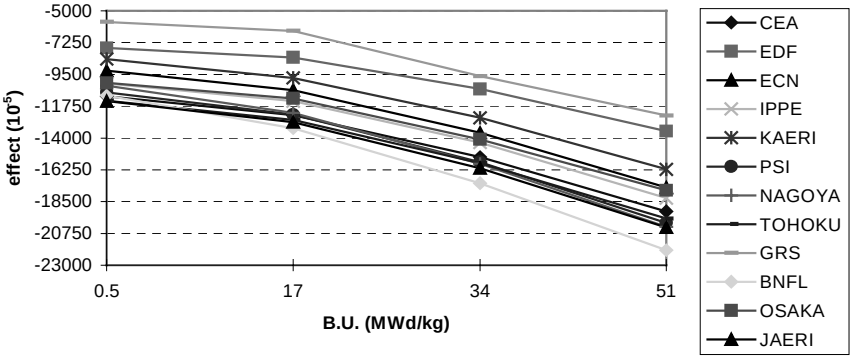

Figure 4.38. STD PWR – Stage II – Fifth recycle: Global void effect with no leakage

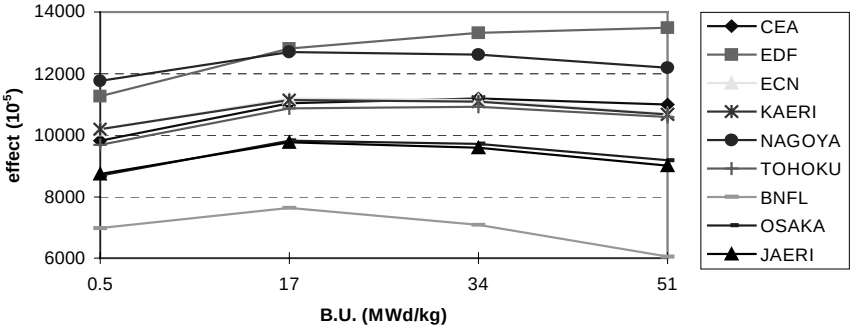

Mass balance

Figures 4.39 and 4.40 show the plutonium mass balance by participant. This is the net **reduction** in plutonium mass during a complete cycle of irradiation of the fuel from initial loading to recycle after pond storage and reprocessing. It therefore accounts for the decay of ^{241}Pu in the period between discharge from the reactor and the subsequent core loading.

Figure 4.39. STD PWR – Stage II – First recycle: Plutonium mass balance (complete cycle)

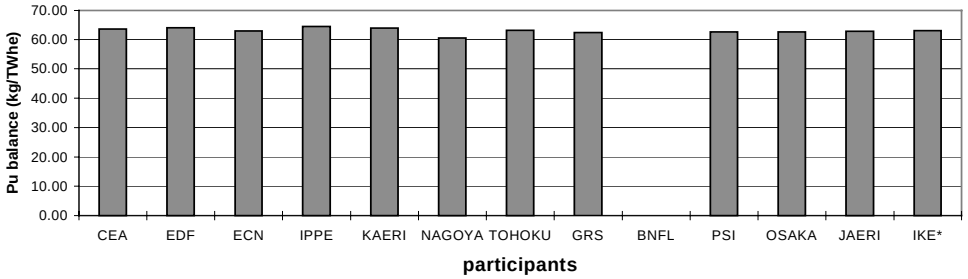

Figure 4.40. STD PWR – Stage II – Fifth recycle: Plutonium mass balance (complete cycle)

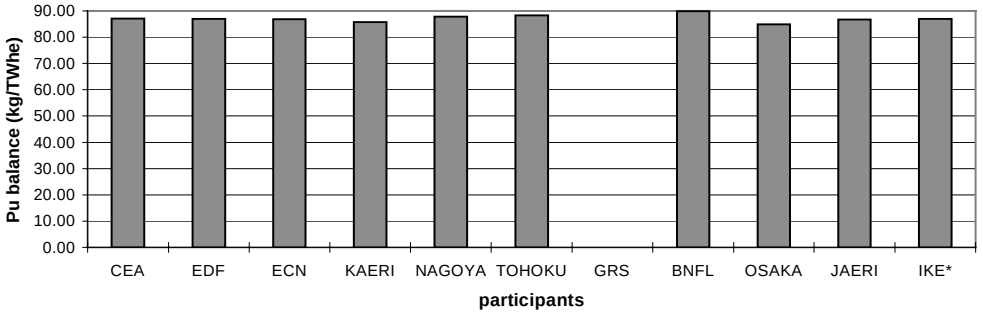

The plutonium mass balance is in good agreement for all participants and is not very sensitive to the initial plutonium content in each recycle generation. The same applies to the americium mass balance, shown in Figures 4.41 and 4.42. For curium, shown in Figures 4.43 and 4.44, the spread is larger in relative terms, though still small in terms of absolute values.

Figure 4.41. STD PWR – Stage II – First recycle: Americium mass balance (complete cycle)

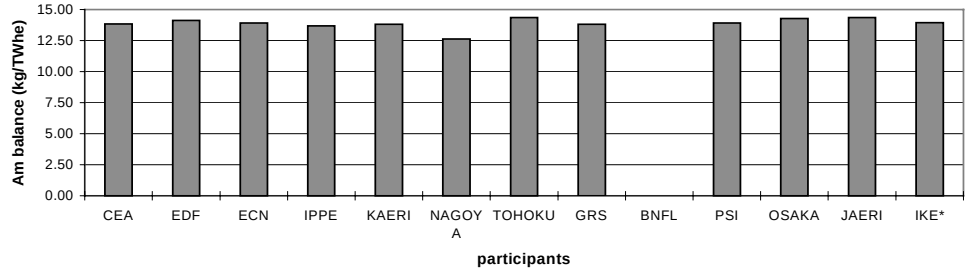

Figure 4.42. STD PWR – Stage II – Fifth recycle: Americium mass balance (complete cycle)

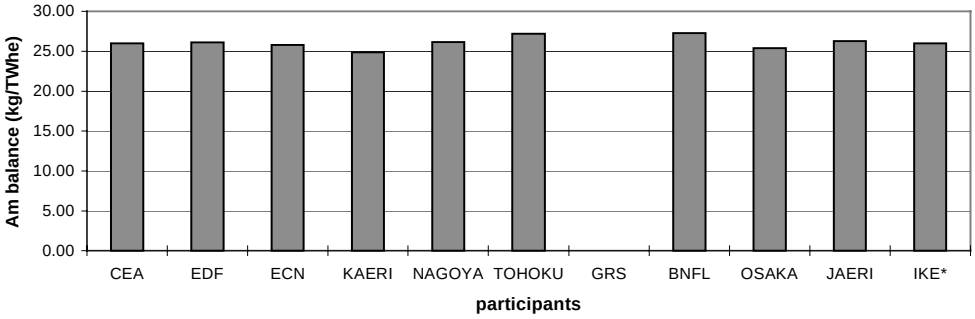

Figure 4.43. STD PWR – Stage II – First recycle: Curium mass balance (complete cycle)

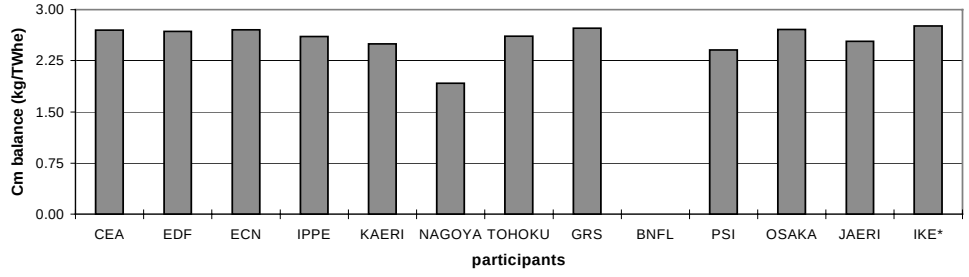

Figure 4.44. STD PWR – Stage II – Fifth recycle: Curium mass balance (complete cycle)

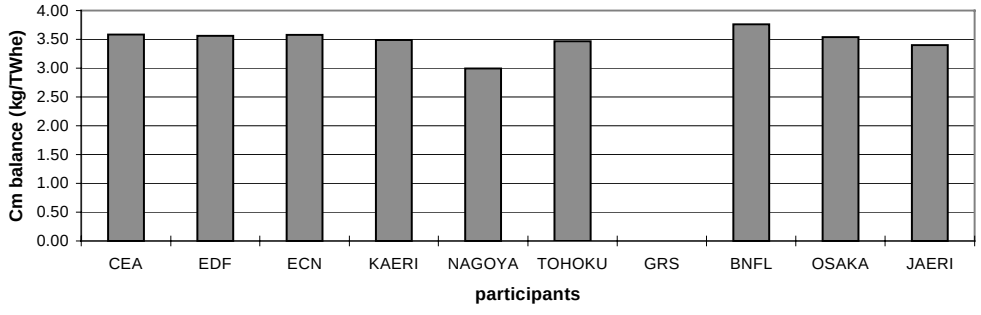

For the long-lived fission products, the production terms are very consistent between all the participants.

Highly moderated PWR – Stage I Benchmark

This section presents the results for the Highly Moderated (HM) PWR, with a moderation ratio of 3.5 (Vm/Vf) or 7.45 ($n_H/n_{H.N.}$), as described in Chapter 2. Only selected results are presented, usually for just the first and fifth recycle generation cases.

Microscopic cross-section spreads: ^{238}U, ^{239}Pu, ^{240}Pu, ^{241}Pu, ^{242}Pu

On the microscopic fission and absorption cross-sections

The comparison of microscopic cross-sections for fission and absorption is shown in Figures 4.45 to 4.51. The comparison is shown for the first recycle generation only, as the results are similar in the subsequent generations. The cross-sections are plotted as a function of cell irradiation.

The spread of values tend to be larger than for the STD PWR case. For the microscopic cross-section of the main isotopes, ^{239}Pu and ^{238}U, spreads over a total range of typically of 6% are seen. For ^{238}U, there are two groups of trends with irradiation, one group which show a tendency for the cross-section to decrease with irradiation and a second one (EDF, TOHOKU, OSAKA) which shows an increasing trend with irradiation compared with CEA.

For higher isotopes, similar spreads are seen:

- from -1% to +4% for ^{240}Pu;
- from ±4% for ^{241}Pu;
- from ±4% for ^{242}Pu.

Figure 4.45. HM PWR – Stage I – First recycle:
^{239}Pu fission cross-section – Comparison with CEA values

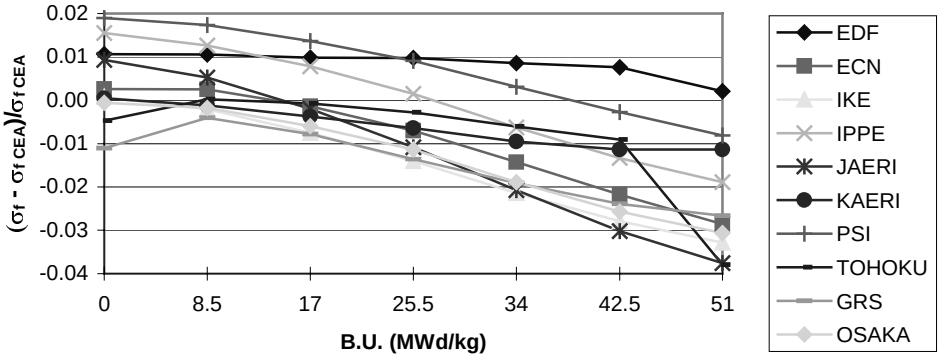

CEA values							
B.U (MWd/kg)	0	8.5	17	25.5	34	42.5	51
σ_f ^{239}Pu (barn)	53.53	57.10	63.48	71.11	80.01	90.02	100.79

Figure 4.46. HM PWR – Stage I – First recycle:
^{241}Pu fission cross-section – Comparison with CEA values

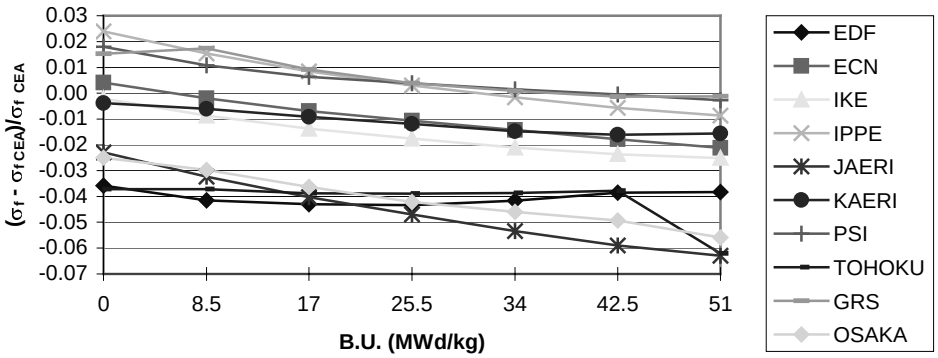

CEA values							
B.U (MWd/kg)	0	8.5	17	25.5	34	42.5	51
σ_f ^{241}Pu (barn)	64.51	68.02	74.71	82.58	91.72	102.04	113.34

Figure 4.47. HM PWR – Stage I – First recycle:
^{238}U capture cross-section – Comparison with CEA values

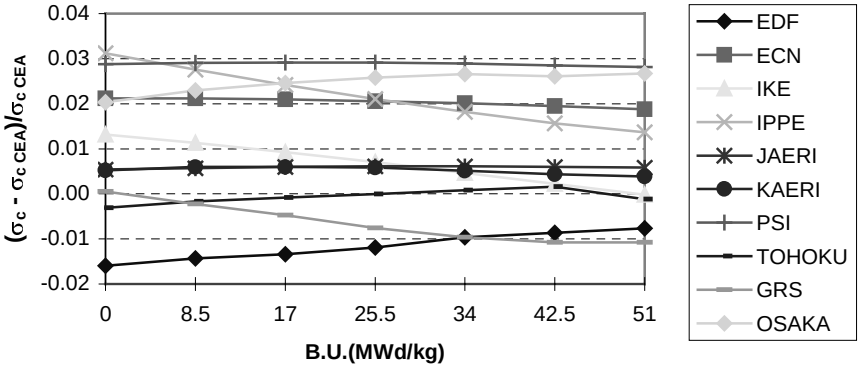

CEA values							
B.U (MWd/kg)	0	8.5	17	25.5	34	42.5	51
σ_c ^{238}U (barn)	0.91	0.91	0.92	0.93	0.94	0.95	0.96

Figure 4.48. HM PWR – Stage I – First recycle:
^{239}Pu capture cross-section – Comparison with CEA value

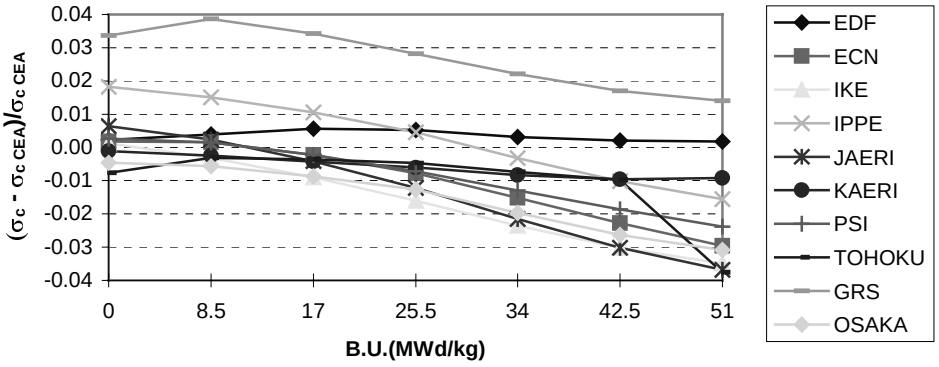

CEA values							
B.U (MWd/kg)	0	8.5	17	25.5	34	42.5	51
σ_c ^{239}Pu (barn)	29.03	31.18	34.70	38.89	43.76	49.19	55.00

Figure 4.49. HM PWR – Stage I – First recycle:
^{240}Pu capture cross-section – Comparison with CEA value

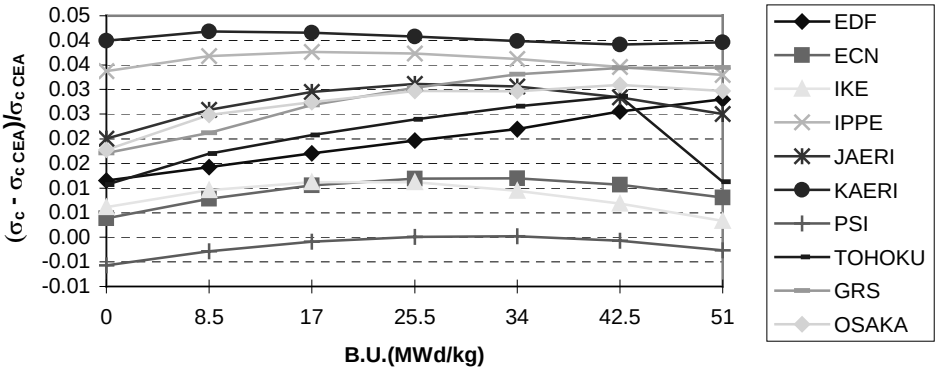

CEA values							
B.U (MWd/kg)	0	8.5	17	25.5	34	42.5	51
σ_c ^{240}Pu (barn)	47.95	47.42	48.18	49.72	52.06	55.19	59.14

Figure 4.50. HM PWR – Stage I – First recycle:
^{241}Pu capture cross-section – Comparison with CEA value

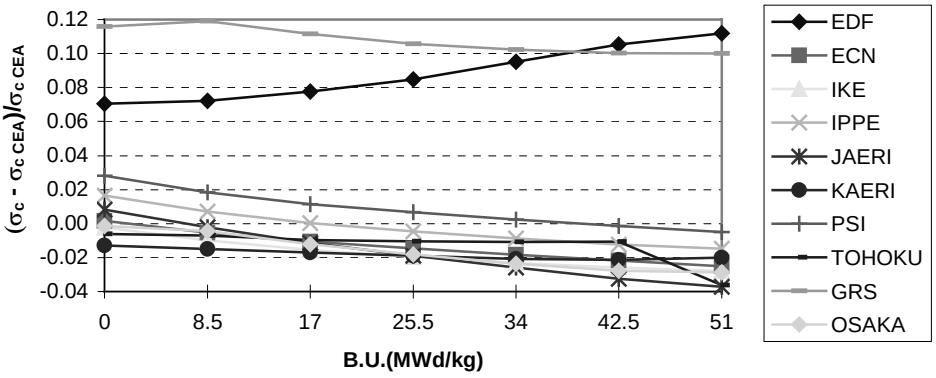

CEA values							
B.U (MWd/kg)	0	8.5	17	25.5	34	42.5	51
σ_c ^{241}Pu (barn)	20.93	22.20	24.50	27.20	30.32	33.84	37.68

Figure 4.51. HM PWR – Stage I – First recycle:
^{242}Pu capture cross-section – Comparison with CEA value

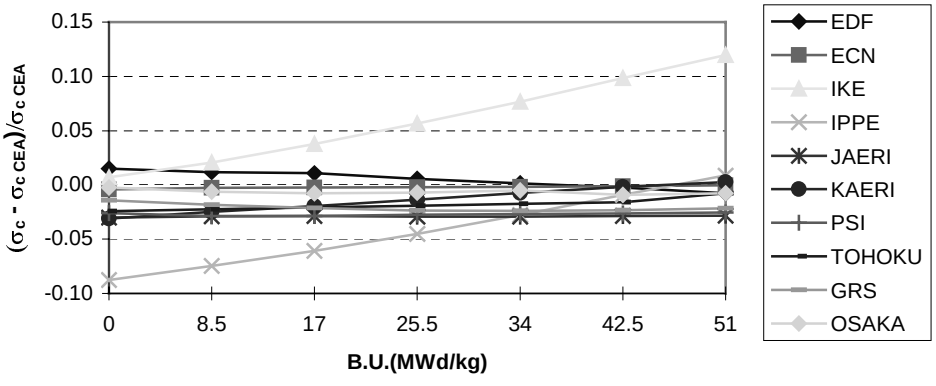

CEA values							
B.U (MWd/kg)	0	8.5	17	25.5	34	42.5	51
σ_c ^{242}Pu (barn)	16.94	16.60	16.23	15.82	15.38	14.94	14.52

On the microscopic (n,2n) cross-sections

Although the higher order reactions are much less important in the overall neutron balance, they nevertheless make a significant contribution. Only ^{238}U and ^{244}Cm are shown in Figures 4.52 and 4.53:

Figure 4.52. HM PWR – Stage I – First recycle:
^{238}U (n,2n) cross-section – Comparison with CEA values

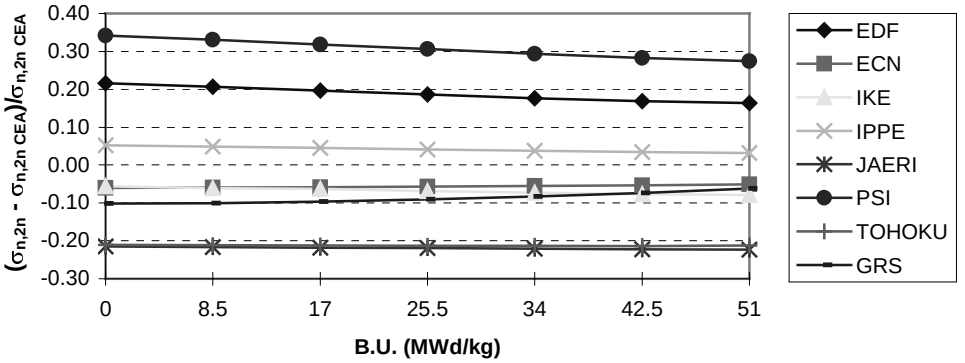

CEA values							
B.U (MWd/kg)	0	8.5	17	25.5	34	42.5	51
$\sigma_{n,2n}$ ^{238}U (barn)	6.20E-03	6.20E-03	6.17E-03	6.13E-03	6.08E-03	6.01E-03	5.94E-03

Figure 4.53. HM PWR – Stage I – First recycle:
^{244}Cm (n,2n) cross-section – Comparison with CEA values

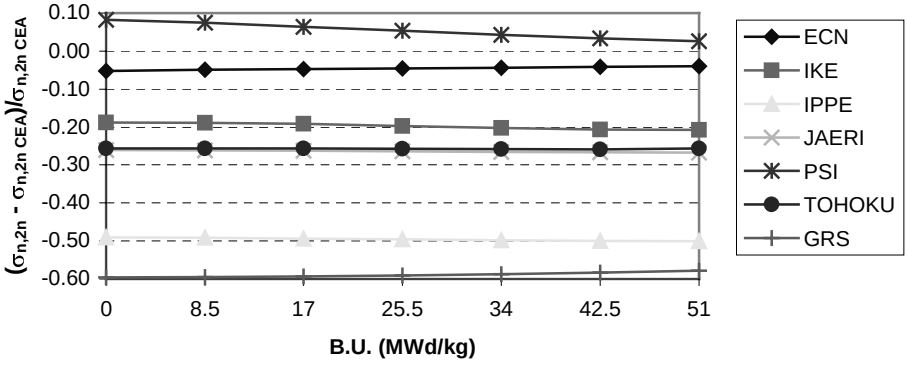

CEA values							
B.U (MWd/kg)	0	8.5	17	25.5	34	42.5	51
$\sigma_{n,2n}$ ^{244}Cm (barn)	2.37E-03	2.37E-03	2.36E-03	2.34E-03	2.33E-03	2.30E-03	2.27E-03

As for the STD PWR, the spread of results is quite large, with the same general trends and similar ranges. The isotopes which show the largest range of values are ^{243}Cm, ^{245}Cm (up to a factor 3) and ^{239}Pu. The other isotopes typically fall within a range of 50%.

On the ν values

Figure 4.54 shows a comparison of ^{239}Pu ν values, the average number of neutrons per fission. These are in reasonably good agreement.

Figure 4.54. HM PWR – Stage I – First recycle: ^{239}Pu ν values

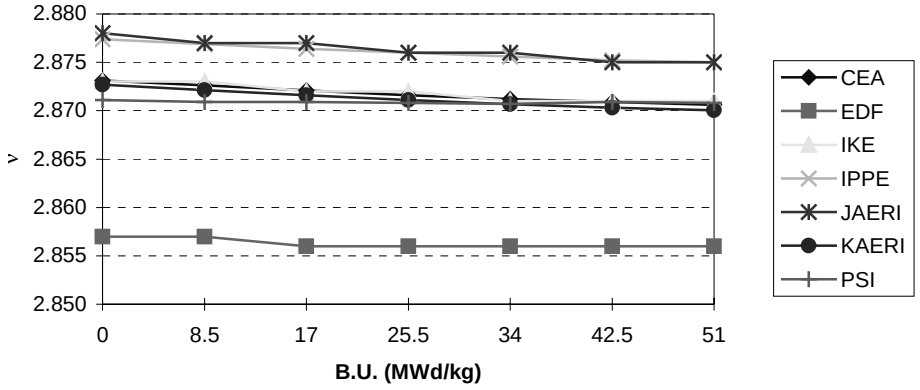

On fission capture cross-sections ratio

The fission/capture ratios are shown for ^{239}Pu in Figure 4.55. Disregarding the clearly discrepant GRS values, all of the participants show positive differentials from 0 to 1% compared with CEA. It implies that the main isotope contributing to reactivity is relatively more fissile and thus the majority of participants should obtain higher reactivities than CEA.

For ^{241}Pu (not plotted), the differences are larger, especially for EDF and GRS (-10%). For the other participants, the differences are in the range +1% to -4%.

Figure 4.55. HM PWR – Stage I – First recycle: ^{239}Pu ratio fission/capture – Comparison with CEA values

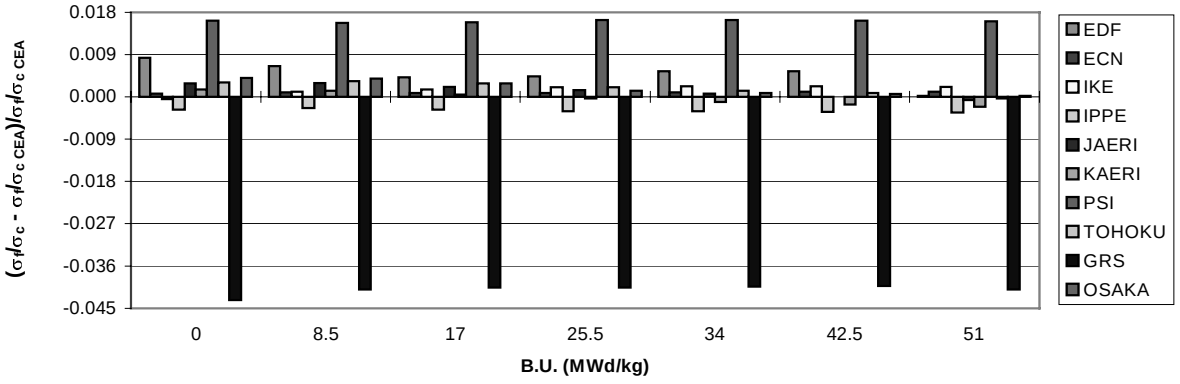

CEA values							
B.U (MWd/kg)	0	8.5	17	25.5	34	42.5	51
σ_f/σ_c ^{239}Pu	1.844	1.831	1.829	1.828	1.828	1.830	1.833

Spread in reactivities

Figures 4.56 and 4.57 show comparisons of reactivities versus cell irradiation, for the first and fifth recycle generations respectively, plotted relative to the CEA values as a reference.

Figure 4.56. HM PWR – Stage I – First recycle:
Reactivity swing – Comparison with CEA values

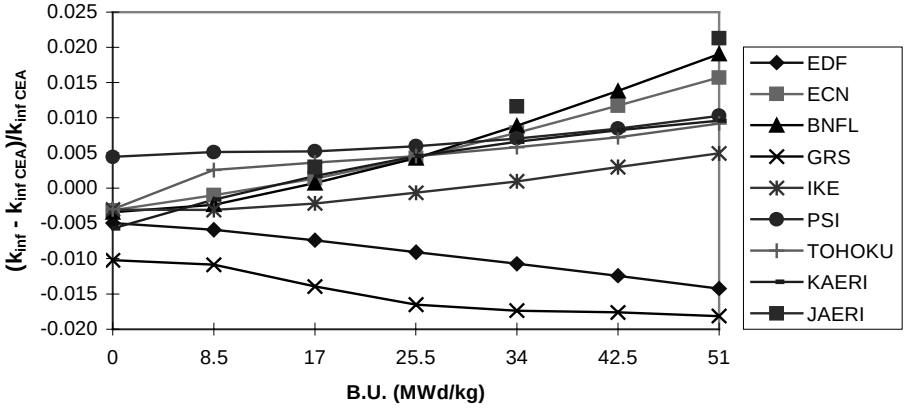

Figure 4.57. HM PWR – Stage I – Fifth recycle:
Reactivity swing – Comparison with CEA values

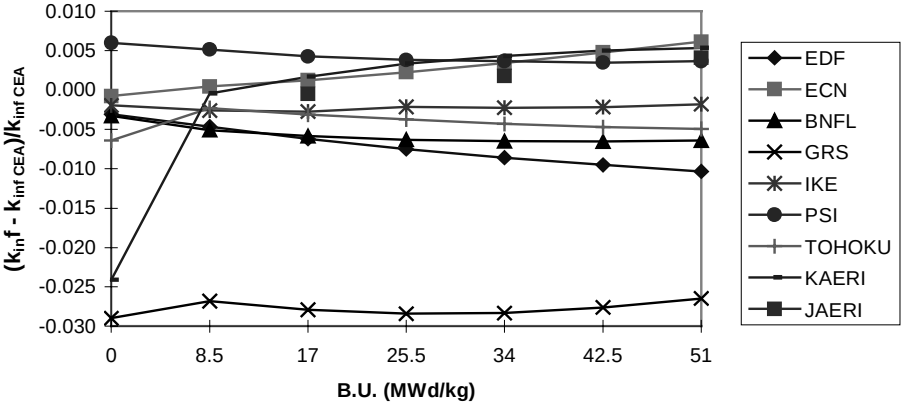

Compared with the STD PWR, the spread of reactivity values is larger for the HM PWR. This is especially evident in the first generation recycle, where there are also significantly discrepant trends with cell irradiation, resulting in a larger spread at high irradiations. There is a tendency for the range of values to converge in subsequent recycle generations.

Reactivity balance under irradiation

The reactivity balance under irradiation is 35% in the first recycle generation and 18% in the fifth generation. These very contrasting behaviours will have an impact on the initial plutonium content and on the reactivity adjustment values. Figure 4.58 shows the comparison of end-of-cycle k-infinities, with the CEA value as the reference. The same data are also listed in Table 4.3, with the minimum and maximum values highlighted in Table 4.4.

Figure 4.58. HM PWR – Stage I:
End-of-cycle reactivity – Comparison with CEA value

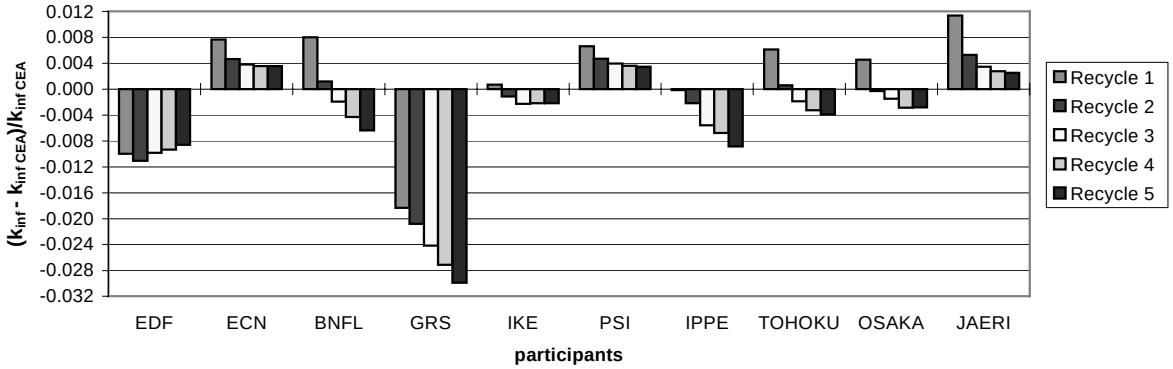

The differences between participants are larger than for the STD PWR due to a larger difference in reactivity values at zero irradiation and the subsequent trend during irradiation.

Table 4.3. End-of-cycle k-infinities by participant and recycle generation

	Recycle 1	Recycle 2	Recycle 3	Recycle 4	Recycle 5
CEA	1.03727	1.03720	1.03732	1.03726	1.03727
EDF	1.02688	1.02573	1.02712	1.02757	1.02835
ECN	1.04522	1.04203	1.04127	1.04095	1.04098
BNFL	1.04560	1.03847	1.03535	1.03280	1.03067
GRS	1.01825	1.01561	1.01224	1.00915	1.00627
IKE	1.03800	1.03600	1.03500	1.03500	1.03500
PSI	1.04411	1.04212	1.04144	1.04101	1.04088
IPPE	1.03713	1.03497	1.03152	1.03027	1.02808
TOHOKU	1.04364	1.03782	1.03537	1.03388	1.03324
OSAKA	1.04198	1.03690	1.03578	1.03431	1.03434
JAERI	1.04904	1.04269	1.04093	1.04014	1.03989

The largest change through the five recycle generations is BNFL (1.5%). The differences between largest and smallest values for each participant are given in the following table.

Table 4.4. End-of-cycle k-infinities – minimum and maximum values by participant

	CEA	EDF	ECN	BNFL	IKE	PSI	IPPE	TOHOKU	OSAKA	JAERI
Min	1.0372	1.02573	1.04095	1.030666	1.035	1.04088	1.02808	1.03324	1.03431	1.039889
Max	1.03732	1.02835	1.04522	1.045604	1.038	1.04411	1.03713	1.04364	1.04198	1.049041
Diff	-0.00012	-0.00262	-0.00427	-0.014938	-0.003	-0.00323	-0.00905	-0.0104	-0.00767	-0.009152

The range covered by the maximum and minimum values, summarised in Table 4.5, tends to decrease during in later recycle generations from 2.2% down to 1.3%. This is opposite to the trend seen with the STD PWR and moreover the spread of values is larger for the HM PWR.

Table 4.5. End-of-cycle k-infinities – extreme values

	Recycle 1	Recycle 2	Recycle 3	Recycle 4	Recycle 5
Min.	1.02688	1.02573	1.02712	1.02757	1.02808
Max.	1.04904	1.04269	1.04144	1.04101	1.04098
Largest difference	0.02216	0.01696	0.01432	0.01344	0.01290

Fission rate discrepancies

Figure 4.59 shows the differences in fission rates relative to CEA as the reference.

Figure 4.59. HM PWR – Stage I:
Differences in fission rates compared with CEA values (in %)

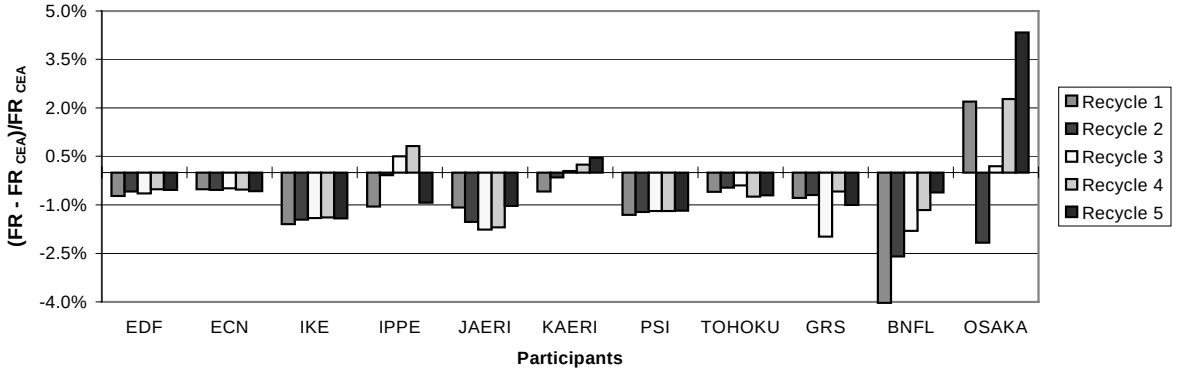

CEA values					
	Recycle 1	Recycle 2	Recycle 3	Recycle 4	Recycle 5
Fission rate (fraction)	0.05216	0.05209	0.05209	0.05209	0.05209

The range of values is larger for the HM PWR than for the STD PWR. 1% in relative difference on the fission rate is equivalent to 0.3% in reactivity in the first generation recycle and to 0.2% for in the fifth generation. The majority of participants are below 2%, thus under 0.6% reactivity difference on reactivity balance under irradiation. Thus the majority of participants obtain smaller fission rates than CEA, which would tend to cause the reactivity balance to be smaller than CEA for the majority of the participants. This actually is not the case, the majority of participants showing a positive increase of reactivity under irradiation.

Spread in reaction rates

Only five participants provided data on the breakdown of reactions rates. These are shown in Figure 4.60. The number is insufficient to reach any definite conclusions, but usefully illustrates the relative contribution of the various reactions and shows order of magnitude of the spread of results. The illustration is for the end of life condition (51 MWd/kgHM) for the first (C1) and fifth (C5) recycle generations. The spread is larger than for the STD PWR.

Absorption and production increase between the first and fifth recycle generations, due to the increasing plutonium content. Also, the reaction rates are increased by the higher moderation ratio and the more thermalised neutron spectrum, compared with the STD PWR.

Figure 4.60. HM PWR – Stage 1 – Reaction rates

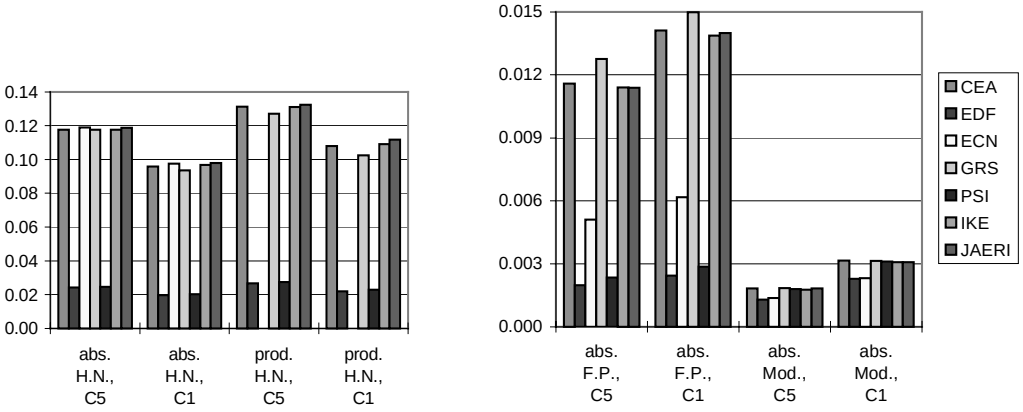

Reactivity coefficients

Figures 4.61 and 4.62 show the boron efficiencies versus cell irradiation for the first and fifth recycle generations. The boron efficiency is in moderately good agreement between the various participants, with acceptable agreement on trends with cell irradiation. In the fifth generation recycle the boron efficiency is reduced compared with the first generation, but is still a factor 2 higher than for the STD PWR. Thus the increase in moderation ratio improves strongly this important control parameter, partly due to the larger mass of boron at a given concentration and partly due to the softer neutron spectrum.

Figure 4.61. HM PWR – Stage I – First recycle: Boron efficiency

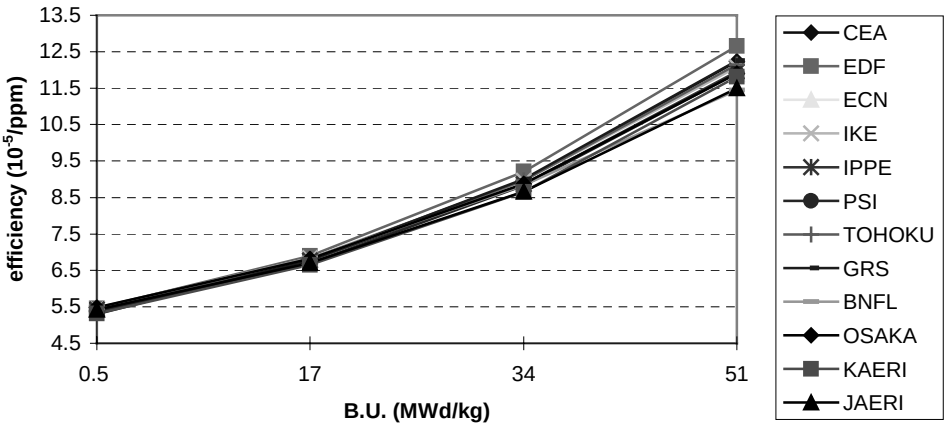

Figure 4.62. HM PWR – Stage I – Fifth recycle: Boron efficiency

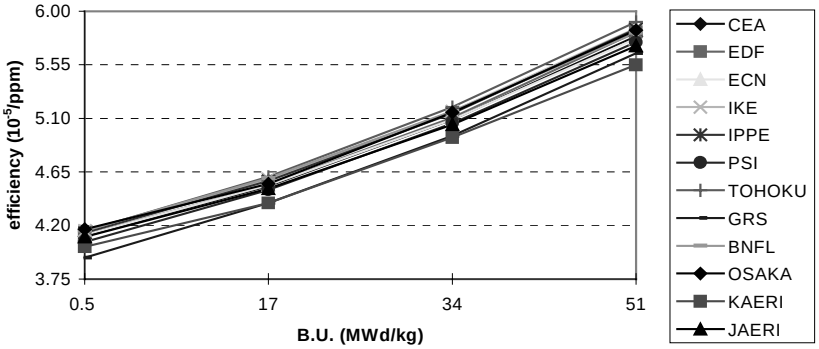

For the first recycle generation at the end of irradiation, the differences are about 10^{-5}/ppm of soluble boron. This corresponds to 2% absolute reactivity difference for 2 000 ppm of soluble boron. This must arise from a combination of discrepancies in the depletion and flux calculations and the nuclear data. The plutonium content is very low and the neutron spectrum is thermal. Nevertheless, the boron efficiency is very high and it will not cause a large impact in terms of safety, only in terms of boron content for the core concept calculations. For the fifth recycle generation, with a harder neutron spectrum, the differences are very small and acceptable.

Figures 4.63 and 4.64 show the moderator temperature coefficients for the first and fifth recycle generations.

Figure 4.63. HM PWR – Stage I – First recycle: Moderator temperature coefficient

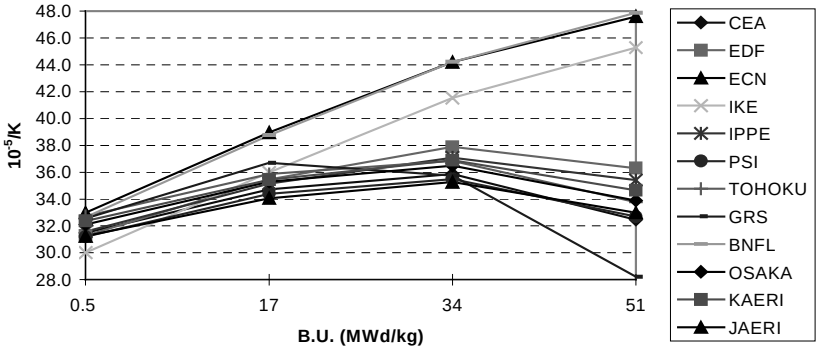

Figure 4.64. HM PWR – Stage I – Fifth recycle: Moderator temperature coefficient

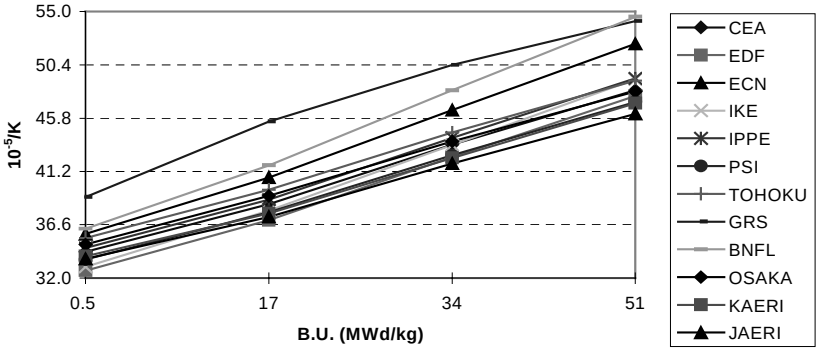

In the first generation recycle, discrepancies are evident in the trend of the moderator temperature coefficient with cell irradiation between ECN, IKE, BNFL and the other participants. This tendency reduces in later recycle generations, disappearing completely by the fourth and fifth generations, although there still remains a large spread in the absolute values three sets of solutions as clear outliers. In terms of absolute values, they are spread over a smaller range than in the STD PWR. The highest absolute values are in the region of -50×10^{-5} /°C. This parameter has an important impact on control and kinetic behaviour for cooling transients; if it is too negative, a faster and a larger increase in reactivity during the transient is implied.

Figures 4.65 and 4.66 show the fuel temperature (Doppler) coefficient for the first and fifth recycle generations. The fuel temperature coefficients are spread over a larger range of values and behavioural trends with cell irradiation than the STD PWR case. Generally, the absolute values are smaller in magnitude, due to the more thermalised spectrum and the increased resonance escape probability. As for the STD PWR, the treatments of temperature dependence of the resonance absorptions and self-shielding differ between the participants.

Figure 4.65. HM PWR – Stage I – First recycle
Fuel temperature coefficient

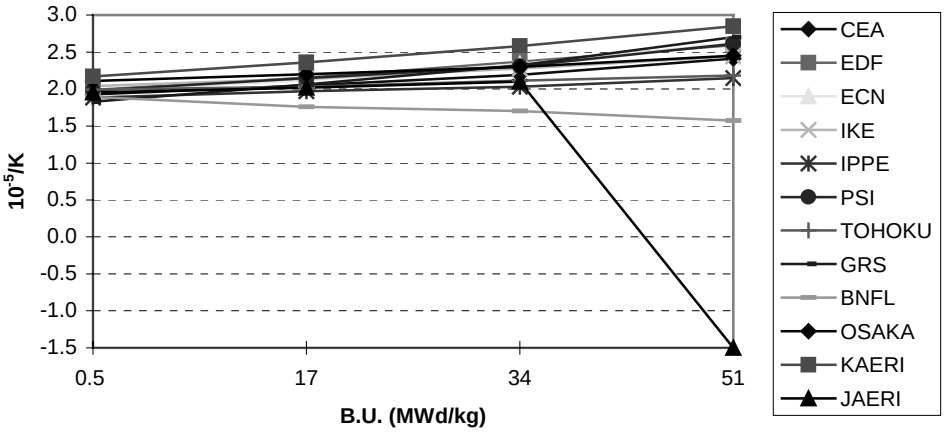

Figure 4.66. HM PWR – Stage I – Fifth recycle:
Fuel temperature coefficient

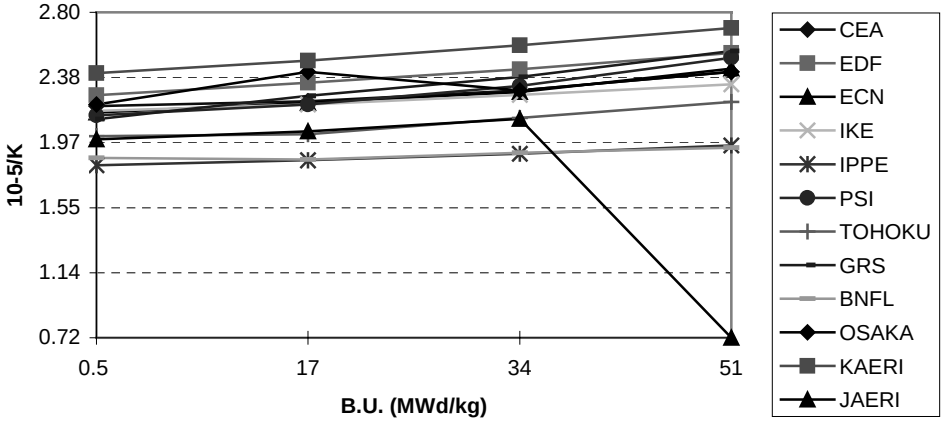

Figures 4.67 and 4.68 show the void effects without leakage. The void effect is the change in reactivity upon complete voiding of the moderator and should be negative to prevent rapid reactivity insertion following void formation in the moderator.

Figure 4.67. HM PWR – Stage I – First recycle:
Global void effect with no leakage

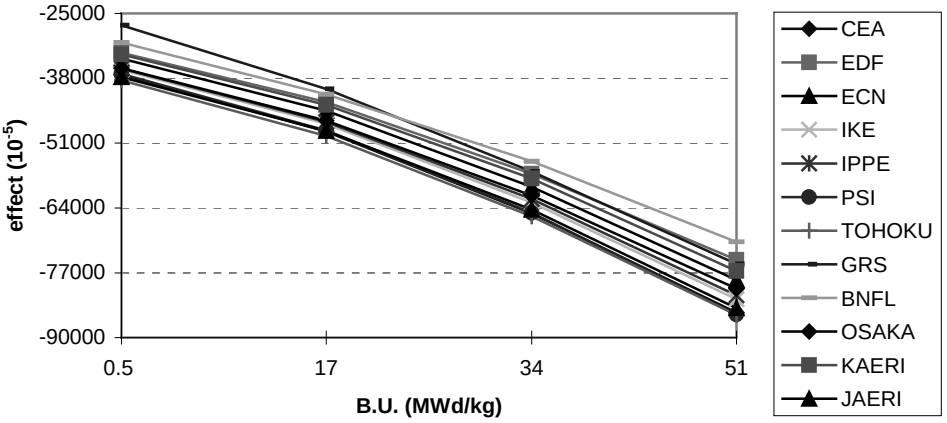

Figure 4.68. HM PWR – Stage I – Fifth recycle:
Global void effect with no leakage

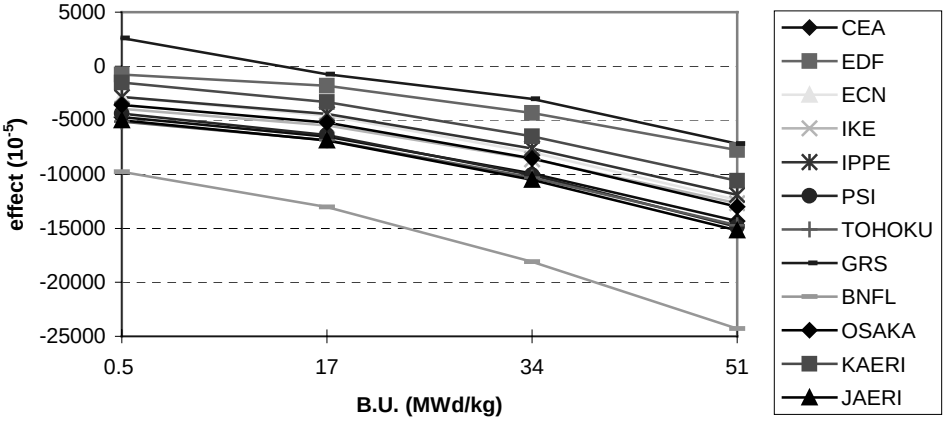

The global void effect falls generally within a range of 10% in reactivity. The trend with cell irradiation is very similar for the various participants, although the BNFL results form an outlier in the later recycle generations. The values remain negative throughout all the recycle generation for almost all the participants. This is a positive advantage of the HM PWR compared to the STD PWR.

Highly moderated PWR – Stage II Benchmark

Since IPPE and PSI did not follow the precise specification with respect to the dilution plutonium from MOX with plutonium from UO_2, their results are not comparable to the others and have been omitted from this section.

Initial plutonium content

Figure 4.69 show the initial plutonium calculated by the various participants relative to CEA as the reference.

Figure 4.69. HM PWR – Stage II: Pu content – Comparison with CEA values

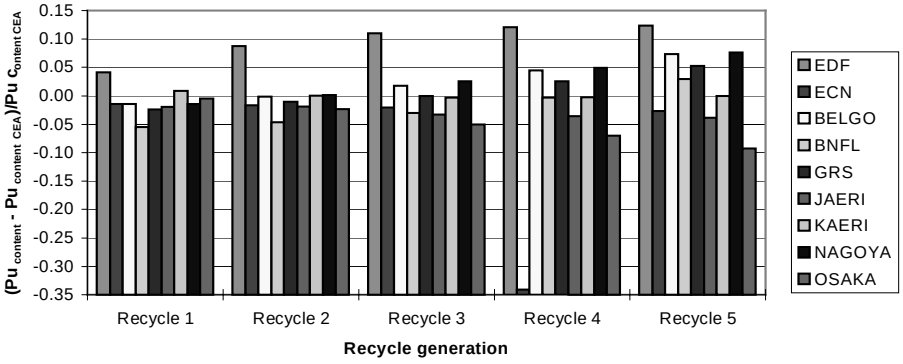

CEA values					
	Recycle 1	Recycle 2	Recycle 3	Recycle 4	Recycle 5
Pu content	6.70%	9.64%	12.11%	14.37%	16.58%

The initial plutonium contents are spread over a range up to ±10% in relative terms and ±1.5% in absolute plutonium content. The differences grow in later recycle generations, as a cumulative effect exists from one recycle generation to the next. The differences represent about one metric tonne for a 1 300 MWe PWR (about 80 metric tonnes of heavy metal), as for the standard PWR.

Adjustment reactivity value

This parameter is a constant for all the cases of plutonium recycling, by definition.

Reactivity coefficients

Figures 4.70 and 4.71 show the boron efficiencies obtained in Stage II as a function of cell irradiation.

Figure 4.70. HM PWR – Stage II – First recycle: Boron efficiency

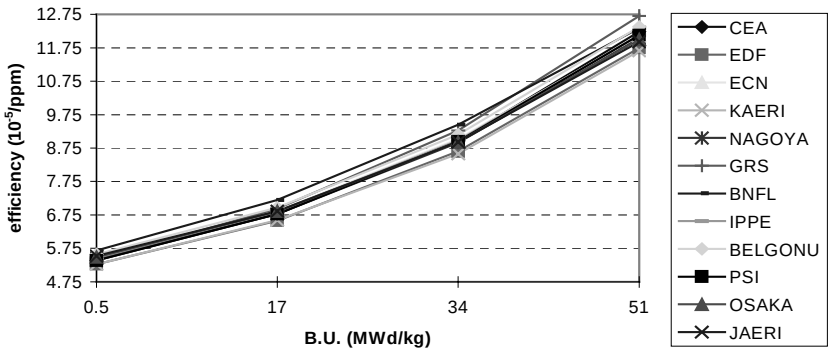

Figure 4.71. HM PWR – Stage II – Fifth recycle: Boron efficiency

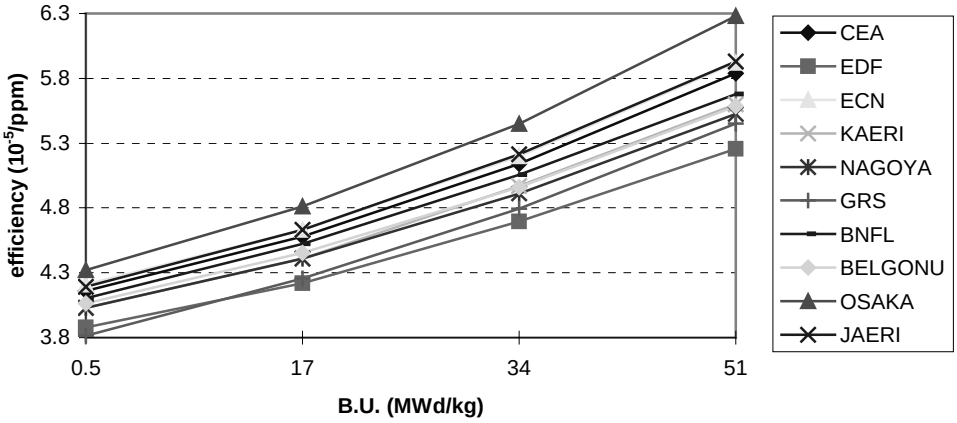

The various participants are in good agreement as to the trend of the boron coefficient with cell irradiation and through the various recycle generations. However, the spread is larger in absolute terms than for the STD PWR, largely because the magnitude of the coefficient is higher. At the end of the irradiation for the fifth generation recycle, the spread is about 10^{-5}/ppm of soluble boron. This difference may be considered as large, and must arise from a combination of plutonium content differences and discrepancies in the depletion calculations. This parameter is sensitive to the dilution factor and initial plutonium content.

Figures 4.72 and 4.73 show the moderator temperature coefficients for the first and fifth recycle generations, as a function of cell irradiation.

Figure 4.72. HM PWR – Stage II – First recycle: Moderator temperature coefficient

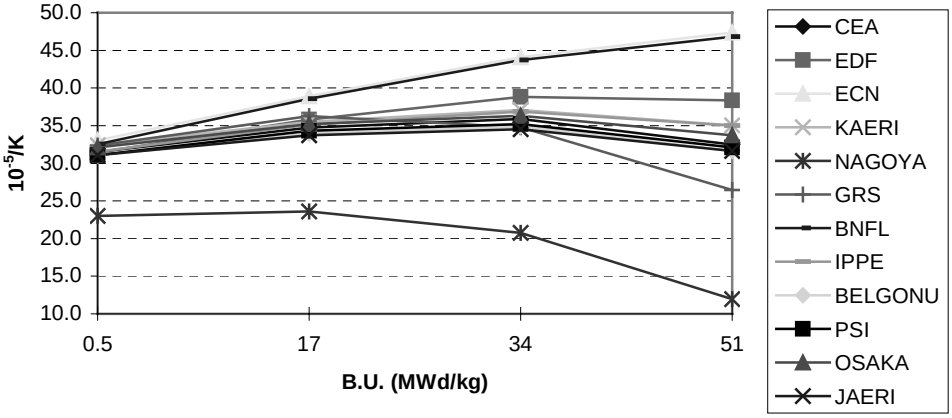

Figure 4.73. HM PWR – Stage II – Fifth recycle: Moderator temperature coefficient

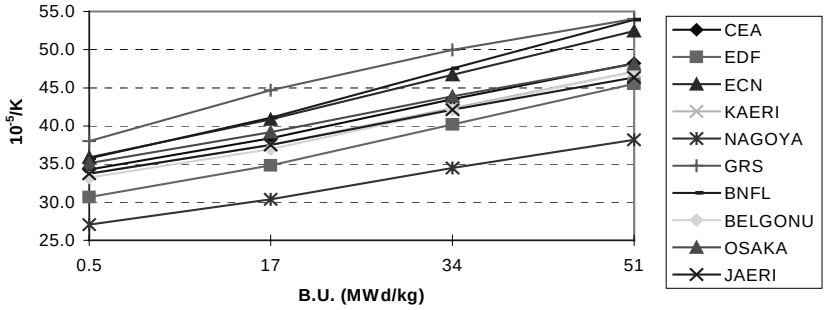

The moderator temperature coefficient has a fairly large spread of results, which tends to increase in the later recycle generations. There is reasonably good agreement regarding the general trend with cell irradiation.

The dilution effect is small for the fifth cycle. As a result, this parameter is more sensitive to the small content of plutonium than for the higher content (more than 12% of initial plutonium content).

Figures 4.74 and 4.75 show the fuel temperature (Doppler) coefficients for the first and fifth recycle generations, as a function of cell irradiation.

Figure 4.74. HM PWR – Stage II – First recycle: Fuel temperature coefficient

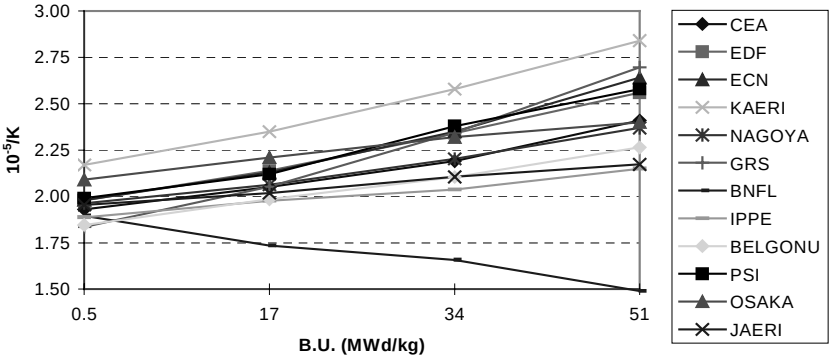

Figure 4.75. HM PWR – Stage II – Fifth recycle: Fuel temperature coefficient

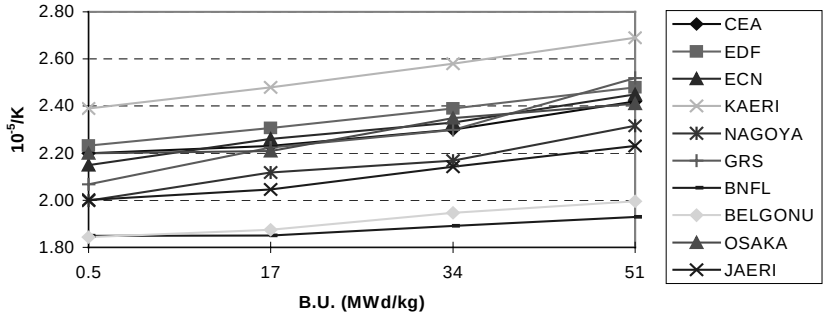

As for the Stage I Benchmark, the fuel temperature coefficient shows large discrepancies. As for the standard case, the BNFL results are clearly anomalous. Even after disregarding the BNFL results, the spread of values is unsatisfactory, approaching 25% of the absolute value of the parameter.

Figures 4.76 and 4.77 show the global void effect (with no leakage) versus cell irradiation.

Figure 4.76. HM PWR – Stage II – First recycle: Global void effect with no leakage

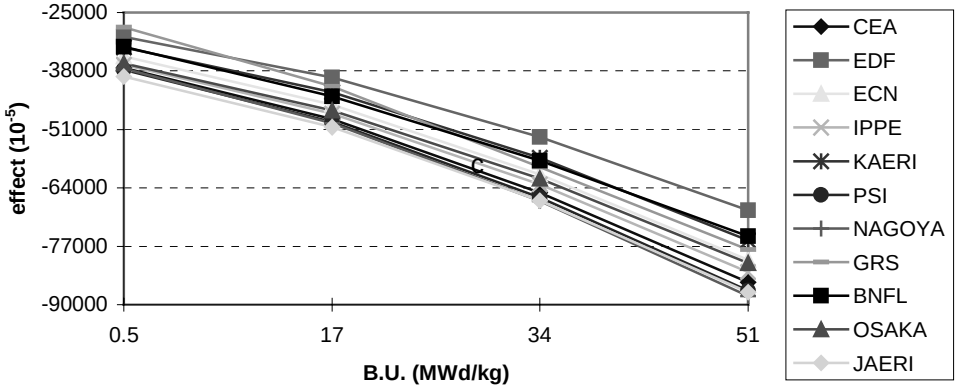

Figure 4.77. HM PWR – Stage II – Fifth recycle: Global void effect with no leakage

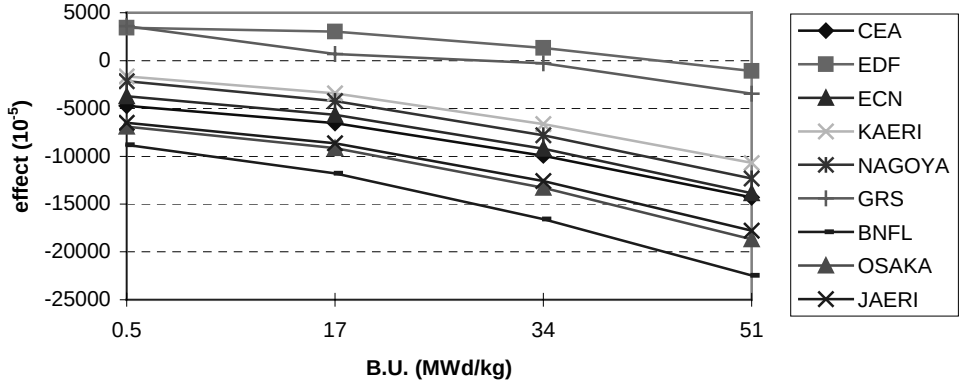

For the global void effect there is good agreement as to the trend with cell irradiation, although there remains a spread in the results which is large in absolute terms. In the fifth recycle generation, EDF, TOHOKU and GRS obtain positive values for the void effect at low irradiations, whereas all the other participants obtain small negative values. The void effect including leakage shows larger discrepancies (about 20%), which must arise from the flux and leakage calculations.

Mass balance

Figures 4.78 and 4.79 show the plutonium mass balances for the first and fifth recycle generations.

Figure 4.78. HM PWR – Stage II – First recycle: Plutonium mass balance (complete cycle)

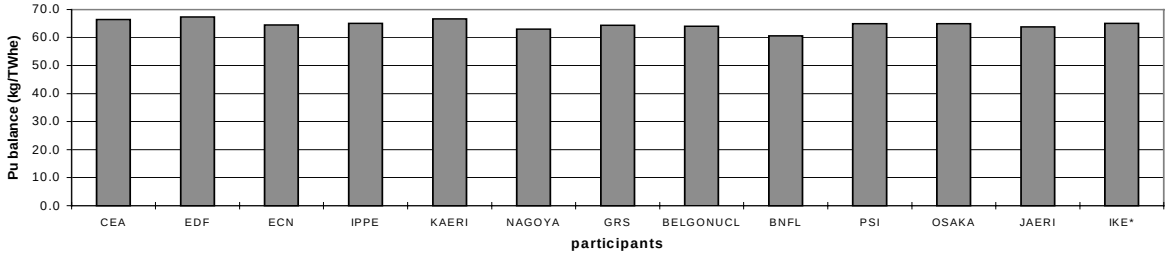

Figure 4.79. HM PWR – Stage II – Fifth recycle: Plutonium mass balance (complete cycle)

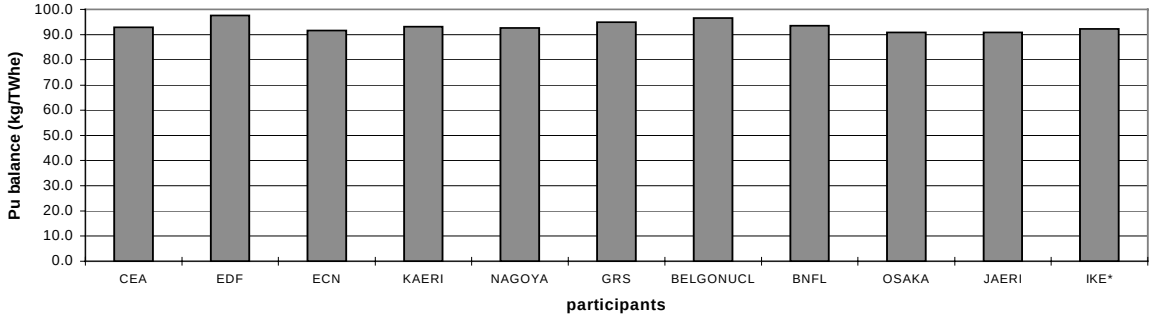

Plutonium consumption (-67 kg/TWhe) is slightly larger in the first recycle generation than for the STD PWR (-64 kg/eTWh) for an initial plutonium content which is some 30% smaller than for the STD PWR. In later recycle generations there is an increase in plutonium consumption to 90 kg/TWhe, higher than attained in the STD PWR. All the participants are in reasonably good agreement.

Figures 4.80 and 4.81 show the mass balances for americium.

Figure 4.80. HM PWR – Stage II – First recycle: Americium mass balance (complete cycle)

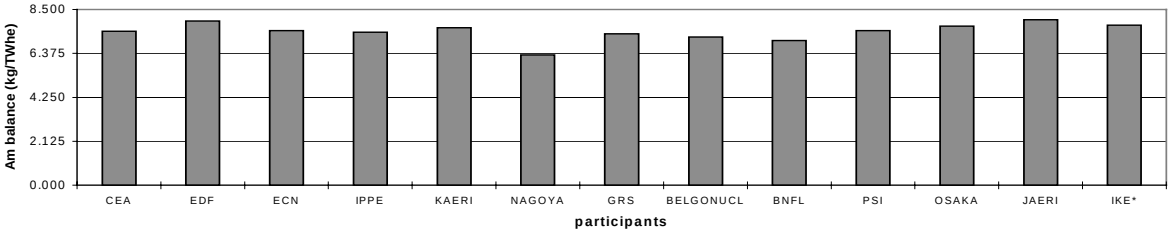

Figure 4.81. HM PWR – Stage II – Fifth recycle: Americium mass balance (complete cycle)

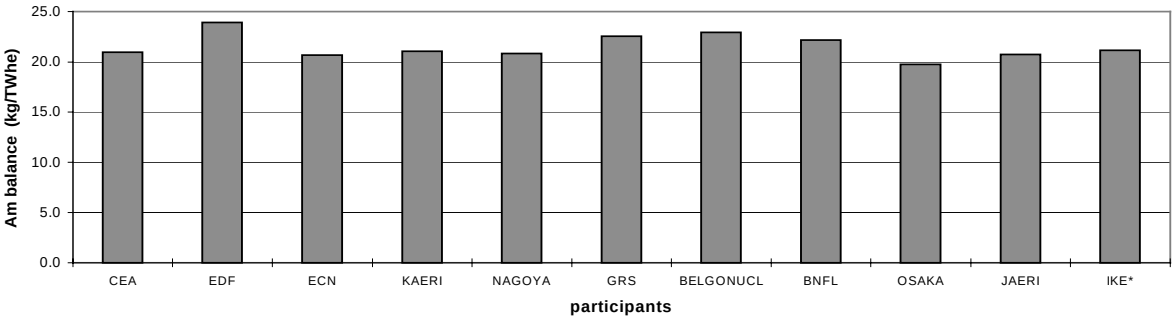

Americium production is a factor 2 lower for the HM PWR, compared with the STD PWR, primarily because of the lower initial plutonium content. The results are in good agreement. For the fifth recycle generation, the americium inventory is some three times that in the first generation, due to the higher initial plutonium content. Generally, the spread of values is larger than for the STD PWR.

Finally, Figures 4.82 and 4.83 show the mass balances for curium.

Figure 4.82. HM PWR – Stage II – First recycle: Curium mass balance (complete cycle)

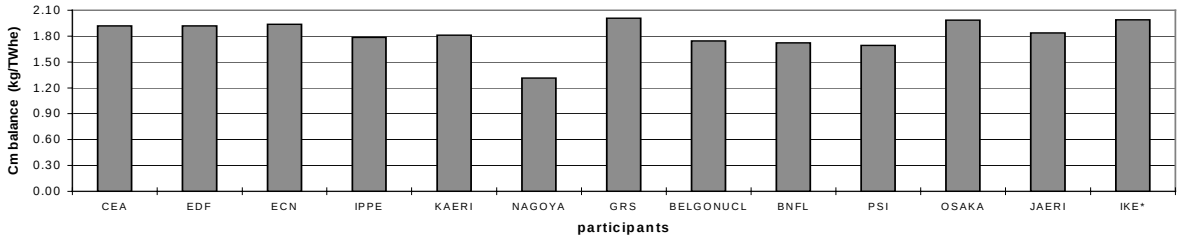

Figure 4.83. HM PWR – Stage II – Fifth recycle: Curium mass balance (complete cycle)

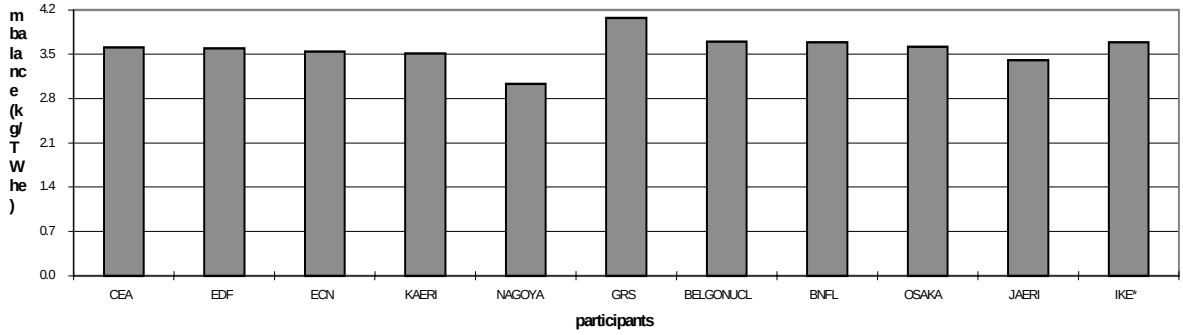

Curium mass balance is smaller for the HM ratio, especially for the first recycling. For the fifth recycling; curium production is similar for the two concepts. The spread between the participants is larger than for the standard PWR and than for the other elements. For the long-lived fission products, the production terms are very close for all the participants.

Activity and radiotoxicity

Comparisons are presented for the fresh fuel (for one metric tonne) and for irradiated fuel after five recycle generations in the STD PWR and in the HM PWR. The comparison is presented for the Stage II Benchmark which accumulates the effects of the different calculations of initial plutonium content and plutonium isotopic evolution.

Activities (for one metric tonne of fresh fuel)

Figure 4.84 shows the global activity levels per metric tonne of initial fuel mass for the first recycle generation fuel of the STD PWR, and Figure 4.85 shows the differences relative to CEA as the reference.

Figure 4.84. STD PWR – Stage II – First recycle:
Global activity of one heavy metal metric tonne of initial fuel

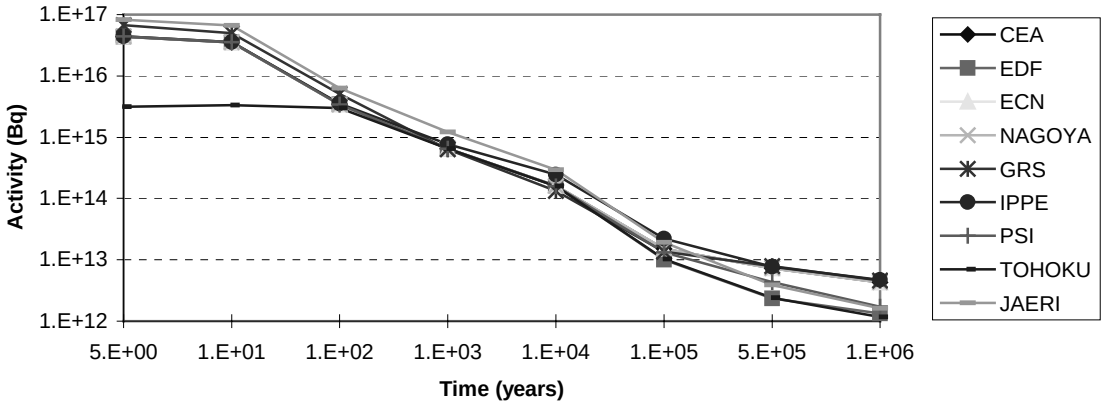

Figure 4.85. STD PWR – Stage II – First recycle:
Global activity of tonne of initial fuel – Comparison with CEA values

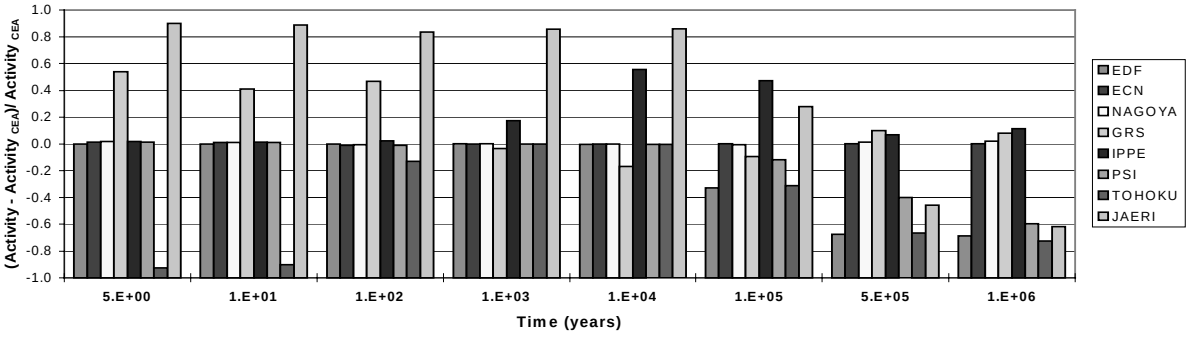

CEA values								
Time (years)	5	10	100	1000	10000	100000	500000	1000000
Activity (Bq)	4.36E+16	3.53E+16	3.46E+15	6.57E+14	1.60E+14	1.50E+13	7.21E+12	4.25E+12

For the shorter term periods, EDF, CEA, ECN, IPPE, PSI are in good agreement. For the long-term period, however, larger discrepancies appear, presumably due mainly to differences the decay chains used. Overall, the agreement is reasonably satisfactory.

Figures 4.86 and 4.87 show the corresponding plots for the STD PWR in the fifth recycle generation. For the STD PWR in the fifth recycle generation, the discrepancies are larger than for the initial step, covering a range +10% to -40%, which may be considered reasonably satisfactory.

Figure 4.86. STD PWR – Stage II – Fifth recycle:
Global activity of one heavy metal metric tonne of irradiated fuel

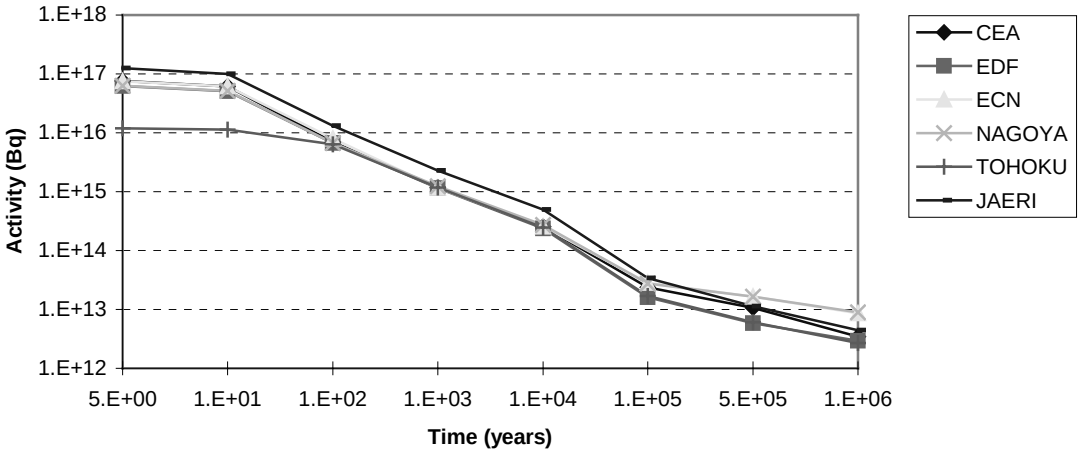

Figure 4.87. STD PWR – Stage II – Fifth recycle:
Global activity of tonne of irradiated fuel – Comparison with CEA values

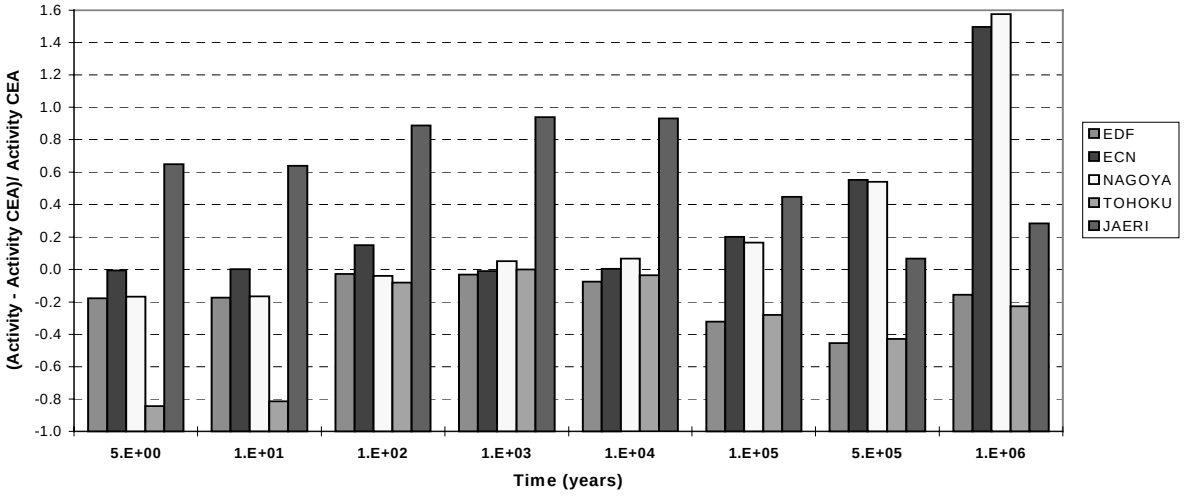

CEA values								
Time (years)	5	10	100	1000	10000	100000	500000	1000000
Activity (Bq)	7.55E+16	6.14E+16	6.93E+15	1.18E+15	2.56E+14	2.36E+13	1.06E+13	3.47E+12

Figures 4.88 and 4.89 present the same plots for the HM PWR in the fifth recycle generation. For the HM PWR, differences are larger, extending over a range of +10% to -60%. Activity is smaller for the irradiated fuel in the HM PWR, about 50% lower, due to the softer neutron spectrum and the lower initial plutonium content.

Figure 4.88. HM PWR – Stage II – Fifth recycle:
Global activity of one heavy metal metric tonne of irradiated fuel

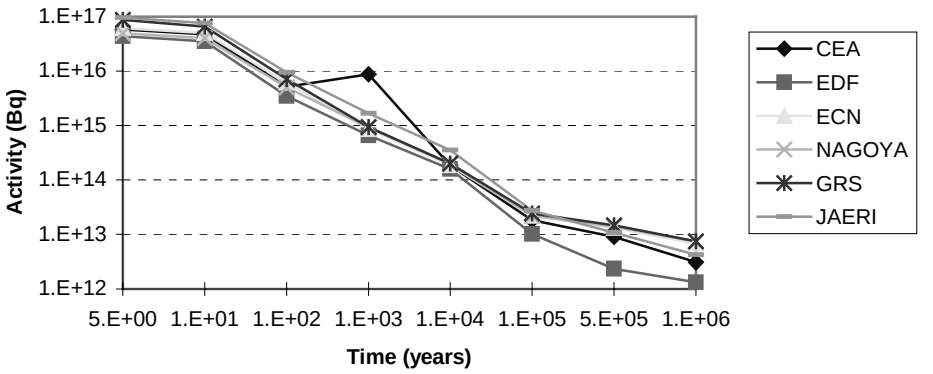

Figure 4.89. HM PWR – Stage II – Fifth recycle:
Global activity of tonne of irradiated fuel – Comparison with CEA values

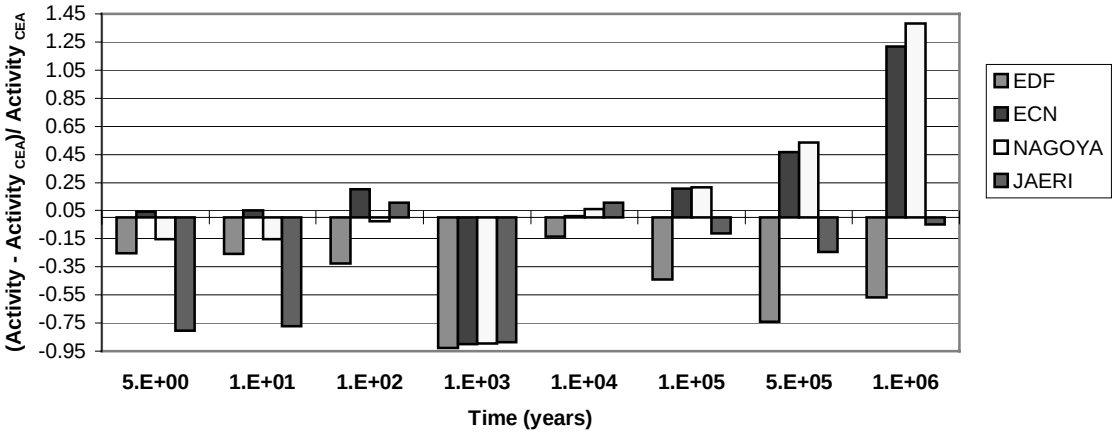

Radiotoxicities

Radiotoxicities depend on the data used for the risk coefficients and on the activities. Only a small number of participants provided results on toxicities and these were presented differently, some of them in Sv, some in CD (Cancer Dose). The following table lists unit each participant used.

Data used	
CEA	Sv
ECN	CD
EDF	Sv
IPPE	Sv
JAERI	CD
PSI	CD

Figures 4.90 and 4.91 plot the radiotoxicities associated with heavy nuclides versus time for the STD PWR. These calculations assume that the multiple recycle is terminated after the fifth recycle generation.

For one metric tonne of fresh fuel

Figure 4.90. STD PWR – Stage II: Radiotoxicity of heavy nuclides of initial fuel

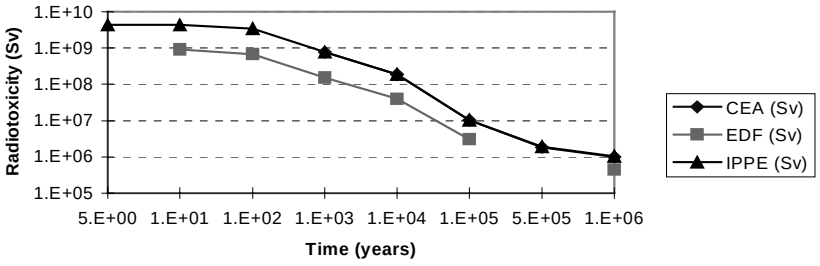

Figure 4.91. STD PWR – Stage II: Radiotoxicity of heavy nuclides of initial fuel

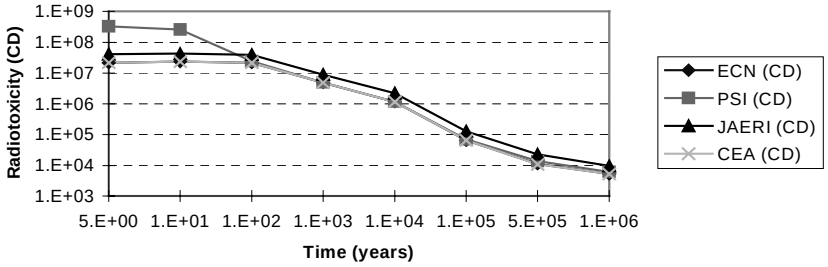

There is a factor up to 5 spread between the participants for the short-term period, reducing to a factor 2 for the long-term period. For comparison, the change from ICRP 30 to ICRP 68 provides a reduction of the radiotoxicity by a factor up to 5.

Annex to Chapter 4

Energy per reaction

This annex provides plots of the energies releases associated with the various reactions obtained by each participant.

Per fission

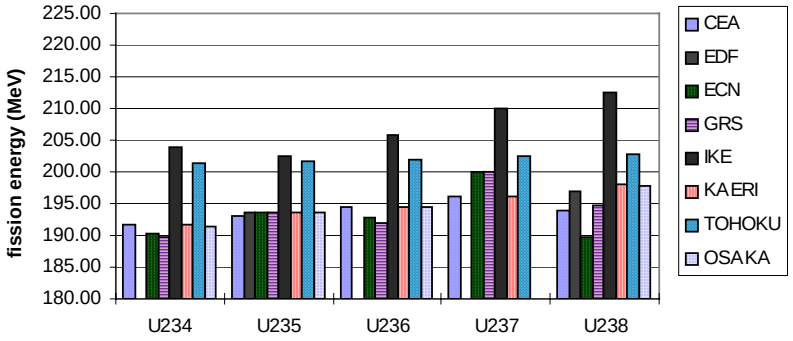

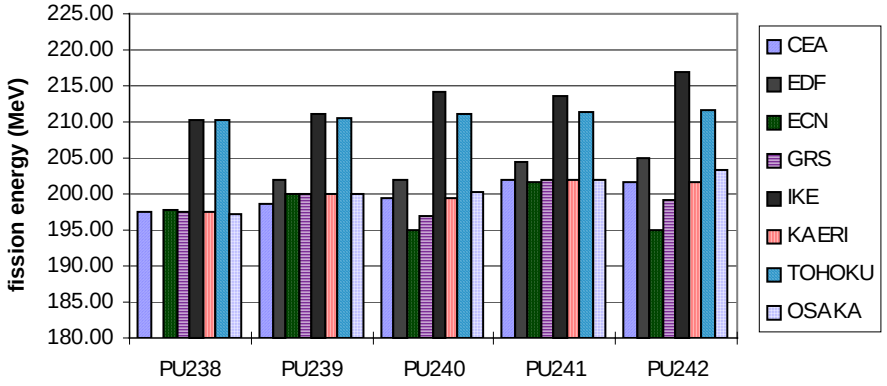

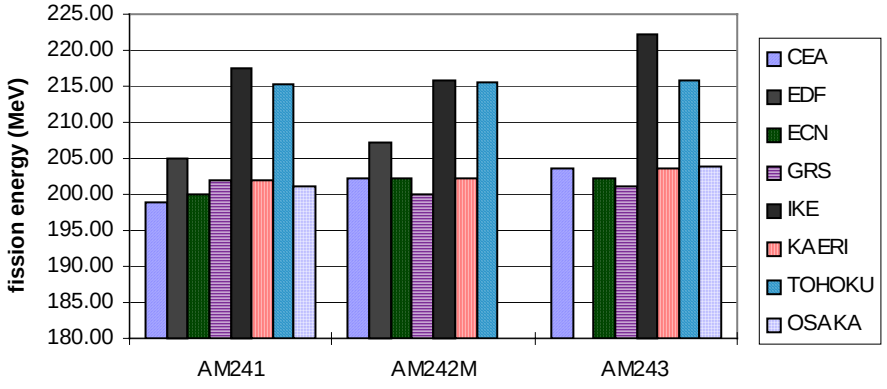

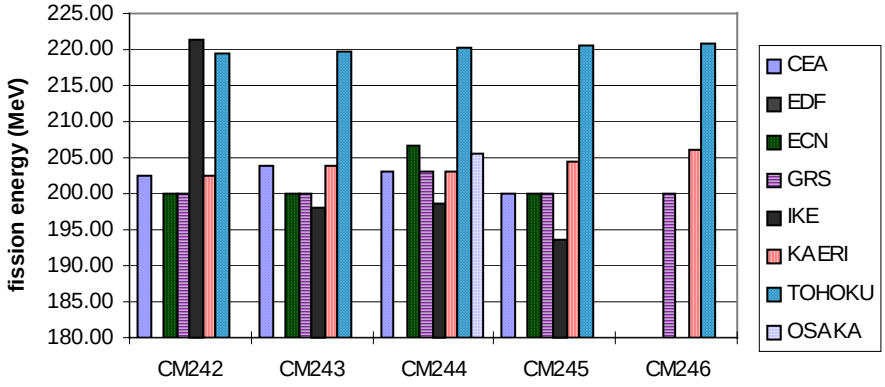
225.00
220.00
215.00
210.00
205.00
200.00
195.00
190.00
185.00
180.00
fission energy (MeV)
CM242
CM243
CM244
CM245
CM246
CEA
EDF
ECN
GRS
IKE
KAERI
TOHOKU
OSAKA

Per capture

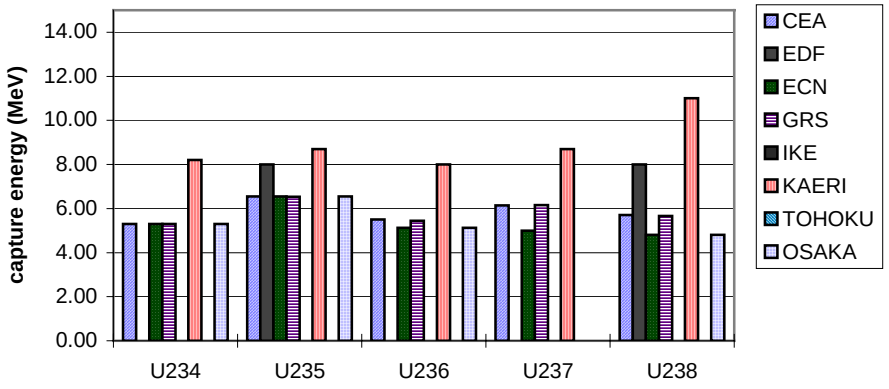
14.00
12.00
10.00
8.00
6.00
4.00
2.00
0.00
capture energy (MeV)
U234
U235
U236
U237
U238
CEA
EDF
ECN
GRS
IKE
KAERI
TOHOKU
OSAKA

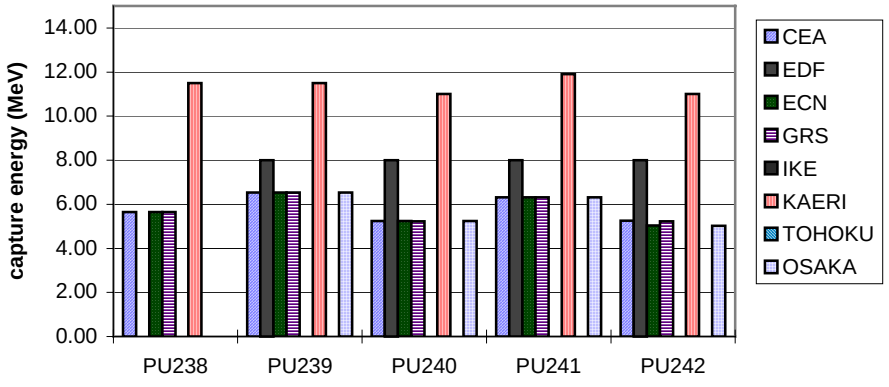
14.00
12.00
10.00
8.00
6.00
4.00
2.00
0.00
capture energy (MeV)
PU238
PU239
PU240
PU241
PU242
CEA
EDF
ECN
GRS
IKE
KAERI
TOHOKU
OSAKA

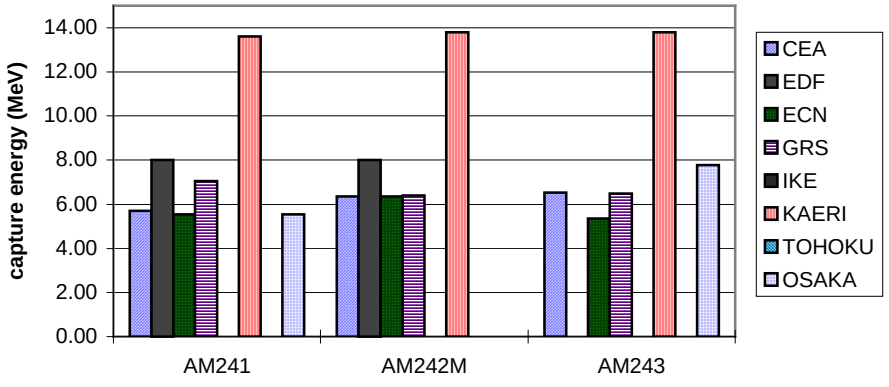
14.00
12.00
10.00
8.00
6.00
4.00
2.00
0.00
capture energy (MeV)
AM241
AM242M
AM243
CEA
EDF
ECN
GRS
IKE
KAERI
TOHOKU
OSAKA

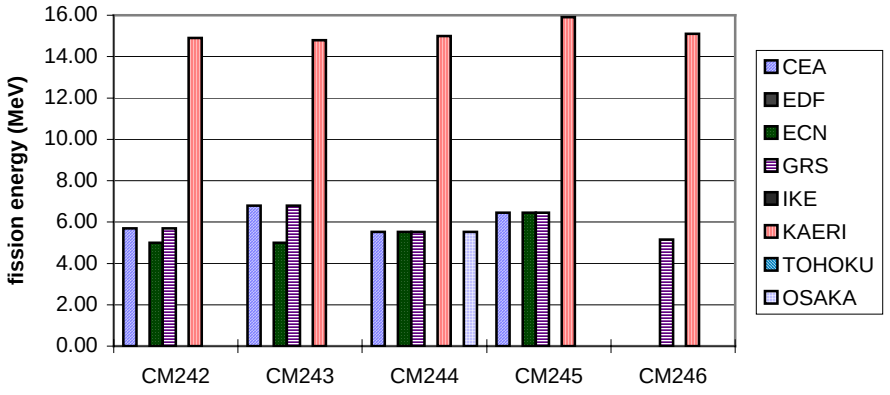
fission energy (MeV)
16.00
14.00
12.00
10.00
8.00
6.00
4.00
2.00
0.00
CM242
CM243
CM244
CM245
CM246
CEA
EDF
ECN
GRS
IKE
KAERI
TOHOKU
OSAKA

Chapter 5

DISCUSSION AND INTERPRETATION OF RESULTS

Objective

The purpose of this chapter is to comment on the results of the STD and HM Benchmarks described in Chapter 4 from the viewpoint of reactor operation and to summarise the lessons that have been learned. This chapter is organised into two parts, the first being a review of all aspects pertaining to the Stage I Benchmark, and the second an equivalent review for the Stage II Benchmark.

Stage I Benchmark

Lifetime average reactivity

This is the determining factor for the fuel cycle length and equivalently, the initial plutonium content needed to achieve a given cycle length. For the STD PWR Benchmark, the spread of reactivities summarised in Table 5.1 (ignoring one outlying solution), varies from 0.9%Δk in the first generation to 1.4%Δk in the fifth generation. For the HM PWR Benchmark, the spreads are somewhat higher, but this time improving from 2.3%Δk in the first generation to 1.3%Δk in the fifth.

Table 5.1. Summary of spread in lifetime average reactivity values

Reactivity (% variation)	STD PWR		HM PWR	
	Cycle 1	Cycle 5	Cycle 1	Cycle 5
Spread (%Δk_{EOI})	0.9	1.4	2.3	1.3

These spreads are considerably better than achieved in the 1994 Benchmark (refer to Vol. I), but are they adequate for operational purposes? This question is not a straightforward one and requires careful consideration: the desired calculational uncertainty on cycle length in conventional PWRs using UOX fuel is usually set at ±20 ppm critical boron, though occasionally errors as high as ±50 ppm are considered acceptable in practice. With a typical boron reactivity coefficient of up to -10 pcm/ppm for UOX, these correspond to reactivity uncertainties in the region of 200 pcm and 500 pcm respectively. Taking the 20 ppm uncertainty as typical, an excess of reactivity in the actual cycle compared with calculation implies that the cycle will end prematurely when the critical boron is still 20 ppm higher than the lowest attainable value (usually about 10 ppm). In the event that the actual reactivity falls short, the 200 pcm reactivity would be made up by continuing operation with the reactor power coasting down gradually, compensating for the reactivity shortfall with the total power coefficient.

Considering, for the sake of argument, an all MOX core, the practicalities are somewhat different. First the boron reactivity coefficient is considerably smaller, as low as -2 pcm/ppm, so that the same reactivity shortfall of 200 pcm would allow the cycle to continue much longer than in the

case of UOX because of the smaller reactivity gradient of MOX. Thus the rate at which the reactivity would fall, and therefore the rate at which the reactor power would need to reduce to compensate, would be much lower. Thus, for example in first generation MOX, the reactivity loss between 0 and 51 MWd/kg is approximately 20%Δk, compared with 50%Δk with UOX. Therefore for first generation MOX, a shortfall in reactivity of 500 pcm would have the same impact in terms of power generation loss as 200 pcm in UOX. For later generations the latitude in reactivity is even higher, as the reactivity gradient is smaller. If -0.2 MWd/kg (5 EFPD) is kept as a target, then MOX uncertainty of 100 pcm is required.

This line of argument would suggest that the reactivity target uncertainty for MOX could possibly be relaxed by a factor of at least 2.5 compared with UOX, with a desirable value of 500 pcm and an upper limit of 1250 pcm. With UOX and MOX assemblies co-resident in a mixed core, the same argument would apply. The observed spread in reactivities in this benchmark is actually not far from the desirable value, suggesting that maybe the current codes are already in acceptable agreement.

In practice, of course, without a set of measurement data we are unable to say what the correct answer should be and it is possible that all the results obtained show systematic errors from the "true" values. This underlines the point that benchmark studies such as this are inadequate without operational data to pin-point the correct values. Moreover, the required level of accuracy will most certainly be beyond any of the codes without empirical guidance. This must be obtained from operational experience, starting with demonstration assemblies with appropriate plutonium isotopics and concentrations.

This conclusion should not be surprising, as it is always necessary to gain operational experience when the design parameters progress sufficiently far from existing experience. What is most relevant now is the question of how reliably the existing codes could be used to predict the behaviour of demonstration assemblies. In this respect the requirements on the codes are not so demanding. First of all, since it is usual to load just a few demonstration assemblies in the core to begin with, the impact of errors on end-of-life reactivity are correspondingly diminished. Moreover, it is usual to ensure that such assemblies are kept well away from being the lead assemblies in terms of rating that define the operational and safety limits. For both these reasons, the same degree of confidence is not required for demonstration purposes and could therefore be argued that the level of agreement already achieved would allow a demonstration assembly programme to go ahead with a good degree of confidence. Of course, as the demonstration programme proceeds, the experimental data obtained allows the code systems to be adjusted empirically to ensure a lower calculational uncertainty for later phases.

All the above comments apply to the standard PWR lattice. For the highly moderated lattice, the same arguments will apply, except that the boron reactivity coefficient will be closer to the values seen in a UOX core and the reactivity gradient with burn-up is slightly steeper than for STD MOX. The desirable uncertainty will also depend on the total power coefficient, which may be different from the standard lattice.

In conclusion, therefore, the observed spread of results from the different participants may possibly be adequate for operational purposes and would certainly be sufficient for supporting a demonstration programme. This would be the next logical step required if multiple recycle MOX was to be pursued in practice. With the relatively small spread in end-of-cycle reactivities obtained in these benchmarks, it will be difficult to identify the precise causes in terms of underlying nuclear data and/or calculational methods, as they are likely to be too small to show up obviously even on

examining the microscopic cross-sections. Moreover, there are likely to be several factors combining together to give the spreads seen here, which would further complicate at attempt to isolate any of them. There seems little point, therefore, in a follow-up benchmark to the present ones.

Reactivity versus burn-up

Reactivity versus burn-up is the determining factor for the variation of critical boron versus cycle burn-up. It is also inter-related with the lifetime average reactivity. For both the STD and HM PWRs, the reactivity versus burn-up curves plotted in Chapter 4 show essentially the same spreads as do the end-of-cycle reactivities. As in the 1994 Benchmark (reference to Vol. I), the gradients of reactivity versus burn-up are fairly consistent between the various participants, at least at first examination, indicating that the solution of the burn-up equations are reasonably consistent and are not greatly affected by the reactivity spread. Table 5.2 summarises the spread in beginning-of-irradiation (0 MWd/kg) and end-of-irradiation (EOI) cycle reactivity spreads seen for Cycles 1 and 5, with the distant outliers excluded.

Table 5.2. Summary of beginning-of-irradiation and end-of-irradiation reactivity spreads

Reactivity (% variation)	STD PWR		HM PWR	
	Cycle 1	Cycle 5	Cycle 1	Cycle 5
Spread (%Δk_{BOI})	0.8	1.0	1.5	1.4
Spread (%Δk_{EOI})	1.2	1.9	4.0	1.7

For the standard PWR the spreads are always no more than 1.0%Δk at BOI and 1.9%Δk at EOI, which are encouragingly tight. More detailed examination of the reactivity gradients for the STD PWR shows that there is a sub-population represented by the three Japanese solutions with systematically different trends. Thus in all generations the Japanese solutions start off at zero burn-up with a reactivity very close to the CEA solution treated as a reference, but a difference accumulates of around +1%Δk by 51 MWd/kg. This is most probably an effect resulting from the nuclear data libraries, with the Japanese libraries giving a slightly different trend to the others.

The same trends are seen for the HM PWR data, except than in this case the spread of values is somewhat larger in the first generation, at 1.5 to 4.0%Δk. The large spread at EOI is due to two solutions showing the opposite trend with burn-up of the other solutions. If these two data sets are omitted, the spread is more than halved. In later cycles the spread decreases (ignoring one outlying solution).

For both STD and HM cases the spreads in EOI reactivities are larger than those for the lifetime average reactivities of the following section, largely because the latter are determined by the 34 MWd/kg burn-up step; the EOI reactivities are determined by the 51 MWd/kg step, with the spread tending to increase with burn-up.

Taking the spreads in Table 5.2 to be representative, they are higher than would be desirable in an operating PWR. The spread of BOI reactivities up 1.0%Δk in the STD case would adversely affect the prediction of the critical boron. For a UOX core, the ideal target would be 0.2%Δk and the maximum permissible 0.5%Δk. The MOX value is considerably higher and the situation is made worse by the very small boron coefficient, such that the 1.0%Δk would translate into a very large uncertainty on initial critical boron. There are limits to which the initial boron could be allowed to deviate, due to requirements to keep within various limits related to guaranteeing sub-criticality in the

shutdown condition and the boration requirements following an emergency shutdown. As previously demonstrated, this further emphasises the need for operational data to tie down the uncertainties.

Boron reactivity coefficient

The boron reactivity coefficient (or boron efficiency) is a simple parameter for the codes to calculate and provided there are no gross spectral differences between the various codes, the spread of values obtained could be expected to be small. Table 5.3 confirms this, giving the spread of values for the first and fifth generation cases and beginning and end of irradiation (BOI & EOI). The boron coefficient is expressed in terms of the reactivity effect in pcm (1E-5 Δk) per ppm increase in boron concentration. Table 5.3 plots the absolute difference (in pcm/ppm) between the highest and the lowest values.

For the STD PWR, the observed spread in values is of the order of 0.3 pcm/ppm or less and shows only a slight trend to worsen in later generations. There is evidence of clustering about a tight spread (ignoring two outlying solutions). The variation of boron coefficient with burn-up is very consistent between the different solutions, and it is quite significant, increasing by around 50% between BOI and EOI. For the STD case the boron coefficients are very small in absolute magnitude, in the region of 20% of that for a normal UOX core. This is the principal reason why current PWRs would not be able to accept a 100% MOX loading, as the boration requirements for normal and emergency shutdown would be excessive.

Table 5.3. Summary of spread in boron reactivity coefficient values

Reactivity Coefficient (pcm/ppm)	STD PWR		HM PWR	
	Cycle 1	Cycle 5	Cycle 1	Cycle 5
BOI	0.21	0.26	0.18	0.24
EOI	0.16	0.32	1.20	0.26

For the HM PWR, the boron efficiencies are much larger in absolute terms, reflecting the more thermalised spectrum and the large volume of moderator in the assembly. The spread of values is generally very small, with the first generation only showing quite a large spread at EOI. Hence the 1.20 pcm/ppm value in Table 5.3 overstates the spread which applies more generally and it is fair to say that with this one exception, there is excellent agreement between the different codes.

An interesting observation is that the boron coefficient varies very dramatically from BOI to EOI in the early generations, but is less sensitive in the later ones. Thus in the first generation, the boron coefficient varies by more than a factor 2 between BOI and EOI. This is a result of the efficient burn-out of the fissile plutonium, with correspondingly lower production of fresh ^{239}Pu from ^{238}U captures, which will affect the level of thermal absorption and the spectrum. In later generations, the non-fissile absorption starts to dominate and the burn-out effect becomes much less evident in the boron coefficient.

In terms of operational requirements, the observed spread in boron coefficient falls within the 10% uncertainty allowance that typically applies to current PWRs and indicates that the boron coefficient calculations are likely to be satisfactory for both the STD and HM cases.

Moderator temperature coefficient

The moderator temperature coefficient (MTC) is important for determining the shutdown margin, the amount of negative feedback in heat-up faults and conversely the amount of reactivity insertion in cool-down faults. The benchmark specifications called for the MTC to be calculated at various cell burn-ups ranging from 0 MWd/kg (BOI) to 51 MWd/kg (EOI). Table 5.4 summarises the absolute spread of values obtained for the STD and HM cases, for the first and fifth generations, in units of pcm/K. The figures quoted exclude one outlying solution.

Table 5.4. Summary of spread in moderator temperature coefficient values

Reactivity Coefficient (pcm/K)	STD PWR		HM PWR	
	Cycle 1	Cycle 5	Cycle 1	Cycle 5
BOI	4.0	4.0	N/A	6.4
EOI	4.5	6.3	N/A	8.4

N/A: Not Applicable

The benchmark specification called for the MTC calculations to be carried out at zero boron, so they are representative of the condition at the end of a refuelling cycle with close to zero boron concentration. For the STD case, the spread in values is quite small, with no evidence of any deterioration with cell burn-up or with recycle generation. There is excellent agreement between the various solutions as to the change in MTC with cell burn-up, all the solutions having virtually the same gradient. This applies to all the recycle generations. Moreover, there is good agreement as to the trend in the absolute value of the MTC in the different generations. In terms of relative error, the spread represents a plus or minus of no more than 5% in the first generation and 10% in the fifth generation. The relative error is higher in the later generations largely because the absolute magnitude of the MTC falls with increasing recycle generation.

For current PWRs, the acceptable uncertainty on MTC in the zero boron end-of-refuelling-cycle condition would typically be set at around 10%. The spread in values obtained here, if they are taken to represent the inherent uncertainty, suggest that the MTC calculations would be acceptable for operational purposes.

In contrast, the situation is less satisfactory for the HM case, especially in the first generation. The problem is that in the first case there is not even agreement between the various solutions as to the trend with increasing cell burn-up. Thus one group of solutions shows a monotonic variation with burn-up, whereas another (larger) group of solutions shows the MTC increasing in magnitude at intermediate burn-ups. This is why no values have been tabulated in Table 5.4 for the first generation case; the spread is meaningless in this case. In the second generation, this behaviour is no longer seen and the dependence on cell burn-up again becomes monotonic for all except one outlying solution. The spread in values tends to improve beyond the second generation, though it remains larger than in the STD case. There is evidence in all generations of two distinct sub-sets of solutions with different gradients of MTC with cell burn-up. Within each of the two sets, the spread is much smaller.

The reason for this less than satisfactory outcome for the HM PWR is not clear, but it must presumably be connected with the different spectral conditions in the HM case. At zero boron, the STD PWR is well undermoderated, so that the competition between moderation and absorption in the water is biased very heavily towards the former. In the HM PWR the balance between these opposing effects is more even, and this would tend to make the calculation more difficult. The suggestion of a

maximum in the MTC at intermediate cell burn-ups in the first generation may well be real. In the first generation the plutonium content is very much smaller than even the second generation and it is conceivable that this could affect the burn-up dependence, given that absorption in the fuel would be relatively low.

Fuel temperature coefficient

The fuel temperature (or Doppler) coefficient is important for ensuring rapid negative feedback in transients involving an increase in reactor power. It is also very important in determining the amount of shutdown margin available, since there is positive reactivity insertion from the decrease of fuel temperature between the operating and zero power conditions. Based on the results presented in Chapter 4, Table 5.5 summarises the spread of the calculated values for the first and fifth recycle generations at BOI and EOI conditions. The observed spreads represent between 20 and 30% of the absolute value of the reactivity coefficient and are quite significant.

Table 5.5. Summary of spread in fuel temperature coefficient values

Reactivity Coefficient (pcm/K)	STD PWR		HM PWR	
	Cycle 1	Cycle 5	Cycle 1	Cycle 5
BOI	0.4	0.6	0.3	0.6
EOI	0.7	0.7	0.6	0.8

For both the STD case the various results are fairly consistent in that the trend with burn-up is in close agreement for all the recycle generations and relative rankings remain consistent throughout. The spread of results is most likely due to differences in the treatment of ^{242}Pu resonance absorptions between the various codes. Some of the codes have a temperature dependent tabulation for all resonance isotopes, whereas others may only have a tabulation for a limited range of isotopes. The resonance absorptions in ^{240}Pu and ^{242}Pu are not important contributors to the fuel temperature coefficient in UOX fuel or in MOX fuel with low levels of these isotopes. However, they are very important contributors for these benchmarks. Therefore a code in which, for example, only the ^{238}U and ^{240}Pu resonance parameters are tabulated versus temperature, the fuel temperature coefficient would be expected to be smaller in magnitude. This is precisely the case for the WIMS code, so that the BNFL solution does not incorporate the contribution of ^{242}Pu to the fuel temperature coefficient. We are therefore led to the conclusion that a full temperature dependent resonance tabulation is essential for the situation examined here. Note that if there is only one resonance temperature in the tabulation, it is usual for a fuel material for it to correspond to full power operation. Therefore predictions of reactivity and power in the full power condition will be correct and it is only with deviations from full power where an error will be incurred.

There is a consistent trend for the fuel temperature coefficient to increase in magnitude with burn-up. Perhaps this is due partly to the increase in concentration of the even isotopes with burn-up. There are only small changes between recycle generations, suggesting that changes in the neutron spectrum in the resonance range are modest. There is only a modest deterioration in the spread of results in later recycle generations.

The HM case shows much the same trends, although in this case there are some anomalous results (showing the opposite trend with burn-up) in the first two generations. The magnitude of the fuel temperature coefficient is a little smaller in this case, presumably due to the softer spectrum and the reduction in resonance capture probability that would be expected with the wet lattice.

Reactivity balance

The reactivity balance is the gradient in reactivity with burn-up during an equilibrium fuel cycle (measured in 10^{-5} Δk/MWd/kg or pcm/MWd/kg). It is important for several reasons, one being that it determines the boron letdown rate during the cycle, and another being that it determines the rate of reduction of power during a power stretchout under which the reactor might operate beyond the natural end of cycle. The various results are reasonably consistent and all participants showed the same trend with increasing recycle generation. Thus the reactivity balance falls dramatically between the first and second generations, but thereafter falls much more slowly, with a gradual levelling off to around 250 pcm/MWd/kg. This is considerably lower than is characteristic of UOX fuel, where a value approaching 1 000 pcm/MWd/kg is more typical. This implies a lower rate at which the critical boron needs to be let down during the cycle. It also implies that reactor power will diminish less rapidly during power stretchout operation, which would be beneficial in terms of total generation capacity.

The HM PWR results are similarly fairly consistent between the various participants. However, in this case the let down rate is much higher in the first recycle generation (~600 pcm/MWd/kg). This is due to the more effective burn-out of ^{239}Pu with the soft spectrum. However, in subsequent generations there is a rapid change towards an asymptotic value of just under 300 pcm/MWd/kg, not far removed from the STD PWR value. The two cases converge because the more rapid deterioration of the plutonium isotopic vector in the HM PWR largely cancels outs the effect of the softer spectrum.

Global void defect

The void defect is the change in reactivity associated with voiding the reactor core, as might happen in the event of steam or gas bubbles displacing the moderator. The design objective is to ensure that the overall void defect of the core is negative, in order to ensure a negative feedback mechanism. In the STD PWR, the MOX assemblies will only constitute a fraction of the core loading and so the positive values obtained in the later recycle generations do not necessarily mean that the core would be unsuitable to licence. Nevertheless, it is worrying that the void defect is positive for all except the first recycle generation, due to the high plutonium concentrations needed.

Two sets of calculations were requested, one for an infinite lattice (no leakage) and one which takes account of the finite diffusion length of fast neutrons and the consequent increase in leakage in the voided condition. The spread of results is already large for the no leakage case and larger still for the case where specified leakages have been applied to the unvoided and unvoided conditions. This probably reflects the nature of the problem where the fully moderated condition corresponds to a normal PWR spectrum and where the voided condition corresponds more closely to a fast reactor spectrum.

The spread may be partly a result of difficulties in some of the codes in calculating the resonance absorption of ^{238}U, ^{240}Pu and ^{242}Pu in the voided condition (where the resonance integrals will be considerably higher than in any normal application of the codes). The larger spread in the presence of leakages suggests that the various participants' codes may not necessarily have been consistent in applying the leakage corrections and therefore the void defects with leakages do not contribute usefully to this comparison.

For the HM PWR the void defects with no leakage are generally in closer agreement. The values are more negative in early recycle generations and remain negative even in the fifth generation. The

spread of values is also in much closer agreement. As with the STD PWR case, introducing leakage greatly increases the spread of results, though all the values remain negative. This implies that the HM PWR does offer benefits over the STD PWR in that a negative void defect is virtually assured in all recycle generations. This is an essential requirement, since in this case there are no UOX assemblies in the core which might tilt the balance from positive to negative.

Stage II Benchmark

Lifetime average reactivity

For the Stage II Benchmarks, the specification calls for each participant to adjust the initial plutonium content in order that the same lifetime average reactivity matches that obtained in the first generation of Stage I. Thus, taking CEA as an example, the k-infinity at 34 MWd/kg, zero boron in the first generation was 1.037. In subsequent generations, the initial plutonium was adjusted to preserve this lifetime average. Table 5.6 summarises the spread of results obtained. For the STD PWR, the initial plutonium in the first generation (Cycle 1) was defined as a common starting point in the specification of the benchmark and the spread is therefore zero. This is why Table 5.6 starts with the second generation. For the HM PWR, the participants were asked to calculate the initial plutonium in all generations, including the first.

Table 5.6. Summary of spread in initial plutonium values

Initial Plutonium (atom % variation)	STD PWR		HM PWR	
	Cycle 2	Cycle 5	Cycle 1	Cycle 5
Spread (atom %)	0.8	2.5	0.6	2.9

The values quoted in Table 5.6 are selective in that two of the solutions have been disregarded. For these two cases, the initial plutonium content was not changed beyond the second generation, presumably due to a mis-interpretation of the Benchmark specification and it is therefore not appropriate to include them. For both the STD and HM cases, the spread starts off small (< 1 w/o absolute variation in total plutonium). As the number of generations increases, the spread naturally increases, as in this case both the underlying reactivity calculation differs between the various solutions (as was the case in Stage I) and the plutonium isotopic composition varies as well. The latter is a cumulative effect, since a systematic difference in plutonium evolution carries over from one generation to the next and leads to a spread of approaching 3 w/o in the fifth generation. Although quite large in absolute terms, since the initial plutonium content in the fifth generation is around 20 w/o, the spread represents a relative error of plus or minus 7.5%, which is encouragingly small.

An important point to note is that the rate of increase in initial plutonium between generations is much higher for the HM PWR than for the STD PWR. For the HM case, the first generation requires just over 6 w/o plutonium, rising to around 17 w/o in the fifth generation. The corresponding figures for the STD PWR are 10 w/o and 19 w/o respectively. The reason for this is that the HM PWR is better at fissioning the ^{239}Pu and ^{241}Pu in the soft spectrum, so that the isotopic quality degrades more quickly between generations. Thus, although the HM PWR starts off with a low initial plutonium concentration in the first generation, it has a tendency to catch up with the STD case. This is a significant observation, in that the initial advantage of the HM PWR (*i.e.* lower initial plutonium concentration) is eroded in later generations.

Mass balances

The mass balance of Pu, Am and Cm are important for the Stage II Benchmark, as they are a determining factor for the environmental impact. It is therefore important to be confident that they are calculated consistently between the various participants. The mass balances are defined in terms of the build-up or destruction rate in kg per TWh(electrical). The various solutions are generally in very good agreement with one another, except for two and sometimes three solutions which are systematically lower than the remainder by a few percent. This observation applies equally to both the STD and the HM Benchmarks. Some general remarks are useful here.

- *Plutonium*
  The plutonium mass balance is negative for both the STD and HM cases, due to the destruction of the odd fissile isotopes. For both the STD and HM cases, the plutonium destruction rate increases with recycle generation (being some 40% higher in the fifth generation than in the first generation). In terms of kg/TWh(e), the destruction rate is only marginally higher in the HM case. However, this does not imply that the STD and HM cases are equivalent in terms of plutonium destruction. The point to remember is that the fuel mass is considerably smaller for the HM PWR and, at least in the early recycle generations, the concentration of plutonium is much smaller. Therefore, with reference to the initial plutonium content, the HM PWR is more effective at destroying plutonium.

- *Americium & Curium*
  The mass balances for Am and Cm are positive, meaning that they accumulate with burn-up and the build-up rate is higher in the later recycle generations. This result applies both to the STD and HM cases and is a result of the higher initial plutonium concentrations needed in later recycle generations; the higher initial plutonium mass leads to accelerated production of the trans-plutonium nuclides. In terms of kg/TWhe, the production rate is lower for the HM PWR than for the STD PWR in the early recycle generations, though the difference becomes marginal in the later generations.

Global activities

For the STD PWR global activities in the fuel at loading and at discharge are in reasonable agreement for more than half of the participants, but there some outlying results which deviate significantly. The spread of results is about the same in the first and fifth multiple recycle generations, so there is, encouragingly, no evidence of a worsening of the agreement with multiple recycle generation. The subsequent decay of activity is in reasonable agreement right up to the 1 million year cut-off, after allowing for the range of variation of values at discharge.

For the HM PWR, a similar situation is seen in the first recycle generation, but the spread of results increases noticeably by the fifth generation. This is indicative of strong disagreement between the various participants with respect to isotopic evolution for the HM PWR case. In the first generation recycle, the HM PWR case gives almost a factor 2 reduction in activity levels at discharge, and this persists through to the 1 million year calculation. The calculations suggest that for the fifth recycle generation this advantage of the HM PWR is somewhat eroded, but still persists to a lesser extent.

Radiotoxicities

For the radiotoxicity comparison, only a small fraction of the participants submitted calculations and those that were submitted are very discrepant. This is presumably due to lack of consistency in toxicity factor used, since the underlying activity levels are in much better agreement. No useful conclusion can be drawn from the information as submitted.

Chapter 6

RESULTS OF THE SPECIAL BENCHMARK ON PWR MOX PIN CELLS

Introduction

In its first phase of the programme of work the Working Party on Physics of Plutonium Recycling (WPPR) had commissioned several benchmarks. Two in particular concerned PWR pin cells with MOX of isotopic Pu vectors of different quality: from a first recycle (B) and a fifth recycle (A). Although the results from participants were found to agree considerably better than in a similar study carried out a decade earlier, they were still not completely satisfactory. For these benchmarks the spread in k-infinity after removing outlying solutions is in excess of 1%; this value would be unacceptable if it were representative of the uncertainty on lattice design calculations.

It was for this reason that a special investigation was proposed with the aim of better clarifying the sources of discrepancies among participants' results. Special emphasis was directed toward applied cross-section processing methods for users of JEF-2 and JENDL-3 evaluated data libraries (see Annex 1 to Chapter 6). The results of this specific benchmark study are the subject of this article.

The calculations were restricted to fresh fuel as in the originally defined benchmarks. A well defined geometry was chosen with a quadratic cell and 6 or 20 subdivisions in the fuel and 3 subdivisions in the moderator. The temperatures were slightly modified to enable continuous energy Monte Carlo calculations.

The participants were originally restricted to using JEF-2.2 and JENDL-3.1, but later, calculations applying the newer JENDL-3.2 database were accepted (see Table 6.1).

A request providing a four group rate and cross-section output was added to the specification to allow a more detailed association of the discrepancies to the different energy regions. A slightly different upper energy boundary for the thermal group was used in the SRAC calculations. Participants from JAERI verified that this discrepancy does not significantly influence the results.

General discussion

Tables 6.2a and 6.2b contain the global results of the contributions, the k-infinity values and the reaction rates of the three zones, for the degraded MOX pin cell (Case A) and the classical MOX fuel (Case B), respectively. The rates are normalised to the total absorption rate in the cell equal to 1.

In Tables 6.3a and 6.3b the relative differences of the results with respect to the MCNP4 solution of IKE1 are listed to facilitate an easier overview for comparisons. The production, fission and absorption rates are related to the corresponding total rates and converted to pcm by multiplying by a factor of 10^5.

Table 6.1. Characterisation of the contributions

ESTABL.	IDENTIF.	DATA-SOURCE	CODE	FUEL ZONES	REMARKS
IKE	IKE1	JEF-2.2	MCNP4	6	continuous energy
ECN	ECN1	JEF-2.2	WIMSD6	1	
ECN	ECN2	JEF-2.2	WIMSD6	6	
ECN	ECN3	JEF-2.2	WIMSD6	20	
CEA	CEA1	JEF-2.2	APOLLO-2	6	
CEA	CEA2	JEF-2.2	TRIPOLI-4	6	continuous energy
JAERI	JAE1	JENDL-3.1	SRAC	1	
JAERI	JAE2	JENDL-3.1	SRAC	6	
JAERI	JAE3	JENDL-3.2	SRAC	1	
JAERI	JAE4	JENDL-3.2	SRAC	6	
JAERI	JAE5	JENDL-3.2	MVP	1	continuous energy
JAERI	JAE6	JENDL-3.2	MVP	6	continuous energy

The Monte Carlo (MC) results using JEF-2.2 data (CEA2 and IKE1) differ by 200 pcm for Case A and 300 pcm for Case B. The MC results using JENDL-3.2 data are closer to the MCNP4 values in Case A (-80 pcm), but up to 400 pcm higher in the classical Case B. The difference between the 2 MVP results themselves is 137 pcm.

The deterministic codes using JEF-2.2 yield very different eigenvalues: the differences are between -289 and +354 pcm for Case A and between -204 and +606 pcm for Case B. The results calculated with JENDL data differ between 156 and 725 pcm and between 304 and 906 pcm, respectively. The highest differences occur for the SRAC calculations with six subdivisions of the fuel zone (JAE2 and JAE4).

The columns with production rates in Table 6.2 differ from k-infinity when production only by fission is given, but most participants included the (n,2n) and (n,3n) yields into the production rate. Because of these inconsistencies in the contributions, the production rates are not suitable for detailed comparisons. Instead, the fission rates are discussed. The (n,2n) rate itself is between 130 and 180 pcm. The absorption rates in fuel will be discussed in the next section. Surprising are the significant differences in absorption rates in clad and moderator between calculations with JEF-2.2 and JENDL data. The JAERI results show higher absorption rates in the clad of between 100 and 140 pcm and lower ones in the moderator of up to 80 pcm.

The results of a special study addressing the effects due to the use of cross-sections derived from JENDL-3.2, Jef-2.2 and ENDF/B-VI are given in Annex 2 to this chapter.

Discussion of differences in absorption rates

Tables 6.4 to 6.11 give information regarding the absorption rates for the isotopes in the fuel. The first column refers to the total absorption rates, and the following ones contain four group values corresponding to the requested energy subdivision (MeV, unresolved and resolved resonance and thermal region). In the first two lines the MCNP4 values and the corresponding values for the statistical standard deviations (sigma) in pcm are listed (the sigma values of the other MC calculations

are of the same order of magnitude). The following ones contain the differences between the other contributions and the MCNP4 results. Horizontal lines divide the sections when different databases are used. This representation shows which isotopes in what energy region are responsible for discrepancies in the results, but it cannot be decided if these are caused by differences in basic cross-sections or by different methods in resonance shielding and spectral calculations, respectively.

Tables 6.4a and 6.4b show the absorption rates of ^{235}U for Cases A and B. All results agree well, except those emerging from JENDL-3.1, which show a difference of about 100 pcm originating mainly from the resonance group.

The MC ^{238}U absorption rates (Table 6.5) of the two calculations with JEF-2.2 agree within the sigma interval, the JAERI results are 120 pcm lower caused by differences in the first and third energy groups. CEA1 shows a value of 65 pcm higher for Case A and a vlaue of 81 pcm lower for Case B, both generated in the first and third group. The ECN solutions differ in the MeV group by -120 pcm and in the resolved resonance group in the range of +250 to +270 pcm. The SRAC results for one fuel zone (JAE1 and JAE3) agree rather well, whereas the solutions with six zones have 300 to 400 pcm lower values in the third group for Cases A and B respectively. In addition the JENDL-3.2 solutions have about 100 pcm lower values in the first group.

For ^{238}Pu Table 6.6a shows a good agreement for all participants. The differences of up to 50 pcm originate from the resolved resonance group.

Tables 6.7a and 6.7b show the results for ^{239}Pu. The absorption rates of CEA2 are 100 and 230 pcm higher than the results of MCNP4; the MC results of JAERI are also higher by up to 326 pcm for Case A and up to 480 pcm for Case B, mainly due to differences in the thermal energy group. CEA1 results agree well for the total value for Case A, but show compensating differences of 92 pcm and -80 pcm in the third and fourth group. For Case B the total difference is 193 pcm originating from 74 and 130 pcm in the third and fourth group. The ECN differences are about -300 pcm for Case A, also caused by deviations in the third and (mainly) fourth group. The agreement for Case B is rather good. The differences of JENDL results are all positive and mostly originate from the thermal group. JENDL-3.1 has 160 and 329 pcm higher values for Cases A and B. JENDL-3.2 shows higher results of up to 376 pcm for Case A and up to 516 pcm higher values for Case B.

Table 6.8 compares the absorption rates of ^{240}Pu. The MC results of CEA2 are 132 pcm and 252 pcm lower for Cases A and B, the MVP differences are 175 pcm generated in the third and fourth group for Case A and are low for Case B, where positive and negative values in the third and fourth group of 70 to 80 pcm cancel. CEA1 has a value of 180 pcm lower, caused by +100 pcm in the resolved resonance group and -281 pcm in the thermal group for Case A. For Case B the differences are similar. The ECN and JAERI results agree rather well with the MC results in both cases, but in Case B the deviations in groups three and four are higher and have a compensating effect.

For ^{241}Pu the agreement of the absorption rates calculated by TRIPOLI-4 and MCNP4 is also good, whereas MVP gives values about 100 pcm lower, originating mainly from the thermal energy region. The CEA1 values are 75 and 91 pcm for A and B summed by about +40 pcm in the third and fourth group. The ECN values are higher for Case A by 230 pcm and 95 pcm for Case B. The discrepancies are mainly produced in the resolved resonance group. The JENDL-3.1 results are up to 226 pcm higher for Case A, which is caused by positive differences in the third and fourth groups. In Case B the differences go up to 138 pcm. The JENDL-3.2 solutions are low and all negative. They add up to -90 pcm.

Tables 6.10a and 6.10b show a rather good agreement for the ^{242}Pu absorption rates. The deviations are all generated in the resolved resonance group. The ECN solutions are 90 pcm higher for Case A and 50 pcm lower for Case B than the other JEF-2.2 appliers. The JENDL results are up to 75 pcm lower than those of IKE1.

Table 6.11 shows the differences among the oxygen absorption rates. All JENDL results are about 100 pcm lower than the results calculated with JEF-2.2; the differences are generated in the first energy group. Comparisons of databases show that the reason for this is a lower threshold for the (n,α) reaction in the JEF-2.2 library than in the JENDL-3 database. The discrepancies observed for the moderator have the same explanation.

Discussion of differences in fission rates

Tables 6.12 to 6.17 give detailed information about the fission rates in fuel. Apart from the (n,2n) and (n,3n) reactions the whole differences in k-infinity are projected onto the fission rates because of the applied normalisation condition. Table 6.12 shows a good agreement of MC results for ^{235}U. The deterministic calculations produced moderate deviations of up to 60 pcm for Case A originating mainly in the third group for JEF-2.2 contributions and in the fourth group for the JENDL-3.2 results. In Case B all differences are very small.

For ^{238}U the discrepancies are of course concentrated in the fast range. All MC results show a rather good agreement. The JEF-2.2 solutions have a different behaviour: APOLLO2 gives 84 pcm higher values and ECN between 78 and 122 pcm lower values than MCNP4. The SRAC calculations with JENDL-3.1 are about 240 pcm higher, but are reduced to between 50 to 85 pcm when applying JENDL-3.2.

Tables 6.8a and 6.8b show a good agreement for the ^{238}Pu fission rates.

The main discrepancies arise for the fission rate of ^{239}Pu in Table 6.15. TRIPOLI-4 calculates 159 and 325 pcm higher fission rates for Cases A and B. The MC calculations applying JENDL-3.2 give 560 to 750 pcm higher results for Case A and between 770 and 900 pcm for Case B, originating in group three (about 250 pcm) and mainly in the thermal energy region. CEA1 shows differences in all groups up to 84 pcm with alternating signs for Case A and a total deviation of 300 pcm for Case B, mainly produced in the thermal region. The ECN results are up to 479 pcm lower for Case A; one-third of the difference is produced in the resolved resonance group, while the rest is produced in the thermal region. In Case B the agreement is rather good with highest deviations of -80 pcm in the third group. JAE1 and JAE2 have rather large differences of 318 and 535 pcm in Case A and B, respectively, which mainly originate from the thermal group. The SRAC calculations with JENDL-3.2 are up to 892 and 997 pcm higher than the MCNP4 solutions, due to different results in the resolved resonance group (200 to 286 pcm) and the thermal group (361 to 789 pcm).

Because of the low contribution of ^{240}Pu to the fission rate effects, low discrepancies are also found for the solutions (Table 6.16). The only remarkable difference emerges from the JAERI calculations, which can is found in the third group and is about -60 pcm.

Tables 6.17a and 6.17b show the fission rate results for ^{241}Pu. The solution of TRIPOLI-4 is 98 and 71 pcm higher than that of MCNP4 for Cases A and B, whereas MVP gives differences of -407 to -478 pcm for Case A and between -342 and -353 pcm for Case B, generated about equally in the third and fourth groups. CEA1 gives 70 pcm higher values for both cases which are caused by differences

in the third and fourth groups. The ECN solutions are also higher by 400 pcm in Case A and by 166 pcm in Case B, resulting from about 500 pcm higher fission rates in the resolved resonance region and a value of 100 pcm lower in the thermal group for Case A. In Case B the differences are mainly produced in the third group. SRAC results with JENDL-3.1 data give also higher results between 154 and 259 pcm for Case A and between 90 and 173 pcm for Case B, mainly caused by the thermal group. In contrast to this result, the SRAC solutions applying JENDL-3.2 produce lower fission rates than MCNP4 in the range of 237 and 395 pcm, generated in the third and fourth energy groups.

The contribution of ^{242}Pu to the fission rate is very low and is not a significant contribution to the global discrepancies in both cases.

Local dependency of absorption rates and cross-sections

When defining this benchmark one point of interest has been to obtain information about the influence of the local dependency of spectra and cross-sections in the fuel. In Tables 6.19 to 6.22 the six zone absorption rates are compared for ^{238}U in the second and third groups, for ^{239}Pu in the thermal group and for ^{242}Pu in the third group. Solutions with local and energy dependent result are contributed from IKE1, CEA1, ECN2, JAE2, JAE4 and JAE6. Table 6.19 shows a very good agreement of the solutions for the unresolved resonance absorption of ^{238}U, demonstrating a low influence of the often discussed differences in shielding models in this energy region.

Tables 6.20a and 6.20b show a good agreement for the two MC results in Case A. APOLLO2 has positive and negative differences summed to the values of +40 and -118 pcm reported in Table 6.5.

ECN2 has, in both cases, nearly the same results with +210 pcm in the inner zone decreasing to -130 pcm in the outermost zone. The two SRAC solutions look untypical. The reason for the high deviations in Table 6.5 are deviations of -132 to -354 pcm in the fourth and fifth zones, whereas the agreement with the MC solutions in the outermost zone is rather good.

The absorption rates of ^{239}Pu in the thermal group show a strong local dependency. The surface terms agree well. The deviations increase in the inner zones. Here, APOLLO2 underestimates the absorptions in Case A and overestimates them in Case B. In both cases, ECN2 generates elevated values in the first zone and negative ones in all others. The differences of the JAERI results are all positive for SRAC and MVP calculations.

Table 6.22 shows the absorption rates in the resonance group of ^{242}Pu. The agreement of the MC results is rather good in Case A and very good in Case B. Again the main discrepancies originate from the two innermost zones and the agreement for the surface term is good.

Tables 6.23 to 6.26 show the locally dependent absorption cross-sections as they correspond to the discussed absorption rates. Differences in the databases can be considered responsible for the differences in Tables 6.25 and 6.26. The discrepancies between the SRAC results in Table 6.24 to the other solutions require further explanation by the contributor.

Summary

The main objective of this benchmark – to localise inconsistencies in data and methods applied for MOX pin cell calculations – could be achieved only partially, because a real best-estimate solution is not available. The two MC codes applied with JEF-2.2 data gave differences in k-infinity of 200 to

300 pcm, apparently caused by different conditions in processing the continuous energy libraries with NJOY. (For instance the tolerance for resonance reconstruction uses 0.1% for the results of MCNP4 and 0.5% for TRIPOLI-4. These discrepancies show that the criteria used in the NJOY code to reconstruct resonances to the continuous energy representation are very important and emphasises the necessity to set up a standard procedure to generate data libraries used in calculations.). The results of the two MVP calculations based on JENDL-3.2 data differed by 130 pcm, also well beyond the statistical error bounds. Subdividing the fuel zone in the cell leads to improved results in the SRAC's solutions with six zones seem to show the contrary. However in this case the same Dancoff factor was used for each fuel sub-zone, which is an approximation that cannot be considered adequate.

Detailed comparisons of fission rates of the isotopes in the fuel identified the thermal range of ^{239}Pu as the main source for observed differences between -300 and +270 pcm for the JEF-2.2 users and between +300 and +700 pcm for the JENDL-3.2 calculations. In the resolved resonance group of this isotope the JEF-2.2 results vary from -130 to +84 pcm. The deviations originating from ^{241}Pu are more moderate with about 100 pcm in the resonance and thermal region with the exception of the ECN differences going up to 500 pcm in the resonance group. The results of JENDL-3.2 calculations are about 200 pcm lower in both groups. The fast fission of ^{238}U causes a spread of the JEF-2.2 solutions between -120 and +85 pcm.

Significant contributions to the spread in eigenvalues are caused by the absorptions of the fissile isotopes ^{239}Pu and ^{241}Pu and in addition by ^{240}Pu with differences of -300 pcm for the thermal group in JEF-2.2 solutions and 100 pcm in the resonance group for the users of both databases. The resonance absorption of ^{238}U is still a source of discrepancies at least for the contributions applying JEF-2.2. The resulting differences for group three are between -120 and +280 pcm.

A surprising conclusion resulted from the comparison of the absorption rates of non-actinides in the cell. JENDL-3.2 cell calculations have 110 pcm higher absorption rates in clad and lower ones by 100 pcm for oxygen in fuel and by 80 pcm in the moderator. The reason for the lower oxygen absorption is a different threshold of the (n,α) cross-section in the two databases.

In conclusion, differences emerging from cross-section data used, their processing and differences in the computational schemes still lead to unsatisfactory discrepancies in calculating PWR MOX pin cells by different institutions, although "state-of-the-art" data and methods are used. This means that there is still a need for further analyses of the differences of best estimate solutions with respect to measured data and data processing, and that there is also need for improvement in deterministic methods and basic nuclear data, as well as for better experimental validation.

Table 6.2a. Table of k_∞ and reaction rates, Case A

Participant		Rates				
		Prod.	Fission	Absorption		
	k_∞	Fuel	Fuel	Fuel	Clad	Mod.
IKE1	1.1329	1.1314	0.3936	0.9745	0.0055	0.0200
CEA1	1.1358	1.1341	0.3945	0.9746	0.0052	0.0203
CEA2	1.1352	1.1332	0.3948	0.9754	0.0056	0.0202
ECN1	1.1285	1.1285	0.3927	0.9750	0.0054	0.0196
ECN2	1.1295	1.1295	0.3930	0.9750	0.0054	0.0196
ECN3	1.1295	1.1295	0.3930	0.9750	0.0054	0.0196
JAE1	1.1365	1.1365	0.3951	0.9740	0.0065	0.0195
JAE2	1.1412	1.1412	0.3967	0.9738	0.0065	0.0196
JAE3	1.1347	1.1347	0.3946	0.9735	0.0069	0.0196
JAE4	1.1394	1.1395	0.3962	0.9734	0.0069	0.0197
JAE5	1.1336	1.1352	0.3945	0.9773	0.0066	0.0192
JAE6	1.1320	1.1320	0.3934	0.9750	0.0066	0.0192

Table 6.2b. Table of k_∞ and reaction rates, Case B

Participant		Rates				
		Prod.	Fission	Absorption		
	k_∞	Fuel	Fuel	Fuel	Clad	Mod.
IKE1	1.1839	1.1824	0.4120	0.9634	0.0061	0.0304
CEA1	1.1911	1.1894	0.4144	0.9634	0.0058	0.0309
CEA2	1.1876	1.1874	0.4138	0.9639	0.0062	0.0306
ECN1	1.1815	1.1815	0.4117	0.9639	0.0061	0.0300
ECN2	1.1822	1.1822	0.4119	0.9639	0.0061	0.0301
ECN3	1.1821	1.1821	0.4119	0.9638	0.0061	0.0301
JAE1	1.1892	1.1893	0.4139	0.9630	0.0070	0.0300
JAE2	1.1947	1.1948	0.4159	0.9628	0.0070	0.0302
JAE3	1.1875	1.1875	0.4134	0.9626	0.0073	0.0301
JAE4	1.1930	1.1930	0.4154	0.9624	0.0074	0.0303
JAE5	1.1886	1.1895	0.4140	0.9653	0.0073	0.0297
JAE6	1.1882	1.1875	0.4133	0.9642	0.0074	0.0296

Table 6.3a. Differences of Case A results with respect to the MCNP4 solution (IKE1) in pcm

Participant		Rates				
		Prod.	Fission	Absorption		
	$\Delta k/k$	Fuel	Fuel	Fuel	Clad	Mod.
CEA1	253.6	241.4	238.3	10.3	-35.5	24.5
CEA2	196.4	160.4	302.4	93.4	5.6	17.1
ECN1	-389.0	-250.6	-231.4	56.0	-9.6	-47.0
ECN2	-307.2	-168.9	-149.4	49.1	-9.1	-40.7
ECN3	-307.2	-169.7	-150.1	47.9	-9.2	-39.5
JAE1	311.5	450.1	374.0	-51.3	101.1	-50.3
JAE2	724.7	863.1	787.6	-65.7	103.0	-37.9
JAE3	156.0	295.4	253.4	-92.5	135.8	-43.8
JAE4	571.3	710.3	667.4	-107.2	137.9	-31.3
JAE5	56.5	335.0	237.7	283.9	112.7	-80.9
JAE6	-80.4	53.8	-47.5	49.4	112.3	-80.8

Table 6.3b. Differences in Case B results with respect to the MCNP4 solution (IKE1) in pcm

Participant		Rates				
		Prod.	Fission	Absorption		
	Δk/k	Fuel	Fuel	Fuel	Clad	Mod.
CEA1	606.2	581.8	577.4	-5.5	-38.3	43.8
CEA2	307.4	420.9	432.9	50.7	0.5	20.9
ECN1	-204.8	-81.3	-64.2	49.0	-8.2	-40.9
ECN2	-147.2	-24.2	-7.3	42.2	-7.7	-34.5
ECN3	-149.7	-26.4	-9.5	40.3	-7.7	-32.6
JAE1	449.0	572.4	477.9	-43.8	82.4	-38.7
JAE2	906.5	1031.0	934.2	-64.4	84.7	-20.4
JAE3	304.0	428.2	353.7	-85.9	119.9	-34.1
JAE4	764.4	887.4	815.0	-106.7	122.4	-15.9
JAE5	392.1	594.2	494.6	182.5	110.8	-73.3
JAE6	364.4	423.8	327.1	80.2	121.3	-81.0

Table 6.4a. ^{235}U one-and four-group absorption rates of MCNP4 and corresponding differences of the other results in pcm, Case A

Participant	Energy group numbers				
	1/1	1/4	2/4	3/4	4/4
IKE1	0.0260	0.0007	0.0013	0.0137	0.0103
σ	± 3.2	± 0.1	± 0.1	± 2.2	± 2.4
CEA1	-4.2	0.5	-0.3	-16.4	11.9
CEA2	6.5				
ECN1	-18.1	-1.0	0.4	-17.4	-0.1
ECN2	-13.8	-1.1	0.3	-14.6	1.5
ECN3	-14.1	-1.1	0.4	-15.1	1.7
JAE1	87.2	1.5	1.5	73.0	11.4
JAE2	95.1	1.6	1.7	74.1	17.8
JAE3	15.0	0.3	0.7	-4.3	18.6
JAE4	23.1	0.4	0.8	-3.1	25.1
JAE5	9.7	0.1	0.6	0.3	8.8
JAE6	1.9	0.1	0.6	-2.2	3.4

Table 6.4b. ^{235}U one- and four-group absorption rates of MCNP4 and corresponding differences of the other results in pcm, Case B

Participant	Energy group numbers				
	1/1	1/4	2/4	3/4	4/4
IKE1	0.0144	0.0002	0.0005	0.0056	0.0081
σ	± 1.8	± 0.0	± 0.0	± 0.9	± 1.5
CEA1	9.7	0.2	-0.1	-2.9	12.5
CEA2	3.1				
ECN1	1.9	-0.5	0.3	-4.1	6.1
ECN2	3.9	-0.5	0.3	-2.8	7.0
ECN3	3.8	-0.5	0.3	-3.0	7.1
JAE1	37.4	0.9	0.5	28.6	7.4
JAE2	43.1	0.9	0.6	29.4	12.2
JAE3	7.9	0.4	0.2	-3.2	10.4
JAE4	13.6	0.4	0.3	-2.3	15.2
JAE5	4.5	0.0	0.2	-1.9	6.2
JAE6	4.1	-0.1	0.3	-1.5	5.4

Table 6.5a. ^{238}U one- and four-group absorption rates of MCNP4 and corresponding differences of the other results in pcm, Case A

	Energy group numbers				
Participant	1/1	1/4	2/4	3/4	4/4
IKE1	0.2071	0.0312	0.0222	0.1466	0.0071
σ	± 47.0	± 4.6	± 2.3	± 47.2	± 1.5
CEA1	64.7	34.5	-13.6	40.4	3.3
CEA2	46.0				
ECN1	119.4	-137.6	1.1	257.6	-1.7
ECN2	110.6	-140.6	0.6	251.4	-0.7
ECN3	114.0	-140.9	0.9	254.8	-0.7
JAE1	-32.1	-29.9	-26.7	32.4	-7.6
JAE2	-369.3	-22.8	-24.8	-318.1	-3.3
JAE3	-61.1	-98.8	-22.9	56.4	4.2
JAE4	-400.3	-91.9	-21.1	-295.6	8.6
JAE5	-53.4	-36.8	-17.5	2.0	-1.1
JAE6	-41.0	-37.7	-21.1	21.5	-3.7

Table 6.5b. ^{235}U one- and four-group absorption rates of MCNP4 and corresponding differences of the other results in pcm, Case B

	Energy group numbers				
Participant	1/1	1/4	2/4	3/4	4/4
IKE1	0.2348	0.0326	0.0230	0.1638	0.0155
σ	± 50.4	± 4.8	± 2.4	± 50.7	± 2.8
CEA1	-81.0	35.7	-12.8	-118.5	14.8
CEA2	19.4				
ECN1	128.2	-163.9	3.7	280.8	7.6
ECN2	119.6	-166.7	3.2	273.9	9.2
ECN3	124.1	-166.3	3.6	277.6	9.2
JAE1	-65.0	-34.5	-27.2	7.3	-11.1
JAE2	-424.3	-26.7	-25.1	-370.1	-2.3
JAE3	-109.0	-112.1	-23.7	17.3	10.0
JAE4	-469.6	-104.5	-21.7	-362.2	19.0
JAE5	-117.7	-42.6	-20.2	-57.1	2.1
JAE6	-118.8	-55.1	-17.2	-45.5	-1.0

Table 6.6a. ^{238}Pu one- and four-group absorption rates of MCNP4 and corresponding differences of the other results in pcm, Case A

	Energy group numbers				
Participant	1/1	1/4	2/4	3/4	4/4
IKE1	0.0118	0.0009	0.0008	0.0051	0.0050
σ	± 2.5	± 0.1	± 0.1	± 2.0	± 1.4
CEA1	38.7	0.7	-0.3	31.1	7.2
CEA2	2.5				
ECN1	13.6	-0.4	-0.1	12.4	1.7
ECN2	14.8	-0.5	-0.1	12.7	2.7
ECN3	14.7	-0.5	-0.1	12.5	2.8
JAE1	-43.8	4.3	4.4	-53.5	1.0
JAE2	-8.2	4.4	4.5	-21.3	4.2
JAE3	-41.1	2.5	4.4	-52.5	4.5
JAE4	-5.6	2.7	4.6	-20.6	7.7
JAE5	45.0	0.9	4.8	42.3	-2.9
JAE6	39.2	0.9	4.8	39.4	-5.9

Table 6.6b. ^{238}Pu one- and four-group absorption rates of MCNP4 and corresponding differences of the other results in pcm, Case B

	Energy group numbers				
Participant	1/1	1/4	2/4	3/4	4/4
IKE1	0.0037	0.0002	0.0001	0.0012	0.0022
σ	± 0.7	± 0.0	± 0.0	± 0.5	± 0.5
CEA1	6.8	0.1	-0.1	3.0	3.7
CEA2	0.5				
ECN1	0.3	-0.2	0.0	-1.9	2.5
ECN2	0.7	-0.2	0.0	-1.9	2.8
ECN3	0.7	-0.2	0.0	-1.9	2.8
JAE1	-4.6	0.8	0.8	-5.6	-0.6
JAE2	-1.5	0.8	0.9	-3.8	0.7
JAE3	-4.1	0.4	0.9	-5.5	0.1
JAE4	-1.0	0.5	0.9	-3.8	1.4
JAE5	7.8	0.1	0.9	8.4	-1.7
JAE6	7.5	0.1	0.9	8.1	-1.7

Table 6.7a. ^{239}Pu one- and four-group absorption rates of MCNP4 and corresponding differences of the other results in pcm, Case A

	Energy group numbers				
Participant	1/1	1/4	2/4	3/4	4/4
IKE1	0.3651	0.0070	0.0093	0.0984	0.2504
σ	± 59.3	± 0.8	± 0.7	± 19.8	± 57.5
CEA1	-2.3	5.4	-19.1	91.7	-79.7
CEA2	99.1				
ECN1	-325.9	-3.7	6.4	-104.1	-224.0
ECN2	-302.8	-4.5	6.1	-94.9	-208.9
ECN3	-301.3	-4.5	6.3	-98.5	-204.1
JAE1	-3.1	12.6	-14.9	-8.7	9.0
JAE2	155.6	13.8	-13.6	-6.1	162.5
JAE3	216.9	-0.5	-14.4	23.1	209.0
JAE4	376.1	0.7	-13.1	25.3	364.3
JAE5	326.1	-10.7	-12.5	9.0	340.9
JAE6	206.4	-10.9	-12.9	24.2	206.5

Table 6.7b. ^{239}Pu one- and four-group absorption rates of MCNP4 and corresponding differences of the other results in pcm, Case B

	Energy group numbers				
Participant	1/1	1/4	2/4	3/4	4/4
IKE1	0.4590	0.0050	0.0065	0.0803	0.3672
σ	± 69.4	± 0.6	± 0.5	± 16.2	± 67.3
CEA1	193.9	3.5	-13.6	74.1	129.4
CEA2	229.3				
ECN1	-62.0	-5.8	5.1	-30.0	-31.9
ECN2	-41.9	-6.2	4.9	-21.7	-19.5
ECN3	-43.6	-6.1	5.1	-24.4	-18.8
JAE1	121.5	8.1	-10.8	5.8	117.7
JAE2	341.7	9.0	-9.8	14.2	328.9
JAE3	293.5	-1.8	-10.5	20.3	285.7
JAE4	515.8	-0.9	-9.5	28.5	497.4
JAE5	479.2	-8.7	-9.4	35.1	461.4
JAE6	410.7	-9.6	-8.3	47.6	380.4

Table 6.8a. ^{240}Pu one- and four-group absorption rates of MCNP4 and corresponding differences of the other results in pcm, Case A

	Energy group numbers				
Participant	1/1	1/4	2/4	3/4	4/4
IKE1	0.1838	0.0048	0.0025	0.0318	0.1447
σ	± 53.3	± 0.6	± 0.2	± 10.9	± 52.4
CEA1	-180.1	3.9	-1.7	98.9	-281.3
CEA2	-132.0				
ECN1	-28.7	-3.1	6.9	-14.9	-17.6
ECN2	-65.3	-3.6	6.8	-11.4	-57.1
ECN3	-68.8	-3.7	6.8	-12.2	-59.9
JAE1	-51.2	11.3	2.8	87.5	-152.9
JAE2	9.3	12.1	3.2	81.0	-87.1
JAE3	34.8	2.1	3.0	100.4	-70.9
JAE4	95.7	2.9	3.5	94.0	-4.7
JAE5	175.5	-5.5	4.8	92.3	83.9
JAE6	105.8	-5.6	5.0	126.1	-19.8

Table 6.8b. ^{240}Pu one- and four-group absorption rates of MCNP4 and corresponding differences of the other results in pcm, Case B

	Energy group numbers				
Participant	1/1	1/4	2/4	3/4	4/4
IKE1	0.1386	0.0017	0.0009	0.0145	0.1215
σ	± 45.1	± 0.2	± 0.1	± 5.2	± 44.7
CEA1	-228.7	1.3	-0.6	69.5	-298.9
CEA2	-251.8				
ECN1	-36.3	-2.2	0.7	44.3	-79.1
ECN2	-69.0	-2.3	0.7	46.6	-114.0
ECN3	-72.3	-2.3	0.7	46.3	-117.0
JAE1	-88.8	3.7	1.0	62.8	-155.7
JAE2	-32.6	4.1	1.1	60.9	-98.7
JAE3	-50.8	0.3	1.1	65.7	-117.7
JAE4	5.1	0.6	1.2	63.9	-60.6
JAE5	-15.7	-2.3	1.7	73.8	-88.8
JAE6	-18.9	-2.6	1.8	68.1	-86.1

Table 6.9a. ^{241}Pu one- and four-group absorption rates of MCNP4 and corresponding differences of the other results in pcm, Case A

	Energy group numbers				
Participant	1/1	1/4	2/4	3/4	4/4
IKE1	0.1330	0.0022	0.0040	0.0588	0.0681
σ	± 18.9	± 0.3	± 0.3	± 10.3	± 16.1
CEA1	75.3	1.6	-0.9	49.9	24.8
CEA2	42.9				
ECN1	216.9	-3.9	0.0	288.3	-67.6
ECN2	237.6	-4.2	-0.1	300.0	-58.2
ECN3	236.4	-4.2	0.0	297.1	-56.6
JAE1	170.2	-6.7	-10.1	133.7	52.9
JAE2	226.0	-6.3	-9.6	146.1	95.8
JAE3	-90.8	-10.5	-10.5	-37.7	-31.9
JAE4	-35.0	-10.2	-10.0	-25.4	10.7
JAE5	-92.9	-10.6	-9.6	-10.8	-62.0
JAE6	-130.8	-10.6	-9.6	-6.9	-103.7

Table 6.9b. ^{241}Pu one- and four-group absorption rates of MCNP4 and corresponding differences of the other results in pcm, Case B

	Energy group numbers				
Participant	1/1	1/4	2/4	3/4	4/4
IKE1	0.0978	0.0010	0.0018	0.0300	0.0650
σ	± 13.3	± 0.1	± 0.1	± 5.2	± 12.2
CEA1	90.7	0.6	-0.4	41.6	49.0
CEA2	36.6				
ECN1	83.0	-2.3	0.1	100.2	-14.8
ECN2	95.7	-2.4	0.0	107.1	-9.0
ECN3	95.1	-2.4	0.1	105.9	-8.4
JAE1	91.6	-3.1	-4.4	65.5	33.8
JAE2	137.9	-3.0	-4.2	73.4	71.8
JAE3	-93.2	-4.9	-4.6	-22.5	-61.1
JAE4	-47.2	-4.8	-4.4	-14.6	-23.5
JAE5	-102.5	-4.9	-4.3	-16.6	-76.7
JAE6	-107.2	-5.0	-4.0	-12.7	-85.4

Table 6.10a. ^{242}Pu one- and four-group absorption rates of MCNP4 and corresponding differences of the other results in pcm, Case A

	Energy group numbers				
Participant	1/1	1/4	2/4	3/4	4/4
IKE1	0.0451	0.0029	0.0013	0.0391	0.0017
σ	± 24.7	± 0.4	± 0.1	± 24.8	± 0.3
CEA1	16.0	2.3	-1.0	13.9	0.6
CEA2	28.8				
ECN1	94.1	-2.6	-0.5	97.7	-0.5
ECN2	83.5	-2.9	-0.6	87.3	-0.3
ECN3	82.5	-3.0	-0.6	86.3	-0.3
JAE1	-74.3	4.9	0.6	-75.8	-4.0
JAE2	-71.1	5.4	0.8	-74.2	-3.0
JAE3	-64.0	-0.6	0.7	-61.3	-2.9
JAE4	-60.8	-0.1	0.9	-59.8	-1.9
JAE5	-29.3	-4.4	1.7	-24.4	-2.3
JAE6	-35.5	-4.4	1.8	-30.3	-2.6

Table 6.10b. ^{242}Pu one- and four-group absorption rates of MCNP4 and corresponding differences of the other results in pcm, Case B

	Energy group numbers				
Participant	1/1	1/4	2/4	3/4	4/4
IKE1	0.0126	0.0003	0.0001	0.0119	0.0003
σ	± 8.9	± 0.0	± 0.0	± 8.8	± 0.0
CEA1	-1.5	0.2	-0.1	-1.9	0.3
CEA2	10.1				
ECN1	-52.5	-0.4	0.0	-52.2	0.1
ECN2	-53.0	-0.4	0.0	-52.7	0.1
ECN3	-53.6	-0.4	0.0	-53.3	0.1
JAE1	-37.2	0.4	0.1	-37.4	-0.3
JAE2	-31.8	0.5	0.1	-32.3	-0.1
JAE3	-34.9	-0.1	0.1	-34.8	-0.2
JAE4	-29.5	0.0	0.1	-29.5	0.0
JAE5	17.8	-0.4	0.1	18.1	0.0
JAE6	-4.2	-0.5	0.2	-3.7	-0.1

Table 6.11a. Oxygen one- and four-group absorption rates of MCNP4 and corresponding differences of the other results in pcm, Case A

	Energy group numbers				
Participant	1/1	1/4	2/4	3/4	4/4
IKE1	0.0026	0.0026	0.0000	0.0000	0.0000
σ	± 1.2	± 1.1	± 0.0	± 0.0	± 0.0
CEA1	2.3	2.3	0.0	0.0	0.0
CEA2	-0.4				
ECN1	-15.2	-15.2	0.0	0.0	0.0
ECN2	-15.4	-15.4	0.0	0.0	0.0
ECN3	-15.5	-15.5	0.0	0.0	0.0
JAE1	-99.6	-99.6	0.0	0.0	0.0
JAE2	-98.9	-98.9	0.0	0.0	0.0
JAE3	-103.2	-104.4	1.1	0.0	0.0
JAE4	-102.5	-103.7	1.1	0.0	0.0
JAE5	-96.8	-98.0	1.2	0.0	0.0
JAE6	-96.5	-97.7	1.2	0.0	0.0

Table 6.11b. Oxygen one- and four-group absorption rates of MCNP4 and corresponding differences of the other results in pcm, Case B

	Energy group numbers				
Participant	1/1	1/4	2/4	3/4	4/4
IKE1	0.0025	0.0025	0.0000	0.0000	0.0000
σ	± 1.1	± 1.1	± 0.0	± 0.0	± 0.0
CEA1	4.7	4.7	0.0	0.0	0.0
CEA2	1.8				
ECN1	-13.5	-13.5	0.0	0.0	0.0
ECN2	-13.7	-13.7	0.0	0.0	0.0
ECN3	-13.7	-13.7	0.0	0.0	0.0
JAE1	-93.4	-93.4	0.0	0.0	0.0
JAE2	-92.7	-92.7	0.0	0.0	0.0
JAE3	-97.6	-98.7	1.1	0.0	0.0
JAE4	-96.8	-98.0	1.1	0.0	0.0
JAE5	-90.8	-91.9	1.1	0.0	0.0
JAE6	-92.7	-93.9	1.1	0.0	0.0

Table 6.12a. ^{235}U one- and four-group fission rates of MCNP 4 and corresponding differences of the other results in pcm, Case A

	Energy group numbers				
Participant	1/1	1/4	2/4	3/4	4/4
IKE1	0.0194	0.0006	0.0011	0.0089	0.0088
σ	± 2.5	± 0.1	± 0.1	± 1.4	± 2.1
CEA1	-15.0	1.3	-0.6	-41.1	25.5
CEA2	15.6				
ECN1	-42.6	-0.6	0.5	-42.1	-0.4
ECN2	-35.5	-0.7	0.4	-38.3	3.2
ECN3	-35.9	-0.7	0.5	-39.1	3.5
JAE1	-18.9	7.3	-2.4	-36.8	13.0
JAE2	-3.1	7.6	-2.0	-35.4	26.8
JAE3	36.6	4.3	-1.1	-11.9	45.4
JAE4	52.8	4.5	-0.7	-10.3	59.3
JAE5	19.1	1.5	-1.0	-6.0	24.7
JAE6	4.8	1.5	-1.0	-8.9	13.3

Table 6.12b. ^{235}U one- and four-group fission rates of MCNP 4 and corresponding differences of the other results in pcm, Case B

	Energy group numbers				
Participant	1/1	1/4	2/4	3/4	4/4
IKE1	0.0111	0.0002	0.0004	0.0036	0.0069
σ	± 1.4	± 0.0	± 0.0	± 0.6	± 1.3
CEA1	15.4	0.4	-0.2	-10.4	25.6
CEA2	8.5				
ECN1	0.5	-0.5	0.4	-12.0	12.6
ECN2	3.8	-0.6	0.4	-10.4	14.5
ECN3	3.7	-0.6	0.4	-10.7	14.6
JAE1	-8.1	2.5	-0.8	-16.2	6.5
JAE2	3.0	2.6	-0.7	-15.0	16.2
JAE3	19.2	1.3	-0.4	-6.6	24.8
JAE4	30.3	1.4	-0.3	-5.4	34.6
JAE5	11.8	0.4	-0.4	-4.6	16.4
JAE6	9.9	0.3	-0.3	-4.8	14.6

Table 6.13a. ^{238}U one- and four-group fission rates of MCNP4 and corresponding differences of the other results in pcm, Case A

	Energy group numbers				
Participant	1/1	1/4	2/4	3/4	4/4
IKE1	0.0275	0.0274	0.0000	0.0000	0.0000
σ	± 4.4	± 4.4	± 0.0	± 0.0	± 0.0
CEA1	84.4	85.0	-0.4	-0.1	0.0
CEA2	24.9				
ECN1	-70.9	-70.5	-0.4	0.0	0.0
ECN2	-77.9	-77.4	-0.4	0.0	0.0
ECN3	-78.8	-78.3	-0.4	0.0	0.0
JAE1	230.7	232.3	-1.5	0.0	0.0
JAE2	247.3	249.0	-1.5	0.0	0.0
JAE3	67.6	69.2	-1.5	0.0	0.0
JAE4	84.5	85.9	-1.4	0.0	0.0
JAE5	-27.9	-26.9	-1.0	0.0	0.0
JAE6	-31.0	-29.9	-1.0	-0.1	0.0

Table 6.13b. ^{238}U one- and four-group fission rates of MCNP4 and corresponding differences of the other results in pcm, Case B

	Energy group numbers				
Participant	1/1	1/4	2/4	3/4	4/4
IKE1	0.0287	0.0286	0.0000	0.0000	0.0000
σ	± 4.6	± 4.6	± 0.0	± 0.0	± 0.0
CEA1	84.2	84.8	-0.5	-0.1	0.0
CEA2	26.1				
ECN1	-116.6	-116.2	-0.4	0.0	0.0
ECN2	-122.9	-122.4	-0.4	0.0	0.0
ECN3	-122.1	-121.7	-0.4	0.0	0.0
JAE1	226.0	227.6	-1.5	0.0	0.0
JAE2	243.0	244.6	-1.5	0.0	0.0
JAE3	50.2	51.8	-1.5	0.0	0.0
JAE4	67.5	69.2	-1.4	0.0	0.0
JAE5	-36.0	-34.9	-1.0	0.0	0.0
JAE6	-66.6	-65.5	-1.0	-0.1	0.0

Table 6.14a. ^{238}Pu one- and four-group fission rates of MCNP4 and corresponding differences of the other results in pcm, Case A

	Energy group numbers				
Participant	1/1	1/4	2/4	3/4	4/4
IKE1	0.0024	0.0009	0.0005	0.0008	0.0002
σ	± 0.3	± 0.1	± 0.1	± 0.3	± 0.0
CEA1	10.3	1.8	-0.8	8.8	0.5
CEA2	-0.8				
ECN1	1.3	-0.9	-0.3	2.4	0.1
ECN2	1.2	-1.1	-0.3	2.5	0.2
ECN3	1.2	-1.2	-0.3	2.4	0.2
JAE1	-3.5	8.1	0.8	-12.3	-0.2
JAE2	5.1	8.4	1.2	-4.6	0.1
JAE3	-7.2	3.7	0.9	-12.0	0.1
JAE4	1.4	4.1	1.3	-4.3	0.4
JAE5	5.3	-0.2	2.1	3.9	-0.5
JAE6	4.6	-0.3	2.1	3.4	-0.7

Table 6.14b. ^{238}Pu one- and four-group fission rates of MCNP4 and corresponding differences of the other results in pcm, Case B

	Energy group numbers				
Participant	1/1	1/4	2/4	3/4	4/4
IKE1	0.0005	0.0002	0.0001	0.0002	0.0001
σ	± 0.1	± 0.0	± 0.0	± 0.1	± 0.0
CEA1	1.7	0.3	-0.2	1.3	0.3
CEA2	-0.3				
ECN1	-0.6	-0.4	-0.1	-0.3	0.2
ECN2	-0.6	-0.5	-0.1	-0.2	0.2
ECN3	-0.6	-0.5	-0.1	-0.3	0.2
JAE1	0.3	1.4	0.1	-1.3	0.0
JAE2	0.9	1.5	0.2	-0.9	0.1
JAE3	-0.4	0.6	0.2	-1.2	0.1
JAE4	0.1	0.6	0.2	-0.9	0.2
JAE5	0.8	-0.1	0.3	0.7	-0.1
JAE6	0.6	-0.2	0.4	0.5	-0.1

Table 6.15a. ^{239}Pu one- and four-group fission rates of MCNP4 and corresponding differences of other results in pcm, Case A

	Energy group numbers				
Participant	1/1	1/4	2/4	3/4	4/4
IKE1	0.2335	0.0069	0.0076	0.0571	0.1619
σ	± 37.8	± 0.8	± 0.6	± 11.5	± 36.2
CEA1	-21.5	13.6	-44.7	83.9	-74.5
CEA2	159.3				
ECN1	-479.0	-5.8	2.9	-143.3	-333.4
ECN2	-437.9	-7.6	2.1	-128.2	-304.5
ECN3	-435.0	-7.7	2.6	-133.5	-296.7
JAE1	55.2	45.9	-28.6	8.9	29.1
JAE2	318.1	48.8	-25.3	15.5	278.8
JAE3	630.5	13.1	-27.4	281.9	361.1
JAE4	892.2	16.0	-24.1	286.9	613.5
JAE5	755.6	-17.3	-21.5	255.3	538.9
JAE6	559.1	-17.6	-22.5	277.9	321.1

Table 6.15b. ^{239}Pu one- and four-group fission rates of MCNP4 and corresponding differences of other results in pcm, Case B

	Energy group numbers				
Participant	1/1	1/4	2/4	3/4	4/4
IKE1	0.2952	0.0049	0.0053	0.0467	0.2382
σ	± 43.0	± 0.6	± 0.4	± 9.4	± 42.4
CEA1	300.0	8.3	-30.6	52.9	271.0
CEA2	326.8				
ECN1	-86.0	-11.3	2.8	-79.6	2.7
ECN2	-50.9	-12.4	2.3	-66.8	26.6
ECN3	-52.7	-12.2	2.7	-70.5	27.9
JAE1	191.1	29.0	-20.1	-4.4	187.5
JAE2	534.8	31.0	-17.9	7.9	515.3
JAE3	636.4	5.3	-19.3	192.9	458.6
JAE4	984.0	7.3	-17.0	204.3	789.0
JAE5	897.3	-14.2	-15.9	229.8	698.0
JAE6	773.8	-16.5	-14.0	225.0	579.8

Table 6.16a. ^{240}Pu one- and four-group fission rates of MCNP4 and corresponding differences of the other results in pcm, Case A

	Energy group numbers				
Participant	1/1	1/4	2/4	3/4	4/4
IKE1	0.0061	0.0046	0.0010	0.0005	0.0000
σ	± 0.6	± 0.6	± 0.1	± 0.1	± 0.0
CEA1	9.0	9.8	-4.0	3.4	-0.1
CEA2	3.0				
ECN1	3.7	-4.5	-2.3	10.5	0.0
ECN2	2.4	-5.7	-2.5	10.6	0.0
ECN3	2.4	-5.8	-2.4	10.6	0.0
JAE1	-46.7	30.4	-12.1	-64.4	-0.5
JAE2	-43.7	32.3	-11.2	-64.3	-0.5
JAE3	-68.9	7.7	-11.8	-64.3	-0.5
JAE4	-66.0	9.7	-11.0	-64.2	-0.4
JAE5	-86.8	-13.7	-6.7	-66.0	-0.4
JAE6	-86.6	-14.0	-6.2	-66.0	-0.5

Table 6.16b. ^{240}Pu one- and four-group fission rates of MCNP4 and corresponding differences of the other results in pcm, Case B

	Energy group numbers				
Participant	1/1	1/4	2/4	3/4	4/4
IKE1	0.0022	0.0017	0.0004	0.0002	0.0000
σ	± 0.2	± 0.2	± 0.1	± 0.1	± 0.0
CEA1	3.2	3.0	-1.4	1.7	-0.1
CEA2	0.6				
ECN1	-1.9	-4.0	-0.9	3.0	0.0
ECN2	-2.3	-4.4	-1.0	3.1	-0.1
ECN3	-2.2	-4.3	-0.9	3.1	-0.1
JAE1	-20.2	9.6	-4.2	-25.2	-0.4
JAE2	-19.1	10.3	-3.9	-25.2	-0.4
JAE3	-28.3	1.4	-4.1	-25.2	-0.4
JAE4	-27.2	2.1	-3.8	-25.1	-0.4
JAE5	-33.9	-5.5	-2.4	-25.7	-0.4
JAE6	-34.6	-6.3	-2.2	-25.8	-0.4

Table 6.17a. ^{241}Pu one- and four-group fission rates of MCNP4 and corresponding differences of the other results in pcm, Case A

	Energy group numbers				
Participant	1/1	1/4	2/4	3/4	4/4
IKE1	0.1014	0.0020	0.0033	0.0454	0.0508
σ	± 14.3	± 0.2	± 0.3	± 7.3	± 12.1
CEA1	167.5	3.8	-2.1	119.2	46.7
CEA2	97.7				
ECN1	359.2	-1.5	0.0	487.3	-126.5
ECN2	402.2	-2.0	-0.3	512.6	-107.9
ECN3	399.9	-2.1	-0.1	507.0	-104.8
JAE1	154.0	23.4	6.0	16.6	108.3
JAE2	259.3	24.2	7.1	39.3	188.5
JAE3	-395.0	14.0	5.5	-269.5	-144.7
JAE4	-288.8	14.8	6.6	-245.6	-64.7
JAE5	-406.9	5.3	7.3	-212.6	-206.9
JAE6	-478.1	5.3	7.2	-206.6	-283.9

Table 6.17b. ^{241}Pu one- and four-group fission rates of MCNP4 and corresponding differences of the other results in pcm, Case B

	Energy group numbers				
Participant	1/1	1/4	2/4	3/4	4/4
IKE1	0.0739	0.0009	0.0014	0.0231	0.0486
σ	± 10.0	± 0.1	± 0.1	± 3.7	± 9.1
CEA1	172.7	1.4	-0.9	86.5	85.4
CEA2	71.0				
ECN1	141.2	-1.9	0.1	170.0	-26.9
ECN2	166.4	-2.1	0.0	184.5	-15.9
ECN3	165.2	-2.1	0.1	182.1	-14.8
JAE1	90.0	9.5	2.4	2.9	75.3
JAE2	172.8	9.8	2.9	16.5	143.6
JAE3	-321.0	5.3	2.2	-142.7	-185.6
JAE4	-237.5	5.6	2.7	-128.3	-117.3
JAE5	-342.3	1.8	2.9	-130.8	-216.1
JAE6	-352.7	1.4	3.3	-124.8	-232.6

Table 6.18a. ^{242}Pu one- and four-group fission rates of MCNP4 and corresponding differences of the other results in pcm, Case A

	Energy group numbers				
Participant	1/1	1/4	2/4	3/4	4/4
IKE1	0.0033	0.0028	0.0004	0.0001	0.0000
σ	± 0.4	± 0.3	± 0.1	± 0.0	± 0.0
CEA1	3.6	5.8	-2.4	0.1	0.0
CEA2	2.7				
ECN1	-3.0	-2.4	-1.8	1.2	0.0
ECN2	-3.9	-3.2	-1.9	1.1	0.0
ECN3	-3.9	-3.2	-1.8	1.1	0.0
JAE1	3.1	15.5	-5.6	-6.5	-0.3
JAE2	4.7	16.7	-5.2	-6.5	-0.3
JAE3	-10.2	2.1	-5.5	-6.5	-0.3
JAE4	-8.6	3.3	-5.2	-6.5	-0.3
JAE5	-20.5	-11.1	-2.7	-6.5	-0.3
JAE6	-20.3	-11.2	-2.4	-6.5	-0.3

Table 6.18b. ^{242}Pu one- and four-group fission rates of MCNP4 and corresponding differences of the other results in pcm, Case B

	Energy group numbers				
Participant	1/1	1/4	2/4	3/4	4/4
IKE1	0.0003	0.0002	0.0000	0.0000	0.0000
σ	± 0.0	± 0.0	± 0.0	± 0.0	± 0.0
CEA1	0.2	0.4	-0.2	0.0	0.0
CEA2	0.2				
ECN1	-0.8	-0.6	-0.2	-0.1	0.0
ECN2	-0.9	-0.6	-0.2	-0.1	0.0
ECN3	-0.8	-0.6	-0.2	-0.1	0.0
JAE1	-1.2	1.2	-0.5	-1.8	0.0
JAE2	-1.0	1.3	-0.4	-1.8	0.0
JAE3	-2.3	0.0	-0.5	-1.8	0.0
JAE4	-2.2	0.1	-0.4	-1.8	0.0
JAE5	-3.1	-1.0	-0.2	-1.8	0.0
JAE6	-3.2	-1.1	-0.2	-1.8	0.0

Table 6.19a. Six zone absorption rates of ^{238}U in Group 2 calculated with MCNP4 and corresponding differences of other results in pcm, Case A

	Zone numbers					
Participant	1	2	3	4	5	6
IKE1	0.0089	0.0067	0.0022	0.0022	0.0011	0.0011
σ	± 1.0	± 0.7	± 0.2	± 0.2	± 0.1	± 0.1
CEA1	-5.0	-4.4	-1.4	-1.6	-0.5	-0.7
ECN2	-1.8	2.5	0.5	-0.2	-0.2	-0.3
JAE2	-5.6	-8.8	-2.3	-2.9	-2.3	-3.0
JAE4	-4.1	-7.7	-2.0	-2.5	-2.1	-2.8
JAE6	-9.0	-5.9	-2.0	-2.2	-1.0	-1.0

Table 6.19b. Six zone absorption rates of ^{238}U in Group 2 calculated with MCNP4 and corresponding differences of other results in pcm, Case B

	Zone numbers					
Participant	1	2	3	4	5	6
IKE1	0.0092	0.0069	0.0023	0.0023	0.0011	0.0011
σ	± 1.0	± 0.7	± 0.2	± 0.2	± 0.1	± 0.1
CEA1	-5.3	-4.2	-1.1	-1.3	-0.5	-0.4
ECN2	-1.4	3.4	1.1	0.3	-0.1	0.0
JAE2	-6.1	-9.0	-2.1	-2.7	-2.3	-2.9
JAE4	-4.7	-8.0	-1.8	-2.3	-2.1	-2.7
JAE6	-7.4	-5.2	-1.6	-1.6	-0.7	-0.6

Table 6.20a. Six zone absorption rates of ^{238}U in Group 3 calculated with MCNP4 and corresponding differences of other results in pcm, Case A

	Zone numbers					
Participant	1	2	3	4	5	6
IKE1	0.0425	0.0367	0.0146	0.0179	0.0126	0.0224
σ	± 11.5	± 9.2	± 4.8	± 6.3	± 5.4	± 10.1
CEA1	40.9	12.9	-5.7	7.5	17.7	-32.9
ECN2	207.1	128.6	39.4	33.1	-19.0	-137.8
JAE2	5.3	78.7	8.1	-133.5	-322.5	45.8
JAE4	17.8	86.6	10.3	-131.8	-321.8	43.3
JAE6	-13.1	8.8	1.8	5.6	13.8	4.6

Table 6.20b. Six zone absorption rates of ^{238}U in Group 3 calculated with MCNP4 and corresponding differences of other results in pcm, Case B

	Zone numbers					
Participant	1	2	3	4	5	6
IKE1	0.0479	0.0413	0.0162	0.0198	0.0139	0.0248
σ	± 12.0	± 10.3	± 5.2	± 6.7	± 5.8	± 10.7
CEA1	-42.8	-64.5	-22.7	1.8	17.7	-8.0
ECN2	211.5	115.5	43.1	44.4	-9.9	-130.7
JAE2	6.8	65.6	6.6	-145.9	-354.1	50.9
JAE4	15.4	69.8	7.2	-145.9	-354.5	45.8
JAE6	-33.3	-18.2	-9.5	11.3	7.2	-3.0

Table 6.21a. Six zone absorption rates of ^{239}Pu in Group 4 calculated with MCNP4 and corresponding differences of other results in pcm, Case A

	Zone numbers					
Participant	1	2	3	4	5	6
IKE1	0.0766	0.0742	0.0294	0.0328	0.0180	0.0195
σ	± 19.9	± 15.6	± 6.5	± 6.9	± 4.1	± 4.5
CEA1	-29.6	-38.4	-4.8	-12.1	0.4	4.8
ECN2	94.0	-130.2	-56.7	-53.9	-33.5	-28.5
JAE2	7.0	34.5	38.4	43.7	18.4	20.5
JAE4	72.8	94.2	61.4	68.8	32.0	35.1
JAE6	59.2	63.5	26.5	16.5	16.2	24.6

Table 6.21b. Six zone absorption rates of ^{239}Pu in Group 4 calculated with MCNP4 and corresponding differences of other results in pcm, Case B

	Zone numbers					
Participant	1	2	3	4	5	6
IKE1	0.1257	0.1100	0.0407	0.0435	0.0230	0.0242
σ	± 25.1	± 18.7	± 7.3	± 7.4	± 4.1	± 4.6
CEA1	29.0	33.0	22.4	18.5	20.2	6.3
ECN2	205.6	-113.2	-46.6	-28.8	-19.0	-17.5
JAE2	72.0	82.0	58.6	67.8	27.6	20.9
JAE4	130.0	132.0	77.4	87.9	38.2	31.9
JAE6	128.6	103.6	46.5	48.3	27.2	26.2

Table 6.22a. Six zone absorption rates of ^{242}Pu in Group 3 calculated with MCNP4 and corresponding differences of other results in pcm, Case A

	Zone numbers					
Participant	1	2	3	4	5	6
IKE1	0.0113	0.0110	0.0046	0.0054	0.0032	0.0037
σ	± 7.1	± 6.5	± 3.0	± 3.5	± 2.2	± 2.6
CEA1	24.5	-5.5	-3.2	-3.2	-0.2	1.5
ECN2	85.7	2.6	-4.3	-2.5	0.4	5.4
JAE2	-21.9	-28.1	-7.9	-8.4	-5.7	-2.2
JAE4	-17.9	-24.2	-6.2	-6.3	-4.5	-0.6
JAE6	-12.6	-20.6	-2.7	2.3	1.1	2.1

Table 6.22b. Six zone absorption rates of ^{242}Pu in Group 3 calculated with MCNP4 and corresponding differences of other results in pcm, Case B

	Zone numbers					
Participant	1	2	3	4	5	6
IKE1	0.0045	0.0036	0.0012	0.0013	0.0006	0.0006
σ	± 3.5	± 2.5	± 0.9	± 0.9	± 0.5	± 0.5
CEA1	-0.2	-2.2	-0.4	0.1	0.3	0.6
ECN2	-18.9	-19.4	-5.8	-4.7	-2.3	-1.7
JAE2	-12.2	-11.1	-3.3	-2.9	-1.6	-1.2
JAE4	-11.1	-10.3	-3.0	-2.7	-1.4	-1.0
JAE6	0.5	-1.8	-1.1	-0.5	-0.7	-0.1

Table 6.23a. ^{238}U microscopic absorption cross-sections (barn) of Group 2 in six fuel zones, Case A

	Zone numbers					
Participant	1	2	3	4	5	6
IKE1	0.246	0.248	0.248	0.249	0.249	0.250
CEA1	0.246	0.247	0.248	0.248	0.249	0.249
JAE2	0.243	0.244	0.244	0.245	0.245	0.245
JAE4	0.243	0.244	0.245	0.245	0.245	0.246
JAE6	0.243	0.244	0.245	0.245	0.246	0.246

Table 6.23b. ^{238}U microscopic absorption cross-sections (barn) of Group 2 in six fuel zones, Case B

	Zone numbers					
Participant	1	2	3	4	5	6
IKE1	0.247	0.248	0.248	0.249	0.249	0.250
CEA1	0.246	0.247	0.248	0.249	0.249	0.250
JAE2	0.243	0.244	0.245	0.245	0.245	0.245
JAE4	0.243	0.244	0.245	0.245	0.245	0.246
JAE6	0.243	0.244	0.245	0.246	0.246	0.247

Table 6.24a. ^{238}U microscopic absorption cross-sections (barn) of Group 3 in six fuel zones, Case A

	Zone numbers					
Participant	1	2	3	4	5	6
IKE1	1.927	2.183	2.571	3.139	4.391	7.760
CEA1	1.933	2.187	2.561	3.159	4.468	7.694
JAE2	1.922	2.230	2.582	2.903	3.275	7.948
JAE4	1.923	2.230	2.580	2.899	3.270	7.922
JAE6	1.915	2.184	2.570	3.140	4.427	7.751

Table 6.24b. ^{238}U microscopic absorption cross-sections (barn) of Group 3 in six fuel zones, Case B

	Zone numbers					
Participant	1	2	3	4	5	6
IKE1	1.923	2.181	2.553	3.106	4.341	7.724
CEA1	1.891	2.142	2.514	3.110	4.400	7.733
JAE2	1.919	2.218	1.560	2.874	3.240	7.906
JAE4	1.920	2.217	2.558	2.870	3.235	7.880
JAE6	1.907	2.170	2.536	3.118	4.355	7.693

Table 6.25a. ^{239}Pu microscopic absorption cross-sections (barn) of Group 4 in six fuel zones, Case A

	Zone numbers					
Participant	1	2	3	4	5	6
IKE1	622.1	698.2	752.9	790.2	821.7	844.5
CEA1	621.7	697.5	754.5	790.5	822.4	847.5
JAE2	647.3	723.0	778.0	813.3	843.8	868.3
JAE4	648.4	724.1	779.0	814.3	844.8	869.3
JAE6	638.8	716.2	771.3	807.4	840.3	865.9

Table 6.25b. ^{239}Pu microscopic absorption cross-sections (barn) of Group 4 in six fuel zones, Case B

	Zone numbers					
Participant	1	2	3	4	5	6
IKE1	710.1	762.8	799.8	823.3	844.0	860.5
CEA1	709.4	763.4	801.6	825.3	846.6	862.8
JAE2	728.3	781.4	818.6	842.0	862.6	880.2
JAE4	729.2	782.4	819.6	843.0	863.7	881.3
JAE6	725.8	778.5	817.7	839.6	860.3	877.8

Table 6.26a. ^{242}Pu microscopic absorption cross-sections (barn) of Group 3 in six fuel zones, Case A

	Zone numbers					
Participant	1	2	3	4	5	6
IKE1	60.65	61.56	62.26	62.63	62.97	63.40
CEA1	61.21	61.94	62.43	62.79	63.12	63.47
JAE2	61.98	63.02	63.66	64.16	64.71	65.36
JAE4	60.04	61.08	61.74	62.24	62.78	63.43
JAE6	60.38	61.35	61.91	62.40	62.95	63.41

Table 6.26b. ^{242}Pu microscopic absorption cross-sections (barn) of Group 3 in six fuel zones, Case B

	Zone numbers					
Participant	1	2	3	4	5	6
IKE1	65.71	66.31	66.74	66.99	67.37	67.70
CEA1	66.43	66.99	67.43	67.71	67.78	68.04
JAE2	67.14	67.87	68.30	68.66	69.10	69.66
JAE4	65.12	65.85	66.27	66.63	67.06	67.61
JAE6	65.31	65.93	66.36	66.77	67.18	67.41

Annex 1 to Chapter 6

Specifications of the new benchmark to compare MCNP, WIMS, APOLLO2, CASMO4 and SRAC

S. Cathalau
CEA Cadarache, France

The new benchmark devoted to the comparison of WIMS6, APOLLO2, CASMO4, MCNP4.2 and SRAC codes without any burn-up calculations is described in the following:

Available Libraries: JEF2.2 for APOLLO2, WIMS6, CASMO4 and MCNP4.2 JENDL3.1 and JENDL3.2 for SRAC.

The benchmark specification is as follows:
For the two fuel types (A: poor quality Pu and B: classical Pu) the general geometry and temperatures are described below.

Geometry

- FUEL: External Radius = 0.4095 cm
- CLAD: External Radius = 0.4750 cm
- MODERATOR: External Square pitch = 1.3133 cm

Three types of mesh point discretisations for the fuel are proposed:

- FUEL: a) 1 point as: 0 cm $\Rightarrow$ 0.40950 cm

  b) 6 points as: 0 cm $\Rightarrow$ 0.25889 cm
  0.25889 cm $\Rightarrow$ 0.34261 cm
  0.34261 cm $\Rightarrow$ 0.36627 cm
  0.36627 cm $\Rightarrow$ 0.38849 cm
  0.38849 cm $\Rightarrow$ 0.39913 cm
  0.39913 cm $\Rightarrow$ 0.40950 cm

  c) 20 equivolumetric rings.

For each calculations, the moderator will be discretised in three zones:

- MODERATOR: 0.475 cm ⇒ 0.580 cm
  0.580 cm ⇒ 0.650 cm
  0.650 cm ⇒ edge of the square cell

Temperatures

- FUEL: = 900.0 K = 626.85 °C
- CLAD: = 600.0 K = 326.85 °C
- MODERATOR: = 573.6 K = 300.45 °C

Isotopic compositions (in atom per barn cm)

Fuel	*Poor Quality(A)*	*Classical (B)*
^{234}U	0.0000000	2.4626E-7
^{235}U	1.4456E-4	5.1515E-5
^{238}U	1.9939E-2	2.0295E-2
^{238}Pu	1.1467E-4	2.1800E-5
^{239}Pu	1.0285E-3	7.1155E-4
^{240}Pu	7.9657E-4	2.7623E-4
^{241}Pu	3.3997E-4	1.4591E-4
^{242}Pu	5.6388E-4	4.7643E-5
Oxygen	4.5854E-2	4.3100E-2
Clad		
Natural Zr	4.3248E-2	4.3248E-2
Moderator		
H_2O	2.3858E-2	2.3858E-2
^{10}B	3.6346E-6	3.6346E-6
^{11}B	1.6226E-5	1.6226E-5

Results

- Multiplication Factor K infinite;

FOR EACH MEDIUM in the CELL (mesh point in fuel, clad and moderator).

- One and four energy group cross-sections (absorption, fission and production cross-section information);
- One and four energy group reaction rates (absorption, fission, production);

Energy group boundaries:

20.0 MeV,	820.85 keV,	5.5308 keV,	1.5 eV,	0.00001 eV
1	2	3	4	

- Optionally averaged cross-sections and reaction rates in the cell.

Annex 2 to Chapter 6

Effect of different state-of-the-art nuclear data libraries on the PWR MOX pin cells benchmark of Chapter 6

(special study reported in [1])

The two PWR pin cells at operational conditions (T_{fuel}=660 C, T_{mod}=306 C) fuelled with recycled MOX (A) and standard MOX (B), respectively, have been performed applying the code system RSYST3 [2] coupled with ORIGEN-2 in a multigroup approach. The group cross-sections of 20 actinides, of the fission products ^{135}Xe and ^{149}Sm and of moderator and structural materials have been prepared by separate RESMOD calculations for each of the three databases. Cross-sections of the other fission products and some minor actinides have been taken from the JEF-2.2 library and the decay data from ENDF/B-VI.

In Tables 1 and 2 k-infinity and the most important isotopic reaction rates are shown. The reaction rates are normalised in such a way that they directly represent the influence on k-infinity. The k-values at BOL are in both cases rather close together; differences after irradiation are slightly higher in Case A, but about twice as high in Case B. However the production rates of ^{239}Pu and ^{241}Pu show significantly higher discrepancies. Due to different signs there are compensation effects at BOL and also (in Case A) for 50 MWd/kgHM. The spread in the isotopic absorption rates is lower, but exceeds 100 pcm for the main Pu isotopes. Due to compensation effects the total absorption rates are also low. In both benchmarks JENDL-3.2 cross-sections give nearly 100 pcm higher absorption rates in the clad and 90 pcm lower ones for oxygen in the fuel and in the moderator than the other libraries. The multiplication constants at BOL have also been calculated by MCNP-4A (stat. error 0.0007). The results are included in the Tables 1 and 2.

REFERENCES

[1] M. Mattes, D. Lutz, W. Bernnat: *Application of Nuclear Data Libraries Based on JEF-2.2, ENDF/B VI and JENDL-3.2 to LWR Criticality and Burn-up Problems*, Proc. of Intl. Conference on Nuclear Data for Science and Technology, Trieste, 19-24 May 1997.

[2] R.Rühle: *RSYST, an Integrated Modular System for Reactor and Shielding Calculations*, Conf-730 414-12, 1973.

Table 1. k-infinity, absorption and production rates of MOX benchmark A at BOL and at 50 MWd/kgHM, calculated with JEF-2.2 data and differences for ENDF/B-VI and JENDL-3.2

	BOL			50 MWd/kgHM		
	JEF-2.2	ENDF/B-VI	JENDL-3.2	JEF-2.2	ENDF/B-VI	JENDL-3.2
	k-infinity			***k-infinity***		
	1.1253	1.1241	1.1234	0.9553	0.9541	0.9536
MCNP-4A	1.1261	1.1252	1.1251			
	Prod. rate	Differences, pcm		***Prod. rate***	Differences, pcm	
^{239}Pu	0.665	385	528	0.482	295	293
^{241}Pu	0.295	-432	-492	0.321	-394	-261
	Abs. rate	Differences, pcm		***Abs. rate***	Differences, pcm	
fuel	0.976	-38	-7	0.975	-40	-10
^{235}U	0.026	50	5	0.015	-119	-171
^{239}Pu	0.362	77	123	0.263	51	18
^{240}Pu	0.183	-100	111	0.150	-80	24
^{241}Pu	0.131	-166	-127	0.144	-112	21
Ox-fuel	0.003	-6	-96	0.003	-5	-95
clad	0.005	38	91	0.005	38	92
mod	0.030	-3	-84	0.036	-13	-78

Table 2. k-infinity, absorption and production rates of MOX benchmark B at BOL and at 50 MWd/kgHM, calculated with JEF-2.2 data and differences for ENDF/B-VI and JENDL-3.2

	BOL			50 MWd/kgHM		
	JEF-2.2	ENDF/B-VI	JENDL-3.2	JEF-2.2	ENDF/B-VI	JENDL-3.2
	k-infinity			***k-infinity***		
	1.1806	1.1792	1.1813	0.9213	0.9183	0.9188
MCNP-4A	1.1807	1.1787	1.1815			
	Prod.rate	Differences, pcm		***Prod. rate***	Differences, pcm	
^{239}Pu	0.845	269	584	0.508	-21	120
^{241}Pu	0.215	-351	-371	0.300	-382	-266
	Abs.rate	Differences, pcm		***Abs.rate***	Differences, pcm	
fuel	0.965	-37	-14	0.958	-32	-28
^{239}Pu	0.458	39	180	0.276	-45	-35
^{241}Pu	0.097	-150	-112	0.136	-111	6
^{241}Pu	0.012	94	20	0.022	111	55
Ox-fuel	0.002	-6	-93	0.002	-5	-92
clad	0.006	38	96	0.006	38	99
mod	0.030	-1	-82	0.036	-6	-72

Chapter 7

CONCLUSIONS

While acknowledging that MOX recycle in PWRs is already demonstrated practically at the commercial scale in PWRs, there will evidently be important new issues to address in the future arising from the combined impact of increasing discharge burn-ups and multiple recycle. Plutonium recycle in BWRs has yet to be demonstrated on the commercial scale, and while there is no doubt that it will prove as practicable as in PWRs, it is clear that the issue of degrading plutonium isotopic quality will also have to be addressed.

The Working Group considers that considerable progress has been made in the nuclear data libraries and lattice codes since the earlier benchmarks. The data libraries have converged somewhat and more exact calculational methods, notably a more accurate treatment of resonance self-shielding in the higher plutonium isotopes, has considerably reduced the spread of results. The range of results obtained is now generally within acceptable bounds, although some important parameters, such as end-of-cycle reactivity have not converged sufficiently for practical application. Consequently there remains a need to obtain experimental and operational data to confirm the predicted values in practice. The uncertainties in the basic nuclear data are sufficient to account for the range of results seen in the STD PWR, but this is not the case for the HM PWR where the ranges of results are generally larger. This is surprising, as the sensitivity of the HM PWR to nuclear data differences might be expected to be smaller than for the STD PWR.

There was generally good agreement as to the evolution of plutonium inventories through the recycle generations. The HM PWR is clearly more tolerant of the degradation in plutonium isotopic quality between recycle generations, as would be expected with the softer neutron spectrum. However, the reduced generation of fresh plutonium from ^{238}U captures speeds up degradation of plutonium compared with the STD PWR. The HM PWR is therefore arguably more proliferation resistant than the STD PWR.

The range of disagreement was higher for the minor actinides (around 20% for americium and curium), but still acceptable, being within the range of uncertainties of the underlying data. It was noted that the uncertainties in threshold reactions are relatively large, and this may affect the actinide number inventories. As might be expected, relatively large uncertainties were noted for higher order effects such as elastic scattering in the moderator and the variation of fission spectrum with burn-up. Although not a dominant component, some variation was noted in fission product absorption.

Since the boundaries of current knowledge will inevitably be expanded gradually as more expedience of MOX recycle is gained, the Working Group considers that multiple recycle scenarios will prove to be practicable in PWRs at least in the near term. Questions as to the reliability and applicability of the nuclear data libraries and lattice codes are unlikely to present an insurmountable barrier to the implementation of multiple recycle. A more important restriction is likely to be the need to maintain an acceptable moderator void coefficient for the complete core. In the particular scenarios examined here, questions regarding the acceptability of the void coefficient arise as early as the

second recycle generation, in the case of the STD PWR, due to the high initial plutonium content (<13 w/o) needed. The HM PWR is less restrictive in this sense, in that the initial plutonium content does not exceed this value until the fourth recycle generation.

The precise point at which the void coefficient becomes unacceptable is not clear because both the present and the earlier benchmarks considered only the nuclear behaviour at the level of lattice cells. To make a definitive evaluation core-wide calculations are necessary, but these are beyond the present scope of work agreed by the Working Group. The Working Group still considers, however, that multiple recycle in the STD PWR case will in practice prove practical up to at least the second generation of recycle, because the scenario examined here is more limiting than can be expected in the immediate future in two senses. First, the burn-up target of 51 MWd/kg in a 1/3-core 18 month cycle exceeds current practice. Second, the plutonium isotopic qualities available from MOX assemblies presently in the discharge ponds or scheduled for discharge are not as poor as those assumed here.

Regarding the need for further benchmark exercises of this kind, the Working Group considers that they would be only of very limited value. This is because the benchmarks presented have converged to the point where it is not possible to clearly identify the underlying causes in the nuclear data and lattice code methods without substantial effort. Even with such effort, the differences are likely to be comparable with the underlying uncertainties in the nuclear data libraries. Whilst there may be some merit in making a comparison on a single nuclear data set, to isolate the contribution to the spread from the lattice code methods, future work on the STD and HM scenarios would be better directed towards whole-core type calculations in an effort to identify the practicable limits such as may be defined by the core-wide reactivity coefficients, transient response and other such behavioural characteristics. Particularly important in this respect would be consideration of the boron coefficient and moderator temperature coefficient and their relevance to such transients as cooldown faults.

Overall the Working Party considers that the latest benchmarks have proved to be very valuable in that they have clearly defined the range of parameters that can be expected in realistic multiple recycle scenarios. There is now a clear understanding of the range of discrepancies that are likely to be expected from the underlying nuclear data and the lattice code methods, which will be immensely useful guidance for the various groups working in the area of plutonium recycle in PWRs. The lessons learned here are likely to be useful as well for BWRs, for which experience of MOX usage lags behind that of PWRs. The HM PWR concept shows clear promise, but generally the range of discrepancies tends to be somewhat larger than for the STD PWR. There is a clear need for experimental support for the HM PWR if it is to be further developed.

REFERENCES

Reports and articles issued from the work of the NSC/WPPR

Physics of Plutonium Recycling – Series of six reports published by the OECD/NEA, 1995/1997.

Issues and Perspectives, ISBN 92-64-14538-9.

Plutonium Recycling in Pressurised-Water Reactors, ISBN 92-64-14560-7.

Void Reactivity Effect in Pressurised-Water Reactors, ISBN 92-64-14591-5.

Fast Plutonium-Burner Reactors: Beginning of Life, ISBN 92-64-14703-9.

Plutonium Recycling in Fast Reactors, ISBN 92-64-14704-7.

Multiple Recycling in Advanced Pressurised-Water Reactors, (this Volume).

A. Tudora: *Evaluation of ^{242}Pu Data for the Incident Neutron Energy Range 5-20 MeV*, NEA/SEN/NSC/WPPR(98)1, December 1998.

Benchmark on the Venus-2 MOX Core Measurements NEA/NSC/DOC(2000)7, OECD/NEA 2000.

Benchmark Calculations of Power Distribution Within Fuel Assemblies, Phase II: Comparison of Data Reduction and Power Reconstruction Methods in Production Codes, NEA/NSC/DOC(2000)3, November 2000.

W. Bernnat, D. Lutz, K. Hesketh, E. Sartori, G. Schlosser, S. Cathalau, M. Soldevila: *PWR Benchmarks from OECD Working Party on Physics of Plutonium Recycling*, Proc. GLOBAL'95, pp. 627-635, 1995.

R.N. Hill, G. Palmiotti, D.C. Wade: *Fast Burner Reactor Benchmark Results from the NEA Working Party on Physics of Plutonium Recycle*, GLOBAL'95, pp. 1367-1373, 1995.

W. Bernnat, S. Cathalau, M. Delpech, K. Hesketh, D. Lutz, M. Mattes, M. Salvatores, E. Sartori, H. Takano: *OECD/NEA Physics Benchmarks on Plutonium Recycling in PWRs*, Proc. PHYSOR'96, Mito, Japan, pp. H61-H74, 1996.

K. Hesketh, M. Delpech, E. Sartori: *Multiple Recycle of Plutonium in PWR: A Physics Code Benchmark Study by the OECD/NEA*, Proc. GLOBAL'97, Yokohama, Japan, pp. 287-294, 1997.

K. Hesketh, M. Delpech, E. Sartori: *The Physics of Plutonium Fuels – A Review of OECD/NEA Activities*, Nuclear Technology, Vol. 131, pg. 385-394, September 2000.

Other reports by the OECD/NEA

Plutonium Fuel: An Assessment, 1989.

The Safety of the Nuclear Fuel Cycle, 1993.

The Economics of the Nuclear Fuel Cycle, 1994.

Management of Separated Plutonium – The Technical Options, A Report by OECD/NEA, 1997, ISBN 92-64-15410-8.

Physics and Fuel Performance of Reactor-Based Plutonium Disposition: Workshop Proceedings, Paris, France, 28-30 September 1998, ISBN: 926417338-1.

Appendix A

PHYSICS OF PLUTONIUM RECYCLING
MULTIPLE RECYCLING IN ADVANCED PRESSURISED-WATER REACTORS

Phase II – Benchmark specification
(Revision 2, 15 April 1996)

Table of contents

MULTIPLE RECYCLING IN ADVANCED PRESSURISED WATER REACTORS: PHASE 2 BENCHMARK SPECIFICATION

Introduction

The aims of this benchmark are to analyse the physics of the plutonium consumption during its recycling in PWRs, the build-up of minor actinides due to this consumption, the effect on the core kinetic parameters, the activity and radiotoxicity consequences, the mass in the cycle and in the waste disposal in order to evaluate the PWR's potential for plutonium stockpile stabilisation.

Thus, this benchmark proposes plutonium recycling with dilution using the first generation plutonium at each recycling inside two kinds of PWRs with a different moderation ration.

The choice of reactor is a standard PWR with a moderation ratio close to 2 (standard PWR) and a highly moderated PWR (HM-PWR) with a moderation ratio of about 3.5. Recent studies [1] have shown that this last concept has a higher ability to consume the plutonium while minimising the minor actinides production. These two reactors are loaded with 100% MOX fuel assemblies.

The number of plutonium recycles for this benchmark is taken equal to 5 to illustrate the composition evolution for many recyclings.

The benchmark is divided into two parts:

- PART 1 aims at the physics analysis of methods, codes and data used for the recycling studies. For that purpose, the plutonium content is provided with this specification together with the corresponding plutonium isotopic compositions. The outputs are all the microscopic and macroscopic results.

- PART 2 aims at the comparison in a global approach of the results obtained by participants themselves on their own during the plutonium recycling following the prescribed specification for dilution. The outputs are the global parameters such as mass balance, plutonium content.

The analysis of these two parts will be carried out, first separately and then jointly for better understanding. For the second part, an extrapolation to an asymptotic case is proposed.

In order to compare the so-extrapolated asymptotic cases as a function of the results obtained for the calculated cycles, an equilibrium state will be extrapolated by the co-ordinator to evaluate the impact of the differences in the first plutonium recycles on the asymptotic case. Also, the impact on the stock mass and cycle mass will be evaluated for each calculated set for this equilibrium state.

The results must be provided in terms of isotopic vectors, isotopic balance, activity and radiotoxicity. These parameters will be given for each step in the cycle and for each plutonium recycle. Also, the results will be analysed in terms of reactivity parameters (boron efficiency,

temperature coefficient, reactivity balance, void effect). This might allow preliminary and global understanding of plutonium recycling in PWRs and evaluation of its feasibility.

1. Data

1.1 Geometry

The dimensions are given for hot conditions.

The calculation of the cylindrised cell is carried out based on the following geometry description:

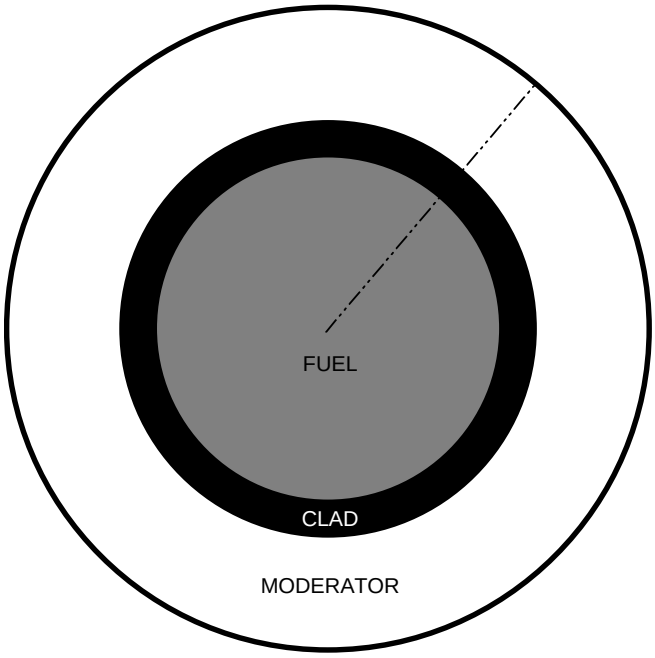

R_3: External radius of the cell.

R_2: External radius of the clad.

R_1: External radius of the fuel pin.

$R_1 = 0.4127$ cm

$R_2 = 0.4744$ cm

For the **standard PWR**..... $R_3 = 0.7521$ cm

For the **HM-PWR**..... $R_3 = 0.9062$ cm

In the different zones, the materials are:

- $0 < R < R_1 \Rightarrow$ The fuel material
- $R_1 < R < R_2 \Rightarrow$ The clad
- $R_2 < R < R_3 \Rightarrow$ The moderator (*The water at nominal conditions, pressure 155 bars and temperature 313°C*)

1.2 Materials

There are three materials in the model:

- The MOX fuel.
- The clad material.
- The moderator.

Note that the materials temperatures specified in the following are equal to the temperatures of the isotopes in the MCNP libraries used in the previous benchmark of WPPR. They do not correspond exactly to the nominal conditions in a PWR. These temperatures are used only to describe the temperature of the isotopes.

1.2.a MOX fuel

Density: 10.02 g/cm^3

Temperature of isotopes: 900 K (626.84°C)

The initial uranium composition:

^{235}U	0.25%
^{238}U	99.75%

This initial uranium composition is taken unchanged at each beginning of each recycling.

For the first cycle of plutonium recycling, the initial concentration of MOX fuel is (in 10^{24} atoms/cm^3) [after fuel fabrication]:

Initial mass content of plutonium: 10.15%

^{235}U	5.0386 10^{-5}		
^{238}U	2.0028 10^{-2}		
^{238}Pu	9.0777 10^{-5}	*Pu mass fraction:*	*4.0%*
^{239}Pu	1.1390 10^{-3}		50.4%
^{240}Pu	5.1761 10^{-4}		23.0%
^{241}Pu	3.0255 10^{-4}		13.5%
^{242}Pu	2.0310 10^{-4}		9.1%
^{16}O	4.4663 10^{-2}		

It is necessary to take into account the decay due to the ^{241}Pu and ^{238}Pu during the ageing time (2 years) in order to obtain the correct plutonium composition before irradiation including ^{241}Am and ^{234}U.

The plutonium is generated through the irradiation of enriched uranium (4.5% of ^{235}U) with the following fuel management: exit burn-up equal to 55.5 MWd/kg and six batch loading and three years of cooling.*

* MWd/kg = Megawatt days per kilogram of initial heavy metal.

For the next cycles, the composition of plutonium will be changed under irradiation and the initial plutonium content is calculated taking into account:

- The level of reactivity adjustment (see next paragraph).
- The density of the MOX fuel is kept constant (10.02 g/cm^3).
- Thus, the initial concentrations will be changed during the multirecycling. *This aspect is explained later in the paper*.

1.2.b Clad

Density: 0.71395 g/cm^3

Temperature of isotopes: 600 K (326.84°C)

The initial concentration is given in the next table is 10^{24} atoms/cm^3:

^{nat}Zr	4.3248 10^{-2}	*In atom %: ^{90}Zr 51.45%, ^{91}Zr 11.32%, ^{92}Zr 17.19%, ^{94}Zr 17.28%, ^{96}Zr 2.76%*

1.2.c Moderator

Density: 0.71395 g/cm^3

Temperature of isotopes: 573.16 K (300°C)

The initial concentration is given in the next table is 10^{24} atoms/cm^3:

^{nat}B	1.98456 10^{-5}	or ^{10}B	3.92943 10^{-6}
		or ^{11}B	1.59162 10^{-5}
^{16}O	2.386013 10^{-2}	or H_2O	2.386013 10^{-2}
^{1}H	4.772026 10^{-2}		

These concentrations correspond to realistic data of the light water at 306°C under a pressure of 155.5 bars. As explained before, the temperature of the moderator isotopes does not correspond to this state of the water in order to be able to use MCNP data libraries if necessary.

The boron concentration is kept under constant evolution. It corresponds to a mass fraction of 500 10^{-6} of soluble boron in the moderator. The natural boron is composed by 18.3% in mass fraction of ^{10}B and by 81.7% of ^{11}B (or respectively 19.8% and 80.2% for atom fraction).

For the initial plutonium content calculations and for the equivalence of the reactivity readjustment calculations, the boron concentration must be zero at the end of the averaged final burn-up of the core (referred to in the section on equivalence calculations).

Calculations are performed with no leakage.

2. Burn-up parameters

One cycle is described as follows:

- *Two years of ageing* after fabrication and before irradiation (build-up of ^{241}Am and ^{234}U).

- *Irradiation with exit burn-up of 51 MWd/kg and three batches of loading management*.

  During irradiation, the power is kept constant. The unit is given for a slice of 1 cm of the cell model. The value of the power depends on the reactor type. It is expressed for all the cells (fuel, clad and moderator) and in Watt per gram of heavy metal:

  – *178 W/cm for the cell with the moderation ratio of 2 or 37.7 W/g of heavy metal. These values correspond to a standard square lattice of 17 × 17.*

  – *280 W/cm for the cell with the moderation ratio of 3.5 or 59.3 W/g of heavy metal. These values correspond to a square lattice 17 × 17. For a 19 × 19 lattice, the linear power decreases to 146 W/cm.*

  During irradiation, the soluble boron concentration is kept constant (mass fraction in moderator: 500 10^{-6}). The previous moderator concentration (see 1.2.c) takes this boron quantity into account. The irradiation is done in one time, with no cooling time for reloading at each cycle step. The used fission energy releases will be reported in the results.

- *Five years of cooling* before reprocessing.

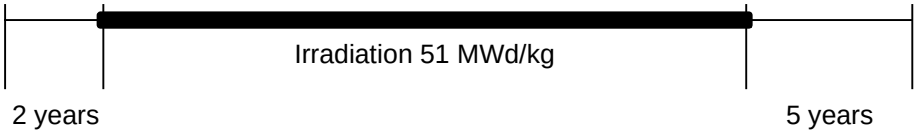

The plutonium recycling with dilution is described as follows:

Only the plutonium is reprocessed at the end of the cycle and put again in reactor after dilution with a first generation plutonium. The rate of the mixture between the first generation plutonium (initial plutonium) and the used plutonium at the end of the cycle is equal to 3. It means that **one assembly** of used plutonium is mixed with **three assemblies** of the first generation plutonium. It means that the electric power share is 25% from the MOX fuel and 75% from the UOX fuel.

The heavy metal mass for one assembly is equal to 540 kg. The plutonium mass per assembly for the UOX irradiated fuel (first-generation plutonium) is equal to 6.7 kg. Thus, we mix 20.1 kg of first generation plutonium with the mass of plutonium contained in one irradiated assembly provided by the MOX fuel.

The other isotopes are extracted, especially the minor actinides (MA) produced by the plutonium under irradiation.

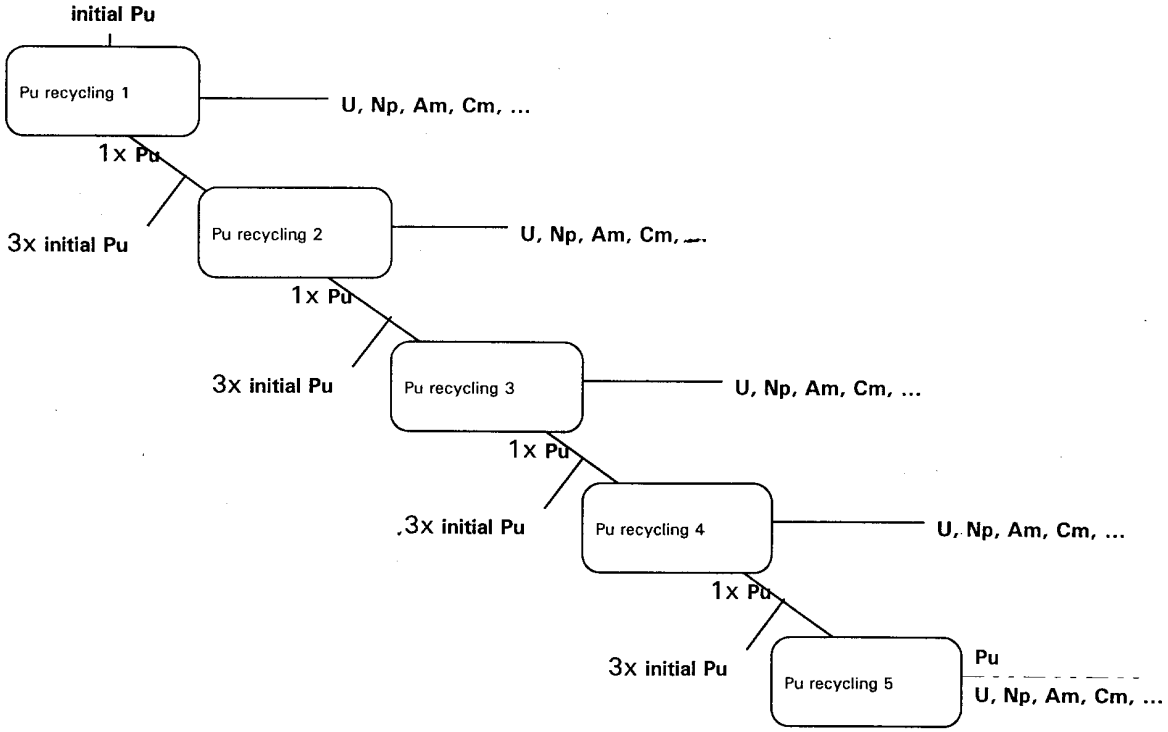

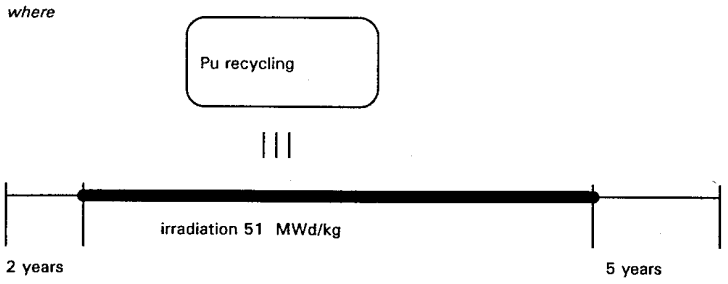

Burn-up model

Usually, the in-core calculations are carried out with boron concentration for all the irradiation time in order to simulate the variation of soluble boron under irradiation. The value of 500 10^{-6} of the mass fraction of soluble boron in the moderator is proper to simulate the effect on the plutonium mass balance.

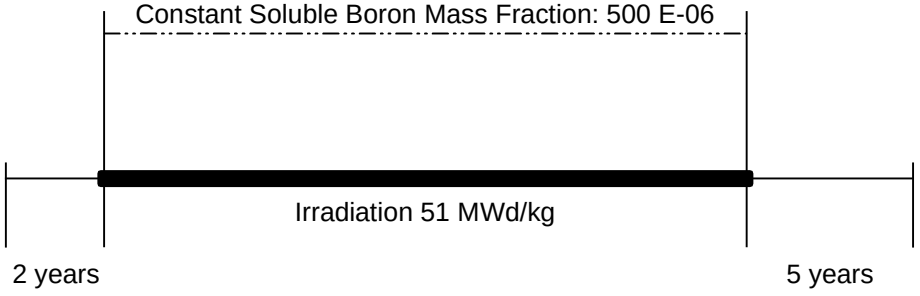

2.1 Part 1: Physics analysis

For this part, the initial plutonium content is given for each cycle:

	STANDARD PWR					**HM-PWR**				
CYCLE	*1*	*2*	*3*	*4*	*5*	*1*	*2*	*3*	*4*	*5*
% Pu	10.1500	13.6250	15.9810	17.7790	19.2280	6.7030	9.6360	12.1070	14.3740	16.5830
^{238}Pu	4.0000	4.8260	5.2880	5.5389	5.6633	4.0000	4.6484	4.9674	5.1382	5.2151
^{239}Pu	50.4000	42.6180	39.1890	37.1235	35.6766	50.4000	36.9325	31.5575	28.5209	26.4344
^{240}Pu	23.0000	26.9270	28.2750	28.9289	29.2940	23.0000	29.0647	29.6867	29.3443	28.7947
^{241}Pu	13.5000	13.4140	12.8570	12.3085	11.8480	13.5000	13.0907	12.7012	12.1591	11.6091
^{242}Pu	9.1000	12.2150	14.3910	16.1003	17.5181	9.1000	16.2637	21.0871	24.8376	27.9467
^{235}U	0.2500	0.2500	0.2500	0.2500	0.2500	0.2500	0.2500	0.2500	0.2500	0.2500
^{238}U	99.7500	99.7500	99.7500	99.7500	99.7500	99.7500	99.7500	99.7500	99.7500	99.7500
at/b•cm										
^{238}Pu	9.0777E-5	1.4695E-4	1.8886E-4	2.2008E-4	2.4337E-4	5.9913E-5	1.0010E-4	1.3440E-4	1.6506E-4	1.9328E-4
^{239}Pu	1.1390E-3	1.2922E-3	1.3938E-3	1.4689E-3	1.5267E-3	7.5174E-4	7.9198E-4	8.5028E-4	9.1235E-4	9.7560E-4
^{240}Pu	5.1761E-4	8.1306E-4	1.0014E-3	1.1399E-3	1.2483E-3	3.4162E-4	6.2066E-4	7.9654E-4	9.3477E-4	1.0583E-3
^{241}Pu	3.0255E-4	4.0335E-4	4.5347E-4	4.8297E-4	5.0279E-4	1.9969E-4	2.7838E-4	3.3938E-4	3.8572E-4	4.2489E-4
^{242}Pu	2.0310E-4	3.6578E-4	5.0547E-4	6.291R3-4	7.4033E-4	1.3404E-4	3.4443E-4	5.6111E-4	7.8465E-4	1.0186E-3
^{235}U	5.0386E-5	4.8875E-5	4.7543E-5	4.6527E-5	4.5708E-5	5.2788E-5	5.1131E-5	4.9734E-5	4.8453E-5	4.7204E-5
^{238}U	2.0028E-2	1.9255E-2	1.8730E-2	1.8330E-2	1.8007E-2	2.0797E-2	2.0143E-2	1.9593E-2	1.9089E-2	1.8597E-2

2.2 Part 2: Global analysis

Adjustment of the plutonium content at each cycle

This reactivity level adjustment permits a coherent evaluation of initial content of plutonium at each cycle of plutonium recycling using only cell calculations and no core calculations.

The initial content of plutonium must be such that it allows to have criticality at the end of each cycle in the core. Our model is based on one cell model calculation and does not take into account the leakage of the core and other penalties. Thus, we propose a model for the cell calculation:

- To adjust the plutonium content for all the cycles of the plutonium recycling.
- To respect core irradiation conditions (leakage and others).
- To respect the reactivity level at the end of one irradiation cycle in the core.

The core average burn-up

The core average burn-up at the end of an equilibrium cycle represents the mean of all the burn-up values for all the assemblies in the core. One equilibrium irradiation cycle in the core starts at 17 MWd/kg (average burn-up value for all the assemblies in the core) and finishes at 34 MWd/kg (average burn-up value for all the assemblies in the core). The core irradiation length between two loadings is 17 MWd/kg.

The core average burn-up at the end of an equilibrium cycle is calculated as:

$$\overline{\text{B.U.}}_{\text{end of cycle}} = 1/\text{n} \sum_{\text{i=1}}^{\text{n}} \text{B.U.}_{\text{end of cycle}}\,(\text{i}) = 34\ \text{MWd/kg}$$

where: n = 3, number of loading batches

$\text{B.U.}_{\text{end of cycle}} = i(\text{B.U.}_{exit}/3)$ for i = 1,2,3, where B.U._{exit} = 51 MWd/kg

$\overline{\text{B.U.}}_{\text{end of cycle}}(\text{i})$ are defined as: i = 1: 17 MWd/kg for the first loading
i = 2: 34 MWd/kg for the second loading
i = 3: 51 MWd/kg for the third loading

Comment: $\text{B.U.}_{exit}/3$ *represents the average burn-up between two loading in the core.*

Reactivity adjustment method

To obtain the initial plutonium content for all cases which allow the fuel management and exit burn-up, we propose a model of in-core irradiation. As described before, the in-core calculations are performed with boron concentration for the full irradiation time in order to take into account a variable quantity of soluble boron under irradiation. The in-core irradiation finishes with no more soluble born in reactor.

The model to calculate the reactivity level at the end of the in-core irradiation is described in two points:

- Settled soluble boron quantity for all the irradiation (500 10^{-6} in mass fraction in the moderator).
- No soluble boron at the end of the averaged burn-up (34 MWd/kg):

$$\overline{\text{B.U.}}_{\text{end of cycle}}$$

The following scheme presents the method:

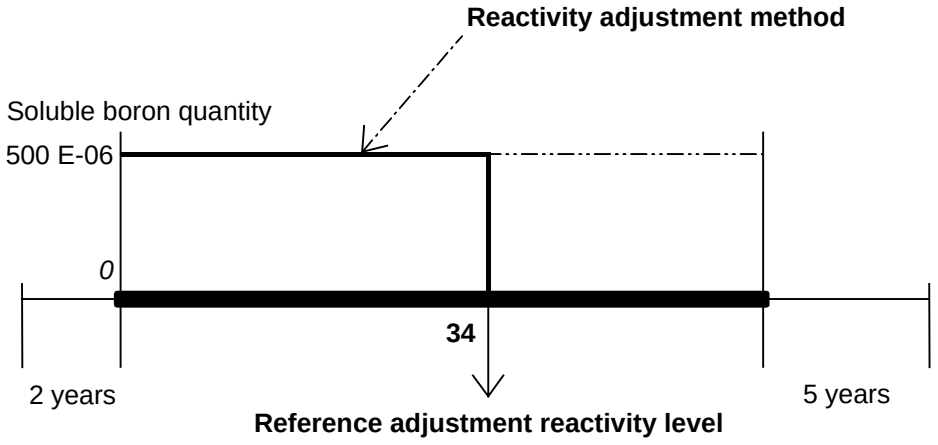

Based on this approach, for each plutonium recycling, we must find the same reactivity level at the averaged burn-up (34 MWd/kg). The first plutonium recycling in standard PWRs (moderation ration equal to 2) gives us this reactivity level. This level takes into account the core leakage and in-core neutron absorption. The plutonium content of the standard PWRs is based on an effective core calculation. In this case, the cell calculation is based on a core calculation with a correct plutonium content, allowing the cycle. This case is named the “Reference Case”.

Reactivity readjustment method for the Reference Case

The first plutonium recycling in standard PWR case with the initial plutonium content, previously given in this benchmark, is the Reference Case.

This reference gives the reference adjustment reactivity level at:

$$\overline{\text{B. U.}}_{\text{end of cycle}}$$

The reference adjustment reactivity level at $\overline{\text{B. U.}}_{\text{end of cycle}}$ is:

$$\rho_{\text{ref}}^{\text{end of cycle}}$$

$\rho_{\text{ref}}^{\text{end of cycle}}$ is calculated as follows:

- An irradiation from 0 MWd/kg to 34 MWd/kg with 500 ppm of soluble boron with no leakage.
- A reactivity calculation at 34 MWd/kg with no soluble boron with no leakage.
- The last step gives the reference adjustment reactivity level: $\rho_{\text{ref}}^{\text{end of cycle}}$.

Reactivity readjustment method for the plutonium recycling cases

All the other cases (others recycling in standard PWR and all the Pu recycling in HM-PWR) are calculated on the base of this Reference Case in a way to find the same reference adjustment reactivity level at:

$$\overline{\text{B. U.}}_{\text{end of cycle}} : \rho_{\text{ref}}^{\text{end of cycle}}$$

Conclusions

The adjustment reactivity level is calculated by each of the participants for the Reference Case (given later) and this level will be kept the same for all the other plutonium recycling cases (**standard PWR and HM-PWR**). This method allows specific and coherent calculations for each set of code and data for all plutonium recycling cases.

Main points of the adjustment methods

Reference Case

- Standard PWR (moderation ration of 2).
- First plutonium recycling (see the previous MOX description).
- Evolution with soluble boron (see the previous moderator description).
- No soluble born for adjustment calculations at 34 MWd/kg.

Thus, in the Reference Case, we obtain:

$$\text{Reference Adjustment Reactivity Level} = k_{\infty}^{ref}(34\ \text{MWd/kgk})$$

Other cycles (during plutonium recycling)

One must adjust the initial plutonium content in order to obtain:

$$k_{\infty}^{\textit{Other cycles}}(34\ \text{MWd/kg}) = k_{\infty}^{\textit{Ref.}}(34\ \text{MWd/kg}) \pm 10^{-4}$$

3. Reactivity coefficients

All of these coefficients are calculated at the beginning and at the end of the irradiation, and also at the beginning of the mean cycle and at the end of the mean cycle:

- At 0.5 MWd/kg.
- At 17 MWd/kg.
- At 34 MWd/kg.
- At 51 MWd/kg.

3.1 Boron efficiency

The boron efficiency is evaluated between two mass boron fractions:

- $500\ 10^{-6}$
- $600\ 10^{-6}$

Moderator composition: boron mass fraction: 500 10^{-6}

B-nat	1.98456 10^{-5}	or B-10 orB-11	3.92943 10^{-6} 1.59162 10^{-5}
O-16	2.386013 10^{-2}	or H_2O	2.386013 10^{-2}
H-1	4.772026 10^{-2}		

Moderator composition: boron mass fraction: 600 10^{-6}

B-nat	2.381472 10^{-5}	or B-10 orB-11	4.71531 10^{-6} 1.90994 10^{-5}
O-16	2.386013 10^{-2}	or H_2O	2.386013 10^{-2}
H-1	4.772026 10^{-2}		

The formula for the boron efficiency is:

$$C_{boron} = \left[1/k_{\infty}\left(600\ 10^{-6}\right) - 1/k_{\infty}\left(500\ 10^{-6}\right)\right]/100$$

The unit is 10^{-5} / ppm.

3.2 Moderator temperature coefficient

The moderator temperature coefficient is calculated between two states. The moderator density variation is calculated when the temperature changes, keeping constant the pressure. The concentrations of the moderator are given as follows:

Unit: 10^{24} atoms/cm^3

	Cold state	**Hot state**
Temperature	569.16 K 296°C	589.16 K 316°C
B-10	0	0
B-11	0	0
H_2O	2.456146 10^{-2}	2.307541 10^{-2}

The formula for the moderator temperature coefficient is:

$$C_{T.Mod.} = \left[1/k_{\infty}\left(\text{Hot State}\right) - 1/k_{\infty}\left(\text{Cold State}\right)\right]/20$$

The unit is 10^{-5} / K.

3.3 Fuel temperature coefficient

The fuel temperature coefficient is evaluated between two states:

- The hot state with a fuel temperature of 910 K (636.84°C).
- The cold state with a fuel temperature of 890 K (616.84°C).

The concentration of all materials are kept equal to those of nominal conditions.

The formula for the fuel temperature coefficient is:

$$C_{T.Comb.} = \left[1/k_{\infty}(\text{Hot State}) - 1/k_{\infty}(\text{Cold State})\right]/20$$

The unit is 10^{-5} / K.

3.4 Reactivity balance

The reactivity balance is defined by:

$$\text{Balance} = \frac{k\infty(0.5\ \text{MWd/kg}) - k\infty(51\ \text{MWd/kg})}{50.5\ \text{MWd/kg}}$$

The unit is 10^{-5} / MWd/kg.

Boron mass fraction in the moderator: 500 10^{-6}.

3.5 Global void effect

The global void effect is calculated between an unvoided state and a voided state at 99% of void. The conditions to calculate the void effect are with no leakage or with leakage.

The formula for the void effect is:

$$E_{void} = 1/K\ (\text{unvoided}) - 1/K\ (\text{voided})$$

The unit is 10^{-5}.

For the unvoided state, the moderator concentrations are (unit: 10^{24} atoms/cm^3):

B-nat	0	or B-10	0
		orB-11	0
O-16	2.386013 10^{-2}	or H_2O	2.386013 10^{-2}
H-1	4.772026 10^{-2}		

For the voided state, the moderator concentrations are (unit: 10^{24} atoms/cm^3):

B-nat	0	or B-10 orB-11	0 0
O-16	$2.386013\ 10^{-4}$	or H_2O	$2.386013\ 10^{-4}$
H-1	$4.772026\ 10^{-4}$		

The two calculations with and without leakage are carried with the following leakage values:

- With no leakage: $B^2 = 0$ for voided state.
  $B^2 = 0$ for unvoided state.
- With critical leakage ($k_{eff} = 1$).

4. Results – Output data

The results must be sent on computer readable medium in order to process them with Microsoft EXCEL software.

The results necessary for Part 1: Physics analysis, and Part 2: Global analysis of the benchmark are:

4.0 A description of

- The computer program.
- The data libraries (number of groups and energy boundaries).
- The self-shielding models and calculations.

4.1 The reactivity value obtained at the end of the mean batch for the reference case

The reactivity values at 0, 8.5, 17, 25.5, 34, 42.5 and 51 MWd/kg*.

4.2 The reactivity parameters for

- Boron efficiency.
- Moderator temperature coefficient.
- Fuel temperature coefficient.
- Reactivity balance.
- Global void effect.

* MWd/kg = Megawatt days per kilogram of initial heavy metal.

4.3 The isotopic composition of the fuel at each cycle step

- Beginning of the cycle.
- Beginning of the irradiation.
- End of the irradiation.
- End of the cooling time (end of the cycle).

4.4 The isotopic composition per elements (uranium, plutonium, neptunium, americium and curium) at each cycle step

- Beginning of the cycle.
- Beginning of the irradiation.
- End of the irradiation.
- End of the cooling time (end of the cycle).

4.5 The one-group microscopic cross-sections and decay values used in the calculations for the first plutonium recycling for all the isotopes. For the microscopic cross-sections, the values are asked at

- Beginning of the irradiation (0 MWd/kg).
- Middle of the first batch (8.5 MWd/kg).
- End of the first batch (17 MWd/kg).
- Middle of the second batch (25.5 MWd/kg).
- End of the second batch (34 MWd/kg).
- Middle of the third batch (42.5 MWd/kg).
- End of the irradiation (51 MWd/kg).

4.6 The macroscopic cross-sections H.N., F.P. and materials (global values for Σ_a **and** $\nu\Sigma_f$ ***for the first step of irradiation and the last step of irradiation***

4.7 The data of fission energy release of all the isotopes

4.8 The β_{eff} ***value at the first and fifth cycles for standard PWR and HM-PWR at the end of irradiation***

4.9 The mass of the fuel at each cycle step

- Beginning of the cycle.
- Beginning of the irradiation.
- End of the irradiation.
- End of the cooling time (end of the cycle).

4.10 The isotopic composition of the fuel at each cycle step

- Beginning of the cycle.
- Beginning of the irradiation.
- End of the irradiation.
- End of the cooling time (end of the cycle).

4.11 The global activity of one heavy metal metric tonne of

- Initial fuel at the beginning of multirecycling for a time scale between 5 years and 1 million years (time steps*).
- Irradiated fuel at the end of multirecycling for a time scale between 5 years and 1 million years (time steps*).

4.12 The radiotoxicity of fission products and heavy nuclides separately for

- Initial fuel at the beginning of multirecycling for a time scale between 5 years and 1 million of years (time steps*), normalised to one heavy nuclide metric tonne.
- Irradiated fuel at the end of multirecycling for a time scale between 5 years and 1 million of years (time steps*), normalised to one heavy nuclide metric tonne (table with factor is given).

* The time steps are defined as: $i\ 10^j$, where i = 1,2,…,9,0 and j = 0,1,2,…,6.

Radiotoxicity data

(CD = Cancer Dose Hazard)

Isotope	Toxicity factor CD/Ci	Half-life Years	Toxicity factor CD/g
Actinides and their daughters			
^{210}Pb	455.0	22.3	3.48E4
^{223}Ra	15.6	0.03	7.99E5
^{226}Ra	36.3	1.60E3	3.59E1
^{227}Ac	1185.0	21.8	8.58E4
^{229}Th	127.3	7.3E3	2.72E1
^{230}Th	19.1	7.54E4	3.94E-1
^{231}Pa	372.0	3.28E4	1.76E-1
^{234}U	7.59	2.46E5	4.71E-2
^{235}U	7.23	7.04E8	1.56E-5
^{236}U	7.50	2.34E7	4.85E-4
^{238}U	6.97	4.47E9	2.34E-6
^{237}Np	197.2	2.14E6	1.39E-1
^{238}Pu	246.1	87.7	4.22E3
^{239}Pu	267.5	2.41E4	1.66E1
^{240}Pu	267.5	6.56E3	6.08E1
^{242}Pu	267.5	3.75E5	1.65E0
^{241}Am	272.9	433	9.36E2
^{242m}Am	267.5	141	2.80E4
^{243}Am	272.9	7.37E3	5.45E1
^{242}Cm	6.90	0.45	2.29E4
^{243}Cm	196.9	29.1	9.96E3
^{244}Cm	163.0	18.1	1.32E4
^{245}Cm	284.0	8.5E3	4.88E1
^{246}Cm	284.0	4.8E3	8.67E1
Short-lived fission products			
^{90}Sr	16.7	29.1	2.28E3
^{90}Y	0.60	7.3E-3	3.26E5
^{137}Cs	5.77	30.2	4.99E2
Long-lived fission products			
^{99}Tc	0.17	2.13E5	2.28E-3
^{129}I	64.8	1.57E7	1.15E-2
^{93}Zr	0.095	1.5E6	2.44E-4
^{135}Cs	0.84	2.3E6	9.68E-4
^{14}C	0.20	5.73E3	8.92E-1
^{59}Ni	0.08	7.6E4	6.38E-3
^{63}Ni	0.03	100	1.70E0
^{126}Sn	1.70	1.0E5	4.83E-2

5. Tables of output data: format and presentation

For greater efficiency, the computed results (1, 2, 3, 4 and 5) must be filled in the following tables for each cycle. For the results concerning activity and radiotoxicity (6 and 7), tables with free format are acceptable.

5.1 The reactivity value (to be provided for Part 1 and Part 2, Section 4.1)

At each cycle:

Reactivity value adjustment	

and k_∞ (B.U.)

5.2 The reactivity parameters for (to be provided for Part 1 and Part 2, Section 4.2)

At each cycle:

	0.5 MWd/kg	17 MWd/kg	34 MWd/kg	51 MWd/kg
Boron efficiency				
Moderator temperature coefficient				
Fuel temperature coefficient				
Reactivity balance				
Global void effect with no leakage				
Global void effect with leakage (k_{eff} = 1)				

- For each parameter: k_∞.
- For the voided state, and the unvoided state: M^2 values.

5.3 The isotopic composition of the fuel (to be provided for Part 1 and Part 2, Sections 4.3 & 4.10)

At each cycle:

- BOC: Beginning of cycle.
- BOI: Beginning of irradiation.
- EOI: End of irradiation.
- EOC: End of cycle.

Unit: 10^{24} atoms/cm^3 at nominal conditions.

	BOC	BOI	EOI	EOC
^{234}U				
^{235}U				
^{236}U				
^{237}U				
^{238}U				
^{237}Np				
^{238}Np				
^{239}Np				
^{238}Pu				
^{239}Pu				
^{240}Pu				
^{241}Pu				
^{242}Pu				
^{241}Am				
^{242}Am				
^{243}Am				
^{242}Cm				
^{243}Cm				
^{244}Cm				
^{245}Cm				
^{246}Cm				
^{79}Se				
^{93}Zr				
^{99}Tc				
^{107}Pd				
^{129}I				
^{135}Cs				
Fission rate				

5.4 The mass composition of the fuel *(to be provided for Part 2, Section 4.9)*

At each cycle:

- BOC: Beginning of cycle.
- BOI: Beginning of irradiation.
- EOI: End of irradiation.
- EOC: End of cycle.

Unit: kilograms per initial metric tonne of heavy metal.

	BOC	BOI	EOI	EOC
^{234}U				
^{235}U				
^{236}U				
^{237}U				
^{238}U				
^{237}Np				
^{238}Np				
^{239}Np				
^{238}Pu				
^{239}Pu				
^{240}Pu				
^{241}Pu				
^{242}Pu				
^{241}Am				
^{242}Am				
^{243}Am				
^{242}Cm				
^{243}Cm				
^{244}Cm				
^{245}Cm				
^{246}Cm				
^{79}Se				
^{93}Zr				
^{99}Tc				
^{107}Pd				
^{129}I				
^{135}Cs				
Fission rate				

5.5 The isotopic composition per elements (to be provided for Part 1, Section 4.4)

At each cycle:

- BOC: Beginning of cycle.
- BOI: Beginning of irradiation.
- EOI: End of irradiation.
- EOC: End of cycle.

Unit: atom mass %.

	BOC	BOI	EOI	EOC
^{234}U				
^{235}U				
^{236}U				
^{237}U				
^{238}U				
^{237}Np				
^{238}Np				
^{239}Np				
^{238}Pu				
^{239}Pu				
^{240}Pu				
^{241}Pu				
^{242}Pu				
^{241}Am				
^{242}Am				
^{243}Am				
^{242}Cm				
^{243}Cm				
^{244}Cm				
^{245}Cm				
^{246}Cm				
^{79}Se				
^{93}Zr				
^{99}Tc				
^{107}Pd				
^{129}I				
^{135}Cs				
Fission rate				

5.6 The microscopic cross-section and decay values

For the first plutonium recycling only, the capture, fission, (n,2n), one-group microscopic cross-sections, the nu values and the decay periods used in the calculations. for the one-group microscopic cross-sections, the values are asked at:

- B: Beginning of the irradiation (0 MWd/kg)
- 1: Middle of the first batch (8.5 MWd/kg)
- 2: End of the first batch (17 MWd/kg)
- 3: Middle of the second batch (25.5 MWd/kg)
- 4: End of the second batch (34 MWd/kg)
- 5: Middle of the third batch (42.5 MWd/kg)
- E: End of the irradiation (51 MWd/kg)

	B	1	2	3	4	5	E
^{234}U							
^{235}U							
^{236}U							
^{237}U							
^{238}U							
^{237}Np							
^{238}Np							
^{239}Np							
^{238}Pu							
^{239}Pu							
^{240}Pu							
^{241}Pu							
^{242}Pu							
^{241}Am							
^{242}Am							
^{243}Am							
^{242}Cm							
^{243}Cm							
^{244}Cm							
^{245}Cm							
^{246}Cm							

5.7 The fission energy release, capture energy release (MeV) *(to be provided for Part 1, Section 4.7)*

	By fission	By capture
^{234}U		
^{235}U		
^{236}U		
^{237}U		
^{238}U		
^{237}Np		
^{238}Np		
^{239}Np		
^{238}Pu		
^{239}Pu		
^{240}Pu		
^{241}Pu		
^{242}Pu		
^{241}Am		
^{242}Am		
^{243}Am		
^{242}Cm		
^{243}Cm		
^{244}Cm		
^{245}Cm		
^{246}Cm		

5.8 Macroscopic cross-sections *(to be provided for Part 1, Section 4.6)*

	0 GWd/kg		**51 GWd/kg**	
	Σ_a	$\nu\Sigma_f$	Σ_a	$\nu\Sigma_f$
HN				
FP				
Clad				
Water				

REFERENCES

[1] M. Salvatores, *et al*., "Nuclear Waste Transmutation: Physics Issues and Potential in Neutron Fields", International Reactor Physics Conference, Tel Aviv, 23-26 January 1994.

Appendix B

LIST OF PARTICIPANTS

(addresses)

BELGIUM

D'HONDT, Pierre
Centre d'Étude de l'Énergie Nucléaire
200 Boeretang
B-2400 MOL

MALDAGUE, Thierry
Belgonucléaire S.A.
Avenue Ariane 4
B-1200 BRUXELLES

CANADA

JONES, Richard T.
Manager, Reactor Physics
AECL Research
Chalk River Nuclear Labs.
CHALK RIVER
Ontario K0J 1J0

DENMARK

HOEJERUP, C. Frank
Senior Scientist
Risoe National Laboratory
P.O. Box 49
DK-4000 ROSKILDE

FRANCE

CATHALAU, Stéphane
CEA – DEN/SPEx/LPE
CEN Cadarache
Bâtiment 230
F-13108 SAINT-PAUL-LEZ-DURANCE CEDEX

COSTE, Mireille
CEA/DEN/DMT
SERMA/LENR
CEA Saclay
F-91191 GIF-SUR-YVETTE CEDEX

DELPECH, Marc
CEA – DER/SERI/LCSI
CEN Cadarache
Bâtiment 230 – B.P. 1
F-13108 SAINT-PAUL-LEZ-DURANCE CEDEX

LEE, Yi-Kang
CEN Saclay
DMT/SERMA/LEPP
F-91191 GIF-SUR-YVETTE CEDEX

PENELIAU, Yannick
CEA/DEN/DMT
SERMA/LEPP
CEA Saclay
F-91191 GIF-SUR-YVETTE CEDEX

POINOT-SALANON, Christine
Société Framatome
EPN
Tour FRAMATOME – Cedex 16
1, Place de la Coupole
F-92084 PARIS LA DÉFENSE

PUILL, André
CEA/DEN/DMT
SERMA/LCA
CEA Saclay
F-91191 GIF-SUR-YVETTE CEDEX

ROHART, Michelle
CEA/DEN/DMT
SERMA/LCA
CEA Saclay
F-91191 GIF-SUR-YVETTE CEDEX

TSILANIZARA, Aimé
CEA/DEN/DMT
SERMA/LEPP
CEA Saclay
F-91191 GIF-SUR-YVETTE CEDEX

GERMANY

BERNNAT, Wolfgang
Universitaet Stuttgart
Institut fuer Kernenergetik und Energiesysteme
Postfach 801140
D-70550 STUTTGART

HESSE, Ulrich
Gesellschaft fuer Anlagen-und Reaktorsicherheit
Forschungsgelaende
Postfach 1328
D-85739 GARCHING

LEHMANN, Sven
Inst. Fuer Raumflugtechnik und Reaktortechnik
Tech. Univ. Braunschweig
Hans-Sommer-Str. 5
D-38106 BRAUNSCHWEIG

LUTZ, Dietrich
Universitaet Stuttgart
Institut fuer Kernenergetik und Energiesysteme
Postfach 801140
D-70550 STUTTGART

MATTES, Margarete
Universitaet Stuttgart
Institut fuer Kernenergetik und Energiesysteme
Postfach 801140
D-70550 STUTTGART

MOSER, Eberhard
Gesellschaft fuer Anlagen-und Reaktorsicherheit
Postfach 1328
D-85739 GARCHING

SCHLOSSER, Gerhard
SIEMENS AG, KWU NBTI
Postfach 3220
Bunsenstr. 43
D-91050 ERLANGEN

JAPAN

AKIE, Hiroshi
Transmutation System Lab.
Dept. of Reactor Engineering
JAERI
TOKAI-MURA, Naka-gun
Ibaraki-ken 319-11

FUJIWARA, Daisuke
Dept. of Quantum Science and
Energy Engineering
Tohoku University
Aoba, Aramaki, Aoba
SENDAI, 980-77

KANEKO, K.
JAERI
Tokai Research Establishment
TOKAI-MURA, Naka-gun
Ibaraki-ken 319-11

MISAWA, Tsuyoshi
Dept. Nuclear Engineering
Nagoya University
Furo-cho, Chikusa-ku
J-NAGOYA-SHI 464-01

TAKANO, Hideki
Pu-Burner Program Team
JAERI
TOKAI-MURA, Naka-gun
Ibaraki-ken 319-11

TAKEDA, Toshikazu
Osaka University
Department of Nuclear Engineering
Graduate School of Engineering
2-1 Yamada-Oka, Suita
OSAKA 565

YAMAMOTO, Toshihisa
Dept.of Nuclear Eng.
Graduate School of Engineering
Osaka University
2-1, Yamada-oka,Suita,
OSAKA 565

KOREA (REPUBLIC OF)

KIM, Young-Jin
Manager, Reactor Physics
Korea Atomic Energy Research
Institute
P.O. Box 105, Yuseong,
TAEJON 305-600

NETHERLANDS

KLOOSTERMAN, Jan Leen
Netherlands Energy Research
Foundation (ECN)
B.U. Nuclear Energy
P.O. Box 1
NL-1755 ZG PETTEN

RUSSIAN FEDERATION

TSIBOULIA, Anatoli
Institute of Physics and Power Engineering (IPPE)
Fiziko-Energiticheskij Inst.
1, Bondarenko Square
249020 OBNINSK

SWITZERLAND

GRIMM, Peter
Paul Scherrer Institute
CH-5232 VILLIGEN PSI

PARATTE, Jean-Marie
Paul Scherrer Institute
CH-5232 VILLIGEN PSI

UNITED KINGDOM

CROSSLEY, Steve
British Nuclear Fuels plc
Springfields
PRESTON
Lancashire PR4 0XJ

HESKETH, Kevin
British Nuclear Fuels plc
Springfields
PRESTON
Lancashire PR4 0XJ

UNITED STATES OF AMERICA

BLOMQUIST, Roger N.
Reactor Analysis Division
Argonne National Laboratory
9700 South Cass Avenue
RA/208
ARGONNE, IL 60439

GRIMM, Karl
Reactor Analysis Division
Argonne National Laboratory
9700 South Cass Avenue
ARGONNE, Il. 60439

HILL, Robert N.
Reactor Analysis Division
Argonne National Laboratory
9700 South Cass Avenue
ARGONNE, Il. 60439

International Organisations

RINEJSKI, Anatoli
Division of Nuclear Power and the Fuel Cycle
I.A.E.A.
P.O. Box 100
A-1400 WIEN

SARTORI, Enrico
OECD/NEA Data Bank
Le Seine-Saint-Germain
12 boulevard des Iles
F-92130 ISSY-LES-MOULINEAUX

List of participants to Annex 1 of Chapter 6

CATHALAU, Stéphane
CEA – DEN/SPEx/LPE
CEN CADARACHE
Bâtiment 230
F-13108 SAINT-PAUL-LEZ-DURANCE CEDEX

LUTZ, Dietrich
Universität Stuttgart
Institut für Kernenergetik une Energiesysteme
Postfach 801140
D-70550 STUTTGART

PEETERS, T.T.J.M.
Netherlands Energy Research Foundation – ECN
P.O. Box 1
NL-1755 ZG PETTEN

PENELIAU, Yannick
CE Saclay
CEA/DRN/DMT
SERMA/LCA
F-91191 GIF-SUR-YVETTE CEDEX

PUILL André
CE Saclay
CEA/DRN/DMT
SERMA/LCA
F-91191 GIF-SUR-YVETTE CEDEX

TAKANO, Hideki
JAERI
Reactor System Laboratory
Tokai Research Establishment
Tokai-Mura, Naka-gun
Ibaraki-ken 319-11

Appendix C

LIST OF SYMBOLS AND ABBREVIATIONS

ANL	Argonne National Laboratory
barn	Nuclear physics' unit for measurement of cross-section (= 10^{-28} m^2)
β_{eff}	Effective delayed neutron fraction
BNFL	British Nuclear Fuels
BWR	Boiling Water Reactor
CEA	Commissariat à l'énergie atomique
ECN	Netherlands Energy Research Foundation
GRS	Gesellschaft fuer Anlagen-und Reaktorsicherheit
HM PWRs	Highly moderated Pressurised Water Reactors
IKE	Institut fuer Kernenergetik und Energiesysteme
IPPE	Institute of Physics and Power Engineering of Obninsk
JAERI	Japan Atomic Energy Research Institute
KAERI	Korea Atomic Energy Research Institute
LWRs	Light Water Reactors
MC	Monte Carlo
MOX	Mixed Oxide (uranium and plutonium)
MWd/t	Mega Watt days per tonne
OECD/NEA	OECD Nuclear Energy Agency

PSI	Paul Scherrer Institute, Switzerland
PWRs	Pressurised Water Reactors
SCK-CEN	Studiecentrum voor Kernenergie-Centre d'études de l'énergie nucléaire
STD PWR	standard 17×17 PWR lattice
TFRPD	Task Force on Reactor-based Plutonium Disposition
UO_2 or UOX	Uranium Oxide
WPPR	Working Party on the Physics of Plutonium Fuels and Innovative Fuel Cycles

Appendix D

CORRIGENDUM FOR PREVIOUS VOLUMES[†]

Corrigendum of corrected specification for Volume II*

Benchmark specification for plutonium recycling in PWRs

Benchmark A: Poor-quality plutonium
J. Vergnes (EdF)

Benchmark B: Better plutonium vector
H. W. Wiese (KfK) and G. Schlosser (Siemens-KWU)

Co-ordinator
H. Küsters, KfK

Benchmark A – poor-isotopic-quality plutonium

The goal of this comparison is to explain the reasons for unexplained differences between results on MOX-PWR cell calculations using degraded plutonium (fifth-stage recycle).

The most important difference is related to the infinite medium multiplication constant k-infinity. We suggest a geometry as simple as possible. We shall describe the proposed options:

- Number of atoms and cell geometry

  Differences could appear for these calculations. So we propose that a number of atoms will be stated for the benchmark.

  For this preliminary calculation, we have taken the geometry of Figure A-1 and the following isotopic balance of plutonium. The plutonium isotopic composition is near the composition at the fifth stage recycle with an average burn-up of 50 MWd/kg.

[†] Corrections are designated by bold characters.

* This section is Appendix A in of *Physics of Plutonium Recycling, Volume II: Plutonium Recycling in Pressurised-Water Reactors*. See pp. 73-78.

Pu-238	4%
Pu-239	36%
Pu-240	28%
Pu-241	12%
Pu-242	20%

The uranium isotopic composition is the following:

U-235	0.711%
U-238	99.289%

The total plutonium concentration proposed is 12.5% (6% of fissile plutonium).

The cladding is only made out of natural zirconium.

In evolution, samarium and xenon concentrations will be self-estimated by each code with a nominal power of 38.3 W/g of initial heavy metal.

- Options of the cell calculation

To ease the comparisons, it is suggested to calculate the cell without any neutron leakage ($B^2 = 0$).

Temperatures will be as follows:

- Fuel 660°C
- Cladding 306.3°C
- Water 306.3°C

Boron concentration is worth **461.4** ppm. Boron composition is as follows:

- B-10 18.3 **w/o**
- B-11 81.7 **w/o**

Table A-1. Number of atoms per cm^3 at irradiation step zero

FUEL	
	ATOMS / cm^3
U-234	0
U-235	$1.4456 \cdot 10^{20}$
U-236	0
U-238	$1.9939 \cdot 10^{22}$
Np-237	0
Pu-238	$1.1467 \cdot 10^{20}$
Pu-239	$1.0285 \cdot 10^{21}$
Pu-240	$7.9657 \cdot 10^{20}$
Pu-241	$3.3997 \cdot 10^{20}$
Pu-242	$5.6388 \cdot 10^{20}$
Am-241	0
Am-242	0
Am-243	0
Cm-242	0
Cm-243	0
CLADDING	
natural Zr	**4.3248** $\cdot 10^{22}$
MODERATOR	
H_2O	$2.3858 \cdot 10^{22}$
B-10	$3.6346 \cdot 10^{18}$
B-11	$1.6226 \cdot 10^{19}$

- Options of the evolution calculation

  We propose an evolution calculation from 0 to 50 MWd/kg including the following time steps (0, 0.15, 0.5, 1, 2, 4, 6, 10, 15, 20, 22, 26, 30, 33, 38, 42, 47 and 50 MWd/kg)

  We take into consideration the following fission products:

  Zr-95, Mo-95, Pd-106, Ce-144, Pm-147, Pm-148, Pm-148m, Sm-149, Sm-150, Sm-151, Sm-152, Eu-153, Eu-154, Eu-155, Gd-155, Gd-156, Gd-157, Tc-99, Ag-109, Cd-113, In-115, I-129, Xe-131, Cs-131, Cs-137, Nd-143, Nd-145, Nd-148,

  and four pseudo fission products in which all the other fission products are grouped.

The energy releases from fission are:

NUCLIDE	ENERGY RELEASE (MeV)
U-235	193.7
U-238	197.0
Pu-239	202.0
Pu-241	204.4
Am-242m	207.0

plus 8 MeV for the n-gamma captures of the other non-fissioning (ν-1) neutrons.

- Results

Results should be provided both on paper and computer-processable medium. A short report should be provided describing:

- The computer program(s) used and their precise version,
- The data libraries used and evaluated data file from which they were derived,
- The list of isotopes for which resonance self-shielding was applied and the method used,
- How the build-up of Xenon was treated,
- How the (n,2n)-reaction was taken into account for the k-infinity calculation.

The following data should be provided in tabular form for the following burn-ups:
0, 10, 33, 42 and 50 MWd/kg.

1. Number densities for all nuclides considered:

	burn-up 1	burn-up 2	.....	burn-up-n
isotope 1				
isotope 2				
.				
.				
.				
.				
.				
isotope -N				

2. k as a function of burn-up,
3. One energy group cross-section (absorption, fission, nu-bar) as a function of isotope and burn-up (see 1.),
4. Reaction rates (absorption, fission) as a function of isotope and burn-up (see 1.),

5. Applied absolute fluxes used in the evolution calculation (and their normalisation factor),

6. Neutron energy spectrum per unit lethargy as a function of burn-up (and its normalisation factor and group structure).

Benchmark B – better plutonium vector

As a second fuel M2, in agreement both with Dr. G. Schlosser, KWU and Dr. J. Vergnes, EdF, a MOX fuel with first-generation-plutonium as used in [1] with the following specifications is suggested:

- 4.0 wt% $\mathbf{Pu_{fiss}}$ in uranium tailings (0.25 wt% U-235),

- Composition of plutonium (wt%):

Pu-238	1.8
Pu-239	59.0
Pu-240	23.0
Pu-241	12.2
Pu-242	4.0

- Composition of uranium (wt%):

U-234	0.00119
U-235	0.25
U-238	99.74881

With the heavy material number density normalised to 2.115×10^{22} atoms /cm^3, the following nuclide number densities are determined:

NUCLIDE	ATOMS / cm^3
U-234	$2.4626 \cdot 10^{17}$
U-235	$5.1515 \cdot 10^{19}$
U-238	$2.0295 \cdot 10^{22}$
Pu-238	$2.1800 \cdot 10^{19}$
Pu-239	$7.1155 \cdot 10^{20}$
Pu-240	$2.7623 \cdot 10^{20}$
Pu-241	$1.4591 \cdot 10^{20}$
Pu-242	$4.7643 \cdot 10^{19}$
heavy metal-atoms	$2.155 \cdot 10^{22}$
O	$4.310 \cdot 10^{22}$

All other specifications shall be the same as in the first benchmark – Case A.

REFERENCE

[1] H. W. Wiese, “Investigation of the Nuclear Inventories of High-Exposure PWR Mixed Oxide Fuels with Multiple Recycling of Self-Generating Plutonium”, Nuclear Technology, Vol. 102, April 1993, p. 68.

Figure A-1. Cell geometry at 20°C

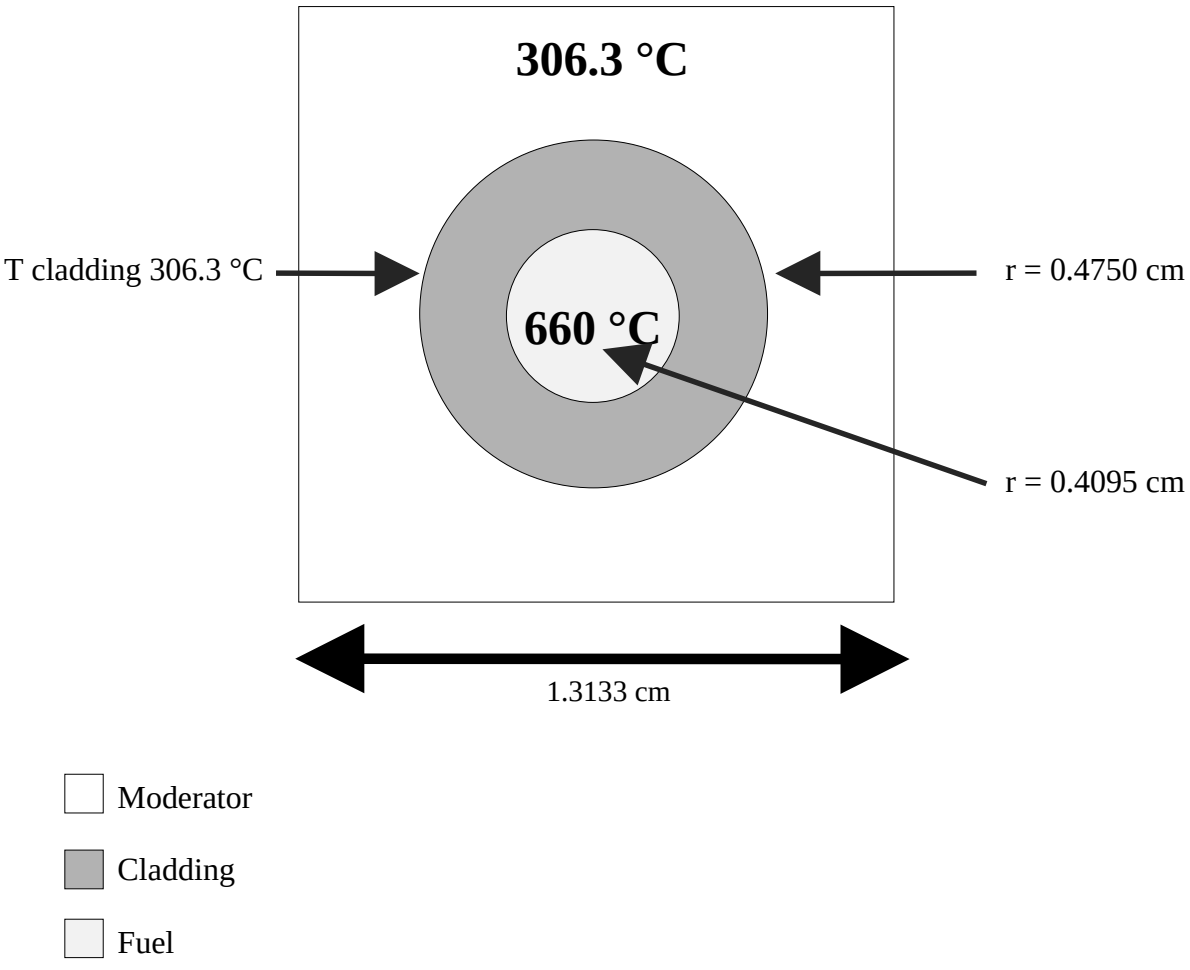

ALSO AVAILABLE

NEA Publications of General Interest

2001 Annual Report (2002) *Free: paper or Web.*

NEA News
ISSN 1605-9581 Yearly subscription: € 40 US$ 45 GBP 26 ¥ 4 800

Geologic Disposal of Radioactive Waste in Perspective (2000)
ISBN 92-64-18425-2 Price: € 20 US$ 20 GBP 12 ¥ 2 050

Nuclear Science

Advanced Reactors with Innovative Fuels (2002)
ISBN 92-64-19847-4 Price: € 130 US$ 113 GBP 79 ¥ 15 000

Basic Studies in the Field of High-temperature Engineering (2002)
ISBN 92-64-19796-6 Price: € 75 US$ 66 GBP 46 ¥ 8 600

Utilisation and Reliability of High Power Proton Accelerators (2002)
ISBN 92-64-18749-9 Price: € 130 US$ 116 GBP 80 ¥ 13 100

Fission Gas Behaviour in Water Reactor Fuels (2002)
ISBN 92-64-19715-X Price: € 120 US$ 107 GBP 74 ¥ 12 100

Shielding Aspects of Accelerators, Targets and Irradiation Facilities – SATIF 5 (2001)
ISBN 92-64-18691-3 Price: € 84 US$ 75 GBP 52 ¥ 8 450

Nuclear Production of Hydrogen (2001)
ISBN 92-64-18696-4 Price: € 55 US$ 49 GBP 34 ¥ 5 550

Pyrochemical Separations (2001)
ISBN 92-64-18443-0 Price: € 77 US$ 66 GBP 46 ¥ 7 230

Evaluation of Speciation Technology (2001)
ISBN 92-64-18667-0 Price: € 80 US$ 70 GBP 49 ¥ 7 600

Comparison Calculations for an Accelerator-driven Minor Actinide Burner (2002)
ISBN 92-64-18478-3 *Free: paper or web.*

Forsmark 1 & 2 Boiling Water Reactor Stability Benchmark (2001)
ISBN 92-64-18669-4 *Free: paper or web.*

Pressurised Water Reactor Main Steam Line Break (MSLB) Benchmark (Volume III) (2002) *In preparation.*

International Evaluation Co-operation *(Free on request - paper or CD-ROM)*
Volume 1: *Comparison of Evaluated Data for Chromium-58, Iron-56 and Nickel-58* (1996)
Volume 2: *Generation of Covariance Files for Iron-56 and Natural Iron* (1996)
Volume 3: *Actinide Data in the Thermal Energy Range* (1996)
Volume 4: *^{238}U Capture and Inelastic Cross-Sections* (1999)
Volume 5: *Plutonium-239 Fission Cross-Section between 1 and 100 keV* (1996)
Volume 6: *Delayed Neutron Data for the Major Actinides* (2002)
Volume 8: *Present Status of Minor Actinide Data* (1999)
Volume 10: *Evaluation Method of Inelastic Scattering Cross-sections for Weakly Absorbing Fission-product Nuclides* (2001)
Volume 12: *Nuclear Model to 200 MeV for High-Energy Data Evaluations* (1998)
Volume 13: *Intermediate Energy Data* (1998)
Volume 14: *Processing and Validation of Intermediate Energy Evaluated Data Files* (2000)
Volume 15: *Cross-Section Fluctuations and Shelf-Shielding Effects in the Unresolved Resonance Region* (1996)
Volume16: *Effects of Shape Differences in the Level Densities of Three Formalisms on Calculated Cross-Sections* (1998)
Volume 17: *Status of Pseudo-Fission Product Cross-Sections for Fast Reactors* (1998)
Volume 18: *Epithermal Capture Cross-Section of ^{235}U* (1999)

Order form on reverse side.

ORDER FORM

OECD Nuclear Energy Agency, 12 boulevard des Iles, F-92130 Issy-les-Moulineaux, France
Tel. 33 (0)1 45 24 10 15, Fax 33 (0)1 45 24 11 10, E-mail: nea@nea.fr**, Internet: www.nea.fr**

Qty	Title	ISBN	Price	Amount
			Total*	

* Prices include postage fees.

❑ Payment enclosed (cheque payable to OECD Publications).

Charge my credit card ❑ VISA ❑ Mastercard ❑ Eurocard ❑ American Express

Card No.	Expiration date	Signature
Name		
Address	Country	
Telephone	Fax	
E-mail		

OECD PUBLICATION, 2, rue André-Pascal, 75775 PARIS CEDEX 16
PRINTED IN FRANCE
(66 2002 17 1 P) – No. 52739 2002